

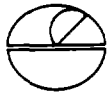
UNDERGROUND VIBRATIONS FROM SURFACE  
BLASTING AT JENNY MINE, KENTUCKY

Prepared for

UNITED STATES DEPARTMENT OF THE INTERIOR  
BUREAU OF MINES

by

Woodward-Clyde Consultants  
4000 West Chapman Avenue  
Orange, California 92668



Bureau of Mines Open File Report 41-80

FINAL REPORT

on

Contract No. J0275030  
Criteria for Proximity of Surface Blasting  
to Underground Mines

#### DISCLAIMER

The views and conclusions contained in this document are those of the authors and should not be interpreted as necessarily representing the official policies or recommendations of the Interior Department's Bureau of Mines or of the U.S. Government.

Reference to specific brands, equipment, or trade names in this report is made to facilitate understanding and does not imply endorsement by the Bureau of Mines.

## FORWARD

This report was prepared by Woodward-Clyde Consultants, Orange, California under USBM Contract number J0275030. The contract was initiated under the Coal Mine Health and Safety Program. It was administered under the technical direction of the Denver Mining Research Center (DMRC) with Mr. Robert Munson acting as Technical Project Officer. Mr. William Battle was the Contract Administrator for the Bureau of Mines. This report is a summary of work recently completed as a part of this contract during the period September 1977 to April 1979. This report was submitted on 1 November 1979.

The underground monitoring program was designed by the DMRC. The instrumentation for measuring and recording underground vibrations was furnished and installed by the Bureau of Mines.

The technical assistance and cooperation of Mr. Munson and other scientists of the DMRC in the conduct of this investigation is gratefully acknowledged. Mr. Lewis Oriard was a consultant to Woodward-Clyde Consultants for this project. His advice and direction were essential to this report.

No reference to patentable features is made herein.



## CONTENTS

	<u>Page</u>
1.0 INTRODUCTION.....	10
1.1 Background.....	10
1.2 Scope of Work.....	11
1.3 Limitations of this Study.....	12
1.4 Related Studies.....	12
2.0 DESCRIPTION OF THE TEST SITE AND MINING OPERATIONS.....	15
2.1 Physiography and Geology.....	15
2.2 Mining Operations.....	15
3.0 INSTRUMENTATION AND MONITORING PROCEDURES.....	23
3.1 Instrumental Recording Program.....	23
3.1.1 Recording Vibrations in the Underground Mine.....	25
3.1.2 Recording Vibrations at the Surface.....	27
3.1.3 Other Vibration Recording.....	29
3.1.4 Convergence Recording.....	29
3.2 Documentation.....	30
3.2.1 Blast Parameters.....	30
3.2.2 Mine Inspection.....	30
4.0 DATA REDUCTION AND STATISTICAL ANALYSIS.....	33
4.1 Vibration Data Reduction.....	33
4.1.1 Reduction of Underground Data.....	33

CONTENTS (continued)

	<u>Page</u>
4.1.2 Reduction of Surface Data.....	38
4.2 Selection of Appropriate Scaling Factors.....	38
4.2.1 Background.....	38
4.2.2 Direct Statistical Analysis.....	40
4.2.3 Range of Regression Coefficients.....	41
4.3 Conventional Presentation of the Data.....	44
5.0 DISCUSSION OF VIBRATION ANALYSIS.....	51
5.1 Propagation Equations for Underground Roof Vibrations.....	51
5.2 Relationship between Floor and Roof Vibrations.....	51
5.3 Relationship between Surface and Roof Vibrations.....	53
6.0 INDICATIONS OF PHYSICAL CHANGES IN THE UNDERGROUND MINE.....	59
6.1 Roof Falls.....	59
6.2 Convergence Measurements.....	60
6.3 Borescope Survey.....	60
6.4 Background Vibration Recording.....	61
6.5 Likelihood of Major Damage.....	61
6.5.1 Crushing, Confined Fracturing and Free Surface Fracturing.....	62
6.5.2 Addition of Dynamic Stresses.....	64
7.0 SUMMARY: OBSERVATIONS AND CONCLUSIONS.....	65

CONTENTS (continued)

	<u>Page</u>
8.0 RECOMMENDATIONS.....	67
8.1 Additional Tests at Jenny Mine.....	67
8.2 Tests at Additional Sites.....	69
8.3 Development of a Model.....	70
REFERENCES.....	71
APPENDIX A - Blast Documentation.....	74
APPENDIX B - Underground Vibration Recording Data.....	88
APPENDIX C - Convergence Measurements.....	95





LIST OF FIGURES

FIGURE		Page
1.	Topographic map showing location and physiographic setting of Jenny mine site.....	16
2	Plan of test site.....	17
3.	Photograph of entrance to Jenny mine.....	18
4.	Cross section through south end of test site illustrating topography and geology.....	19
5.	Location of overburden blasts.....	21
6.	Location of binder blasts.....	22
7.	Plan of test site showing vibration sensor locations.....	24
8.	Photograph of underground instrumentation installation.....	26
9.	Tracings of underground and surface vibration records for blast 6.....	28
10.	Portion of convergence meter record with field and editorial annotation.....	31
11.	Underground roof peak particle velocity versus cube root scaled distance.....	48
12.	Underground floor peak particle velocity versus square root scaled distance.....	49

LIST OF FIGURES (Continued)

FIGURE	Page
13. Maximum peak particle velocity of the three components measured at the surface versus square root scaled distance.....	50
14. Comparison of vibration data from the Jenny mine roof with that collected by Olsen from production blasting monitored in an adjacent underground opening.....	52
15. Data and 95% confidence limits for roof and floor vibration measurements plotted versus square root scaled distance.....	54
16. Distance versus charge weight relationships for peak particle velocity values predicted by regression lines derived from roof and floor data versus square root scaled distance.....	55
17. Roof and surface velocities versus square root scaled distance showing relationships to compilations of previous workers.....	56
18. Distance versus charge weight relationships for peak particle velocity values predicted by regression lines derived from roof and surface data versus square root scaled distance.....	58
A-1. Layout of blasts 1,2,3, and 4.....	76
A-2. Layout of blasts 5,6, and 7.....	77
A-3. Layout of blasts 8 and 9.....	78

LIST OF FIGURES (Continued)

FIGURES	Page
A-4. Layout of blasts 10,11, and 12.....	79
A-5. Layout of blasts 13,14, and 15.....	80
A-6. Layout of blasts 16 and 17.....	81
A-7. Layout of blasts 18,19, and 20.....	82
A-8. Layout of blasts 21,22, and 23.....	83
A-9. Layout of blasts 24 and 25.....	84
A-10. Layout of blasts 26,27A, and 27B.....	85
A-11. Layout of blasts 28 and 29.....	86
A-12. Layout of blast 30.....	87
C-1. Convergence meter deflections, 12 to 30 September, 1977.....	97
C-2. Convergence meter deflections, 1 to 19 October, 1977.....	98
C-3. Convergence meter deflections, 20 October to 12 November, 1977.....	99



LIST OF TABLES

TABLE	Page
1. Data for vibrations recorded underground.....	34
2. Data for the vibrations recorded on the ground surface.....	36
3. Multiple linear regression results.....	42
4. Limits of regression coefficients at the 95% confidence level calculated by non-linear regression.....	43
5. Simple linear regression results.....	45
6. Comparison of correlation coefficients with respect to scaling factors.....	47
A1 Blast data summary.....	75
B1 Sensitivity of underground sensors.....	89
B2 Record-reproduce system calibration factor.....	90
B3 Underground recording information.....	91
C1 Convergence measurements made with modified Philadelphia surveyors rod.....	96



UNDERGROUND VIBRATIONS FROM SURFACE  
BLASTING AT JENNY MINE, KENTUCKY

1.0 INTRODUCTION

1.1 Background

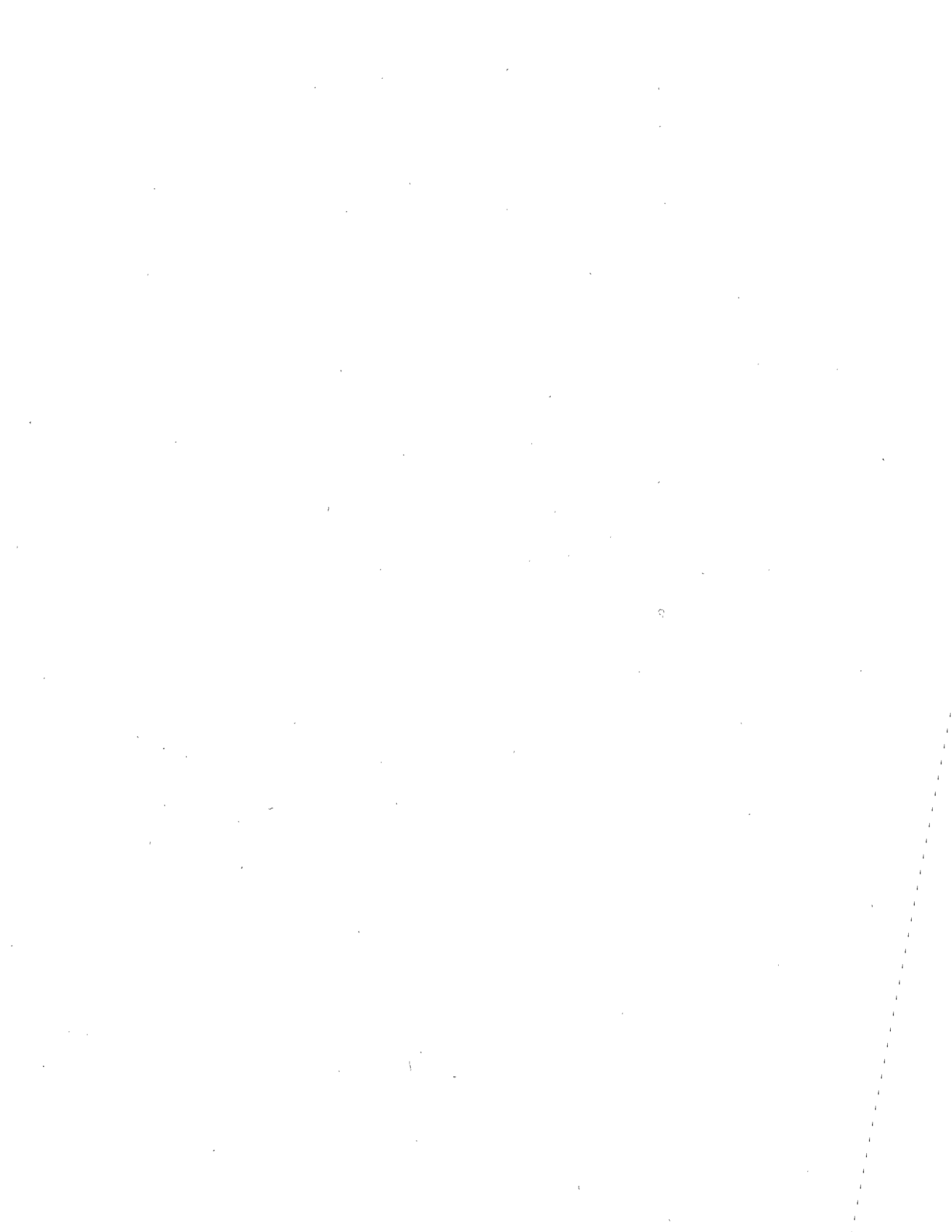
It is a common practice in mining and civil construction to conduct blasting operations in close proximity to underground openings. Underground powerhouses are composed of a number of openings in close proximity to one another which require blasting for excavation. Many mines are developed in a similar manner. Such blasting operations develop a useful background of experience for assessing blasting effects on underground openings. Individuals and organizations may develop considerable experience and skill in predicting blasting effects, but this experience is not passed on to the profession in general unless there is documentation of the physical conditions present at the time of blasting, and the character and intensity of the vibrations are reported.

The U.S. Bureau of Mines, Denver Mining Research Center, is engaged in a research program to document information of this type and in particular to determine suitable criteria for proximity of surface blasting to underground mines. This research has important implications for coal production and operations safety in areas where strip mining is being conducted above or adjacent to existing underground mines. The results of this research may also be applicable to urban blasting projects in the vicinity of subways, drainage channels, and utility tunnels, and construction demolition blasting in the vicinity of dams or tunnels.

The specific objects of the Bureau of Mines research program are:

To establish reliable damage criteria by quantifying the relationship between the level of underground vibrations and damage produced in a mine or underground structure.

To establish the propagation relations for underground vibrations originating from surface blasting so that it is possible to estimate the characteristics of underground vibrations which will occur from a specified blast.





In the fall of 1977 a strip mining operation was conducted above the Jenny mine near Inez, Kentucky. The Jenny mine was under consideration as a demonstration facility for the Bureau of Mines and the blasting for the surface mining operation provided a unique opportunity to collect data relevant to the research program.

This report presents the results of the vibration monitoring and physical observations conducted at the Jenny mine during the surface blasting operations. The data collection, analysis, and subsequent report represent a cooperative effort between Woodward-Clyde Consultants and the U.S. Bureau of Mines, Denver Mining Research Center.

## 1.2 Scope of Work

The purpose of the Jenny mine study was to collect data which would be relevant to the research program for establishing safe operating distances between surface blasting and underground mines. The specific work tasks included:

Recording blast-induced vibrations at three locations in the underground mine. Roof and floor vibrations at all three locations were recorded from 20 of the 31 blasts which occurred. Partial records were collected from 8 additional blasts.

Recording surface vibrations from the blasts in order to investigate the relationship between surface and underground vibrations. Surface vibration measurements were made at one or more locations for 26 blasts.

Direct observation of the mine to identify any immediate damage resulting from the surface blasting.

Making additional measurements and observations which might prove useful to the investigation. These studies included background vibration monitoring, installation of vibration sensors in deep boreholes, measurement of deflections between the roof and floor, and borescope observations of roof strata.

Analysis of the vibration data to identify the empirical relationships between measured vibrations and blast parameters.

Developing recommendations for future studies aimed at establishing blasting proximity criteria.

### 1.3 Limitations of this Study

Although the underground mine was being considered by the Bureau of Mines as a demonstration facility the scope of the investigation was partially restricted due to operating limitations.

Blasting parameters were determined by the surface mine operator. Therefore, the blasts were designed and scheduled to be consistent with efficient strip mining procedures and were not part of the research program design. No visible damage which could be directly attributed to the levels of blasting employed in the strip mining operation was observed. Therefore, correlations between vibration characteristics and damage could not be made.

Access to the site was not available prior to the start of surface mining so that pre-blast monitoring of "routine" failures in the mine could not be accomplished. Without baseline data, potential long range effects of the surface blasting are difficult to identify.

Regression lines that relate vibration levels to distance and charge weights are derived in this report. These data were collected under somewhat uncontrolled field conditions at only one mine. However, the data fall very well within the bounds of previous experience. The data were obtained from a relatively limited range of scaled distances, a factor which often results in distorting regression lines when compared to lines which would be obtained from a larger data bank. Although these data appear to show significant relationships at the Jenny mine, caution should be used in attempting to apply these results elsewhere.

Recommendations are made regarding additional investigations which may eventually lead to the use of the present findings under more general circumstances.

### 1.4 Related Studies

A large number of studies have been conducted on the effects of vibrations generated from blasting. The

studied blasts range from laboratory experiments to full scale nuclear explosions. The topics have included efficiency of explosive products, blasting techniques, behavior of earth and structural materials, energy propagation and damage from vibrations.

Previous studies have shown that theoretical considerations alone are not sufficient for the development of an accurate model for prediction of vibration levels and associated damage. Therefore, the subject of damage potential has been approached primarily from an empirical viewpoint.

None of the published studies referenced in this report have taken place under conditions of geology and blasting geometry which were similar to those found at Jenny Mine. The previous studies do, however, provide the perspective and scientific approach used in this study.

Procedures and instrumentation used in this study for monitoring and analyzing blast vibrations are based on studies conducted by the Bureau of Mines and others over the past 20 years. A comprehensive analysis and review of these studies is presented by Nicholls (12)<sup>1</sup> in a report dealing with potential damage to surface structures from near-surface blasting. His data included quarry blasting measurements by Devine (6) and others gathered over a period of several years. He also presented charge weight and distance criteria for blasting in the vicinity of surface structures in order to avoid damage.

The form of the propagation equation used by Nicholls and previous workers is used in this report for expressing the relationship among peak particle velocity (V), maximum delay charge weight (W), and distance (D). This equation is:

$$V = K (D/W^\alpha)^\beta$$

Nicholls determined that a value of 1/2 for the scaling exponent,  $\alpha$  was sufficient for grouping the data for his

(1) Underlined numbers in parentheses refer to entries in the reference section at the end of the report.

application. Several researchers have noted that the constants  $K$  and  $\beta$  vary widely among different sites. Oriard (18) has further noted that there is an additional influence from other factors including spatial distribution and confinement of the charge, explosive type, sequence of initiation, and geologic conditions.

Since publication of Nicholl's report, several other authors, including Olson (14,15,16) and Siskind (21) have investigated the application of these principles in other situations. They have found not only that  $K$  and  $\beta$  change for each application, but that for some studies of underground explosions a value of  $1/3$  for the scaling exponent results in a better grouping of the data.

Reference to these and other reports are made as part of discussions in later portions of the text.

## 2.0 DESCRIPTION OF THE TEST SITE AND MINING OPERATIONS

### 2.1 Physiography and Geology

The Jenny mine is located in the Appalachian Mountains of eastern Kentucky, approximately 15 miles southwest of the town of Inez. The terrain is hilly with moderate to steep slopes as illustrated on Figure 1. The strip mine site encompassed a north trending ridge which had maximum natural slopes on the order of 1:1. The original ridge top was at an elevation of 1290 ft. Stream valleys both northwest and southeast of the site are at an elevation of 750 ft.

Figure 2 is a sketch plan of the site showing the relationship of the underground mine to the uppermost coal seam which was removed by strip mining. The photograph in Figure 3 illustrates the vertical separation between the underground mine and the surface mining operations.

At Jenny mine the Appalachian coal measures are of Pennsylvanian age and consist of interbedded sandstones, shales and bituminous coal beds. Figure 4 is a cross section showing the generalized stratigraphy at the project site. The strata are nearly flat lying and can be traced from one hill to the next with only small changes in elevation and thickness. The Jenny mine follows the lowest coal seam exposed in the area which is the nominally 5 ft thick Stockton seam at an elevation of about 1000 ft. Above the Stockton is 140 to 150 ft of thinly bedded sandstones and shales with minor coal streaks.

The other two coal seams exposed at the site, the Clarion at about elevation 1150 and the 5-block at an elevation 1180, were removed during stripping operations described in Section 2.2. The lower seam averaged about 4 ft thick; the upper seam, about 8 ft. The seams were separated by strata described as fire clay and sandy shale. The overburden above the 5-block seam was predominantly massive sandstone.

### 2.2 Mining Operations

The underground mine was driven into the Stockton seam from the south end of the ridge during 1974 and 1975. Room and pillar workings extend about 1800 ft into the hill. During the period of this study, the Jenny mine was under lease to the Bureau of Mines and was maintained by a small staff of miners.

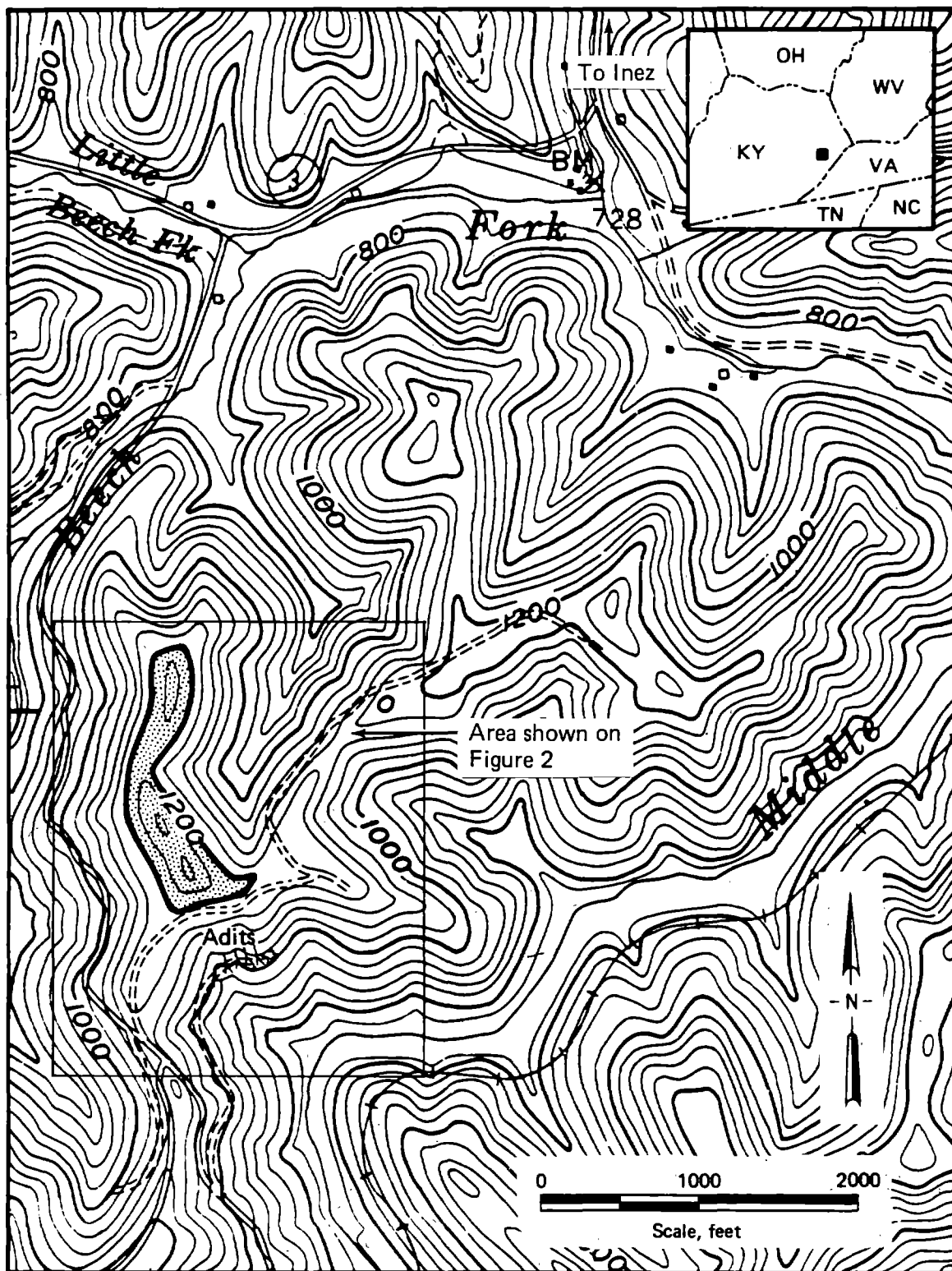


FIGURE 1.—Topographic map showing location and physiographic setting of Jenny mine site.

Dark outline is approximate limit of 5-block coal seam at the site. Adits to the underground mine are also shown. From U.S.G.S. Inez 7½ minute quadrangle, 1954, revised 1978.

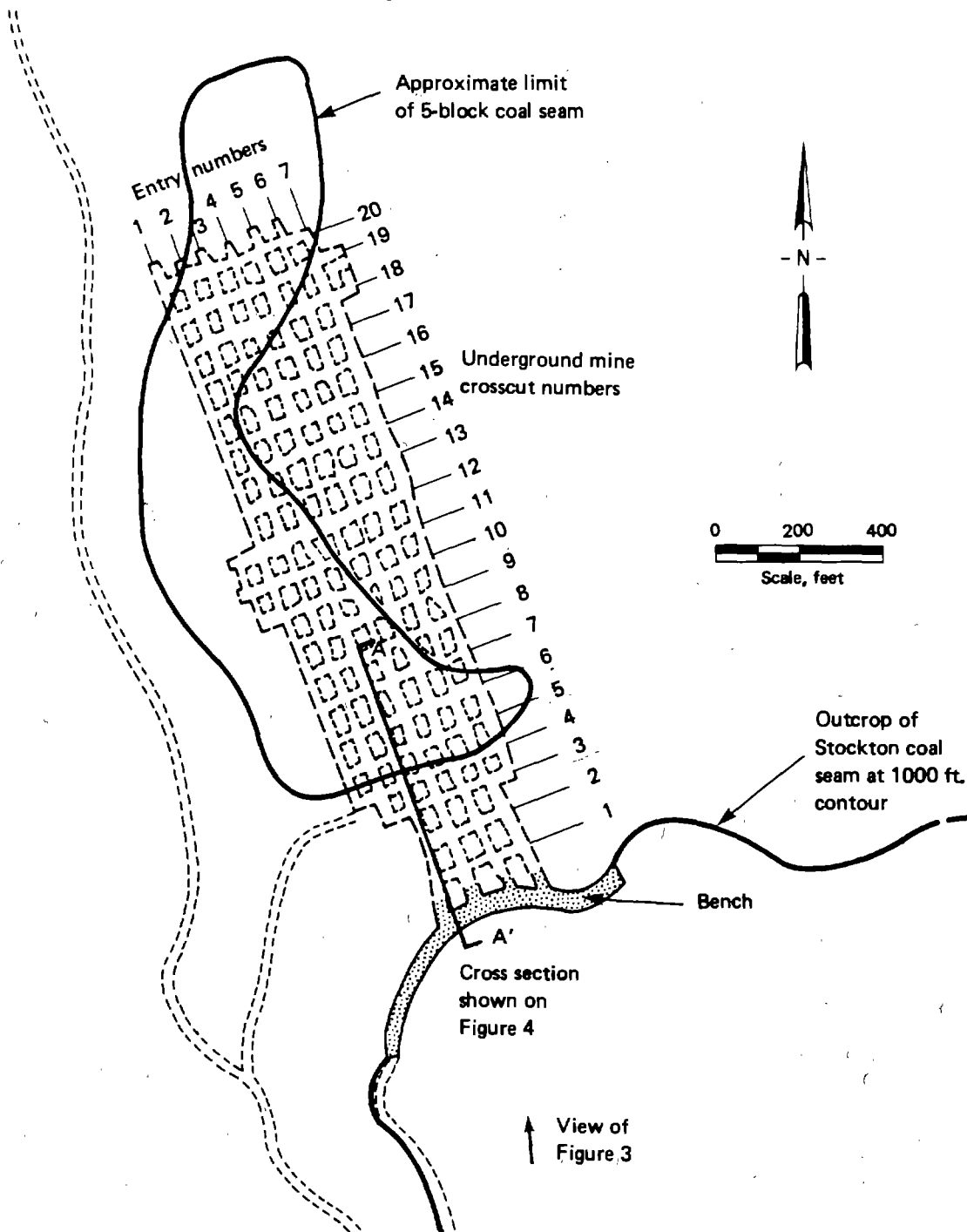
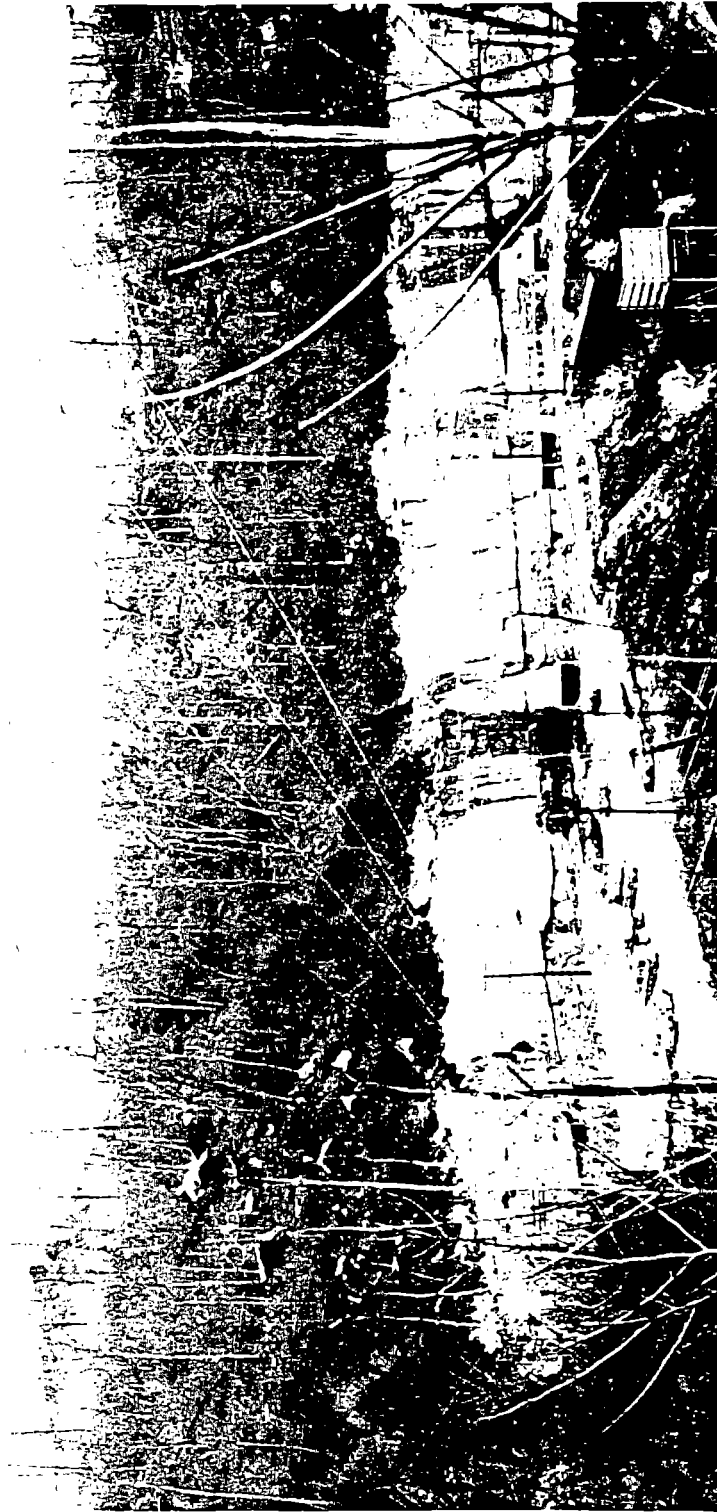


FIGURE 2.—Plan of test site.

The location of the underground mine is related to features shown on Figure 1. Reference locations for Figures 3 and 4 are also shown.



**FIGURE 3.—**Photograph of entrance to Jenny mine.

Three adits appear to the right of the trailer. At the time the picture was taken strip mining operations had removed approximately 50 feet of overburden from the hill above the mine.



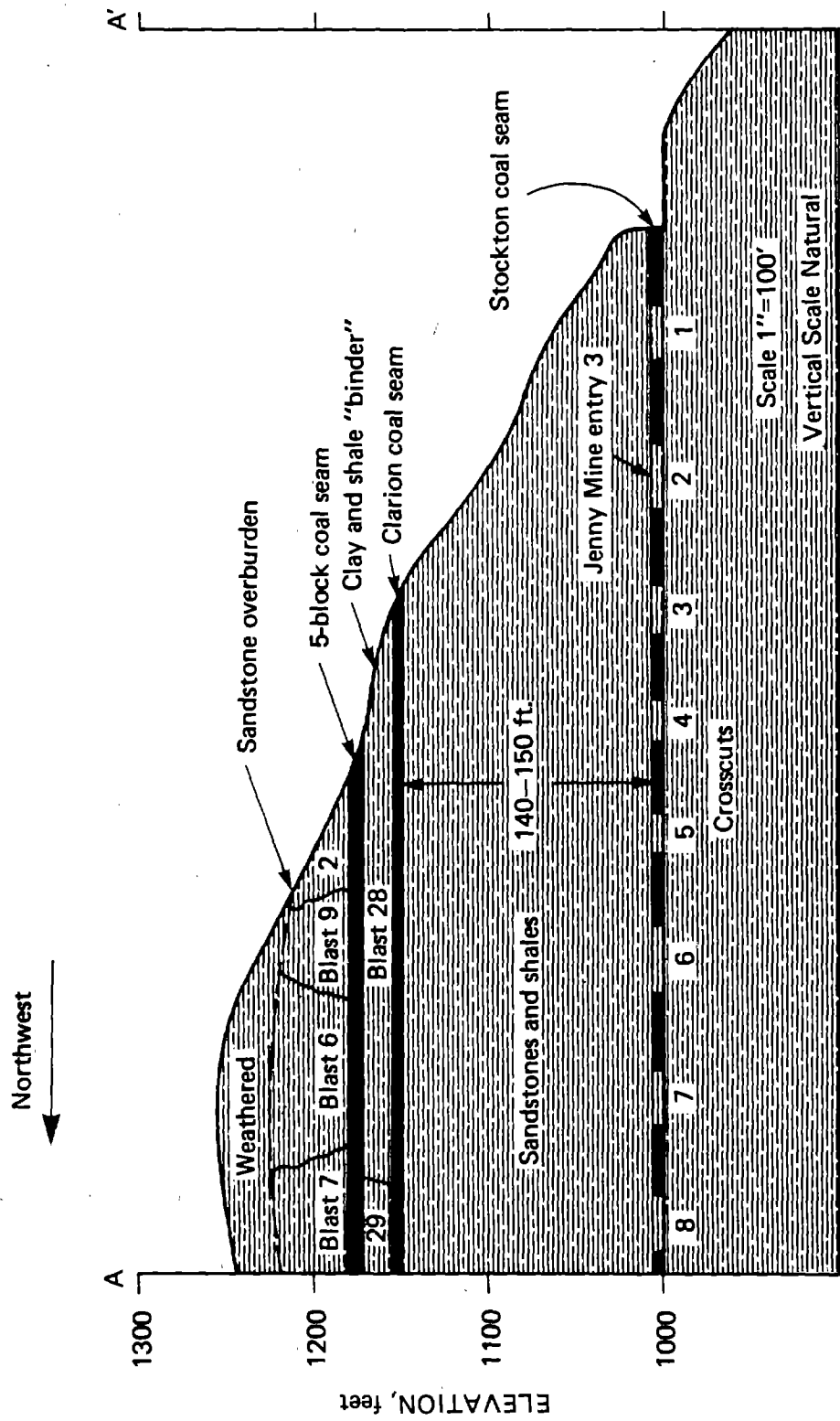


FIGURE 4.—Cross section through south end of test site illustrating topography and geology.

Surface mining operations consisted of blasting and removal of the overburden, excavation of the 5-block seam, blasting and removal of the shale "binder", and excavation of the Clarion seam. Blasting was not required to loosen the coal which was removed by front loader.

The relative locations of 6 of the blasts at the south end of the site are shown on Figure 4. The uppermost portion of the overburden was weathered sufficiently to be removed without blasting.

Figure 5 shows the approximate locations of blasts in the overburden. Holes for these shots ranged from 20 to 40 ft deep and were loaded with 100 to 400 lbs of explosives in each hole. Blasts in the shale "binder" between the coal seams are outlined on Figure 6. These blasts were shallower, from 10 to 15 ft deep, and were loaded with 8 to 25 lbs per hole. Details of the charge weights, location and layouts of the 31 blasts which took place during the monitoring period are included in Appendix A.

Total charge weights for the individual blasts ranged from 1,250 to 51,400 pounds of prilled ammonium nitrate and fuel oil. Each hole was primed with a stick of 60% dynamite and initiated with primacord. Primacord delays of 9, 17, and 25 milliseconds were used to divide most of the blasts into smaller parts. As many as 19 delays but more commonly from 3 to 10 delays were incorporated into most of the blasts. Some shots were designed without delays. The maximum charge weights designed to detonate within a delay period ranged from 276 to 12,400 pounds.

Shot holes were drilled by using 6 in. drills. The holes were 10 to 40 ft deep. Holes approaching a coal seam were generally stopped about 2 ft above it. The arrangement of holes was dictated by existing topography resulting at times in irregular and expansive arrays. Where possible, holes were drilled on 10 to 12 ft centers.

The design and timing of the blasting was solely under the control of the mining company and proceeded in accordance with efficient surface mining operations. The frequency of the blasts was accelerated from the planned one or two per week to as many as two per day. The blasting period, which was to have extended over four to six months, was terminated after less than two months. The monitoring team did not direct or otherwise influence the operations.

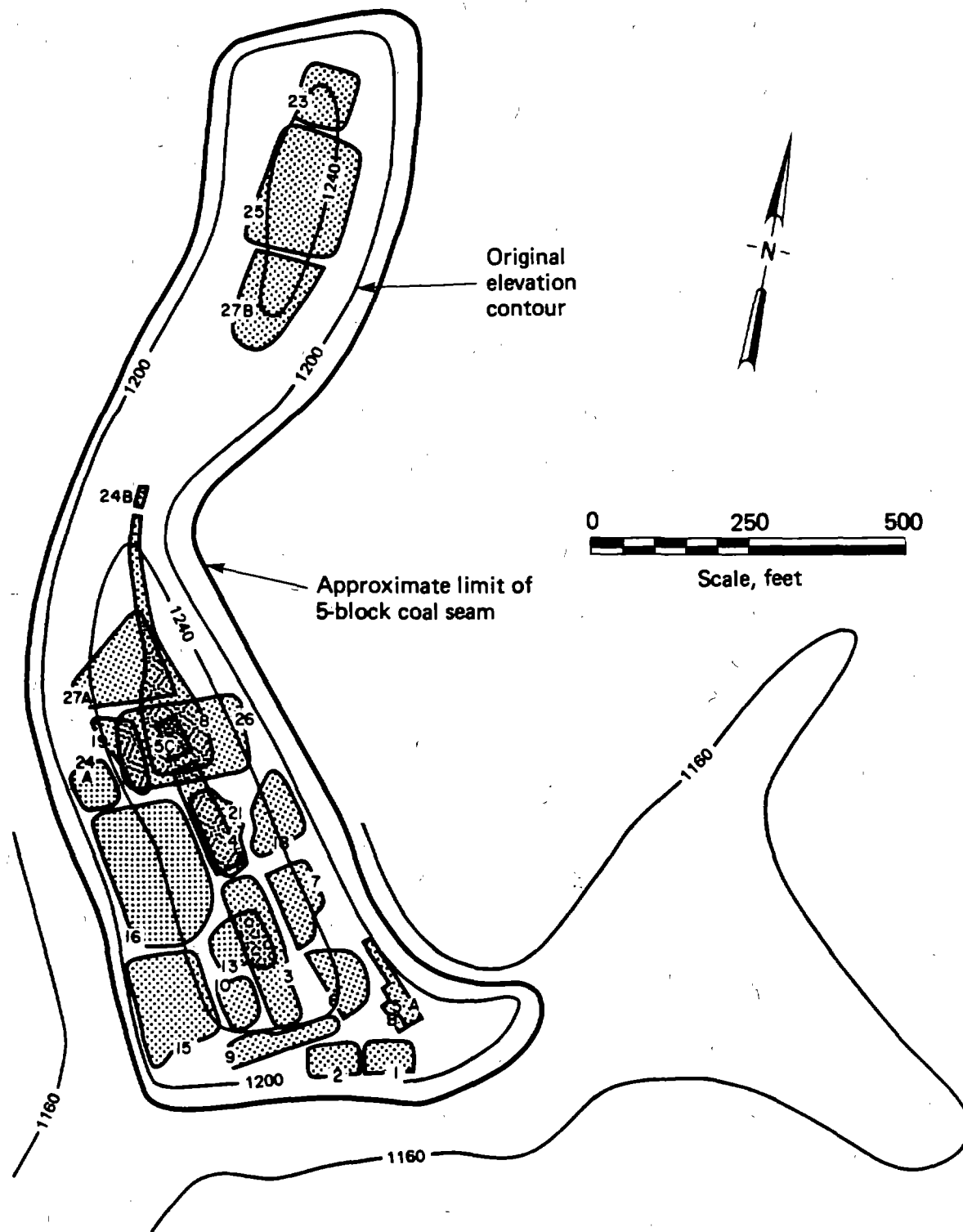


FIGURE 5.—Location of overburden blasts.

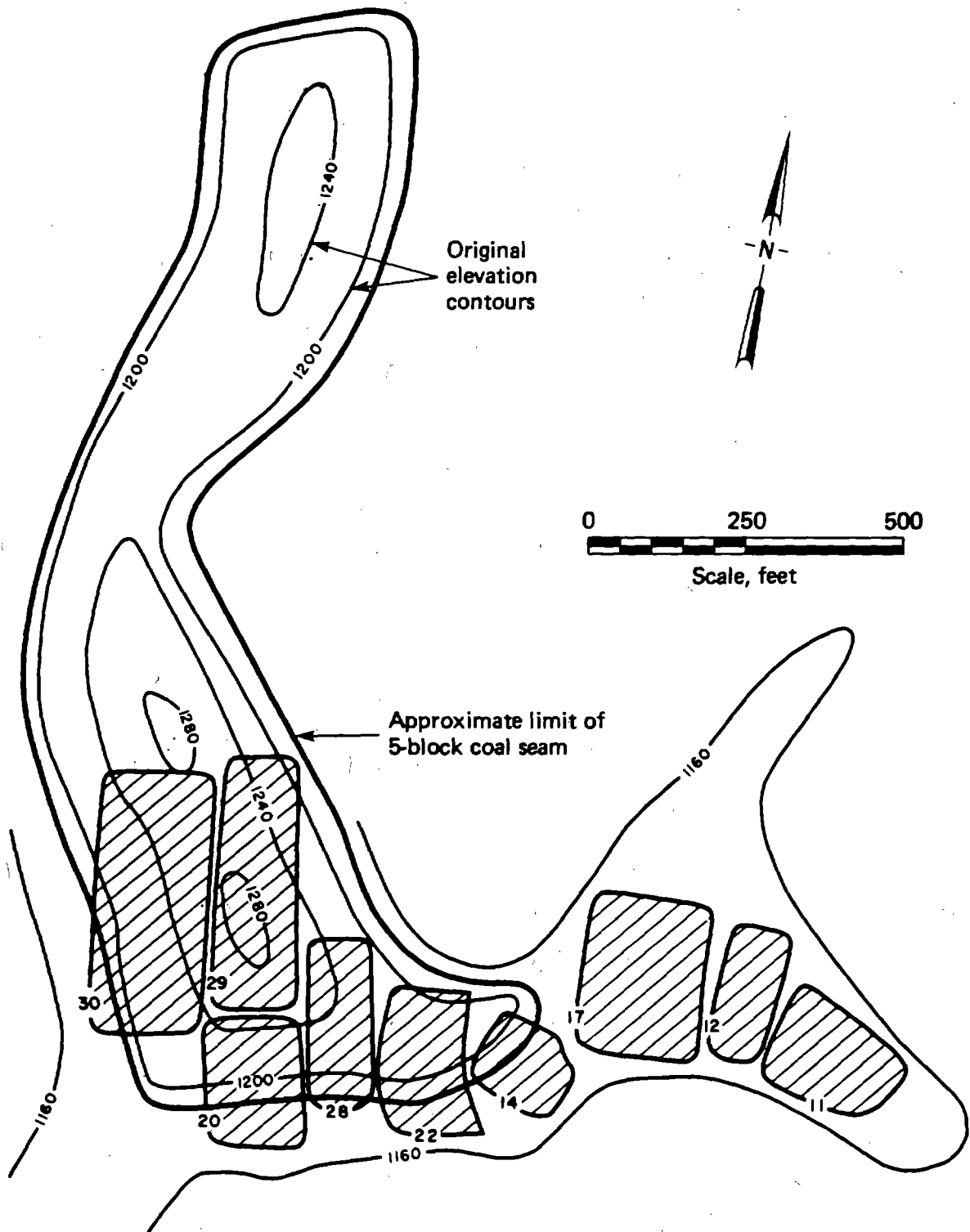


FIGURE 6.—Location of binder blasts.

Elevation contour at 1160 feet shows the approximate limit of the Clarion coal seam.

### 3.0 INSTRUMENTATION AND MONITORING PROCEDURES

The study at Jenny mine is one of the first unclassified programs to specifically monitor the effects of surface blasting on an underground opening. As originally designed, the monitoring program would provide data on both the short term and long term effects of the surface blasting program. Because of the lack of control over the specific geometry of blast location in relation to the structure, it was also an objective of this study to document as many variables as possible in relation to blast design, sensor location, local geology and instrumentation. This data will be useful for identifying anomalous values or situations to future workers who may utilize or expand upon the data base provided by the Jenny mine study.

This section describes instrumentation and field methods used to obtain and document vibration, damage and blast design data. Section 3.1 describes instrumentation and Section 3.2 discusses documentation procedures including measurement of blast parameters and mine inspection reports.

#### 3.1 Instrumental Recording Program

The instrumental recording program was designed to provide data on the underground and surface vibrations resulting from the blasting, background vibrations from other sources and changes in the mine roof height. The location of the sensors is shown on Figure 7. The underground monitoring program was designed by the DMRC. The instrumentation for measuring and recording underground vibrations was furnished and installed by the Bureau of Mines.

Vertical vibration sensors were installed on the roof and floor of the mine at three locations: entry 5, crosscut 6; entry 5, crosscut 11; and entry 3, crosscut 18. A comparison of Figures 5 and 6 with Figure 7 shows the location of each blast with respect to the sensors. From the standpoint of potential damage to the mine, roof vibration levels were the critical parameter to be monitored. Floor vibrations were monitored to identify their scaling law and to investigate the use of floor measurements to estimate roof vibration levels and potential damage.

Surface vibrations were monitored using three three-axis engineering seismometers. Sites S3, S4 and S5 (Figure 7)

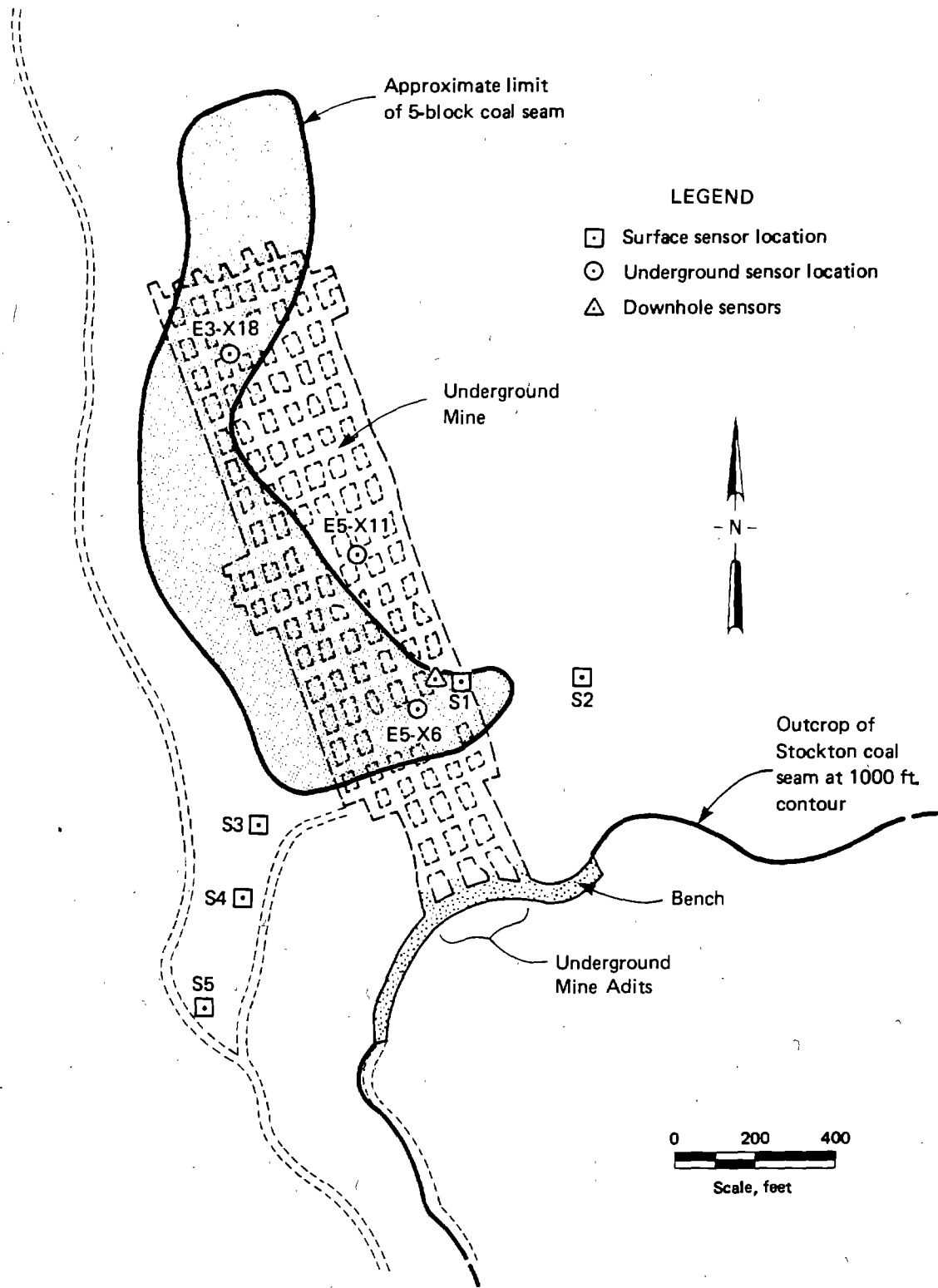


FIGURE 7.—Plan of test site showing vibration sensor locations.

were used for the majority of the blasts. Surface vibrations were measured for comparison with the existing data base and scaling laws in order to identify any anomalous local site conditions. Also, since surface vibrations may be easier to measure, their use as predictors for roof vibrations was investigated as part of this study.

A continuously recording seismograph was maintained to measure background vibrations resulting from major rockfalls, earthquakes, or nearby blasting. The sensor was placed near the instrument trailer west of the mine adits, Figures 7 and 4. Continuously recording drum type extensometers were installed at the three underground instrument locations. The extensometers were provided to monitor short term changes in roof-floor height resulting from blasting or removal of overburden.

### 3.1.1 Recording Vibrations in the Underground Mine

Vertical vibration sensors were attached to both the roof and the floor at the three locations in the underground mine shown on Figure 7. Holes were drilled in the roof and floor and 1/4 inch expansion bolts were used to secure the sensor base plates. Irregular spaces between base plate and rock were filled with dental plaster. Figure 8 is a photograph of one of the installations.

The seismometers used in the underground monitoring were MB Electronics type 125 transducers furnished by the Bureau of Mines. Before installation, each seismometer was adjusted for optimum response to particle motion in the vertical direction. The seismometers have a nominal basic sensitivity of 93.2 millivolts/inch/second (mv/in/sec). In order to reduce the sensitivity to the levels anticipated for this project, a shunt resistance was introduced into the system as part of an impedance matching preamplifier paired with each sensor. This resulted in output values ranging between 18.25 and 19.50 mv/in/sec for a 100 Hz input. General Radio model 1560-P4 preamplifiers were used with a one-to-one gain. The precise outputs of sensor-preamp pairs used in the mine were determined and are tabulated in Appendix B, Table B1.

The signals were transmitted by a four-conductor shielded cable to a Bureau of Mines recording van located near the mine entrance. At that point, signals from the six seismometers were split and fed into 12 Ithaco model 454 amplifiers and then into a Sangamo 14-channel tape recorder. The output of each sensor was thus recorded at

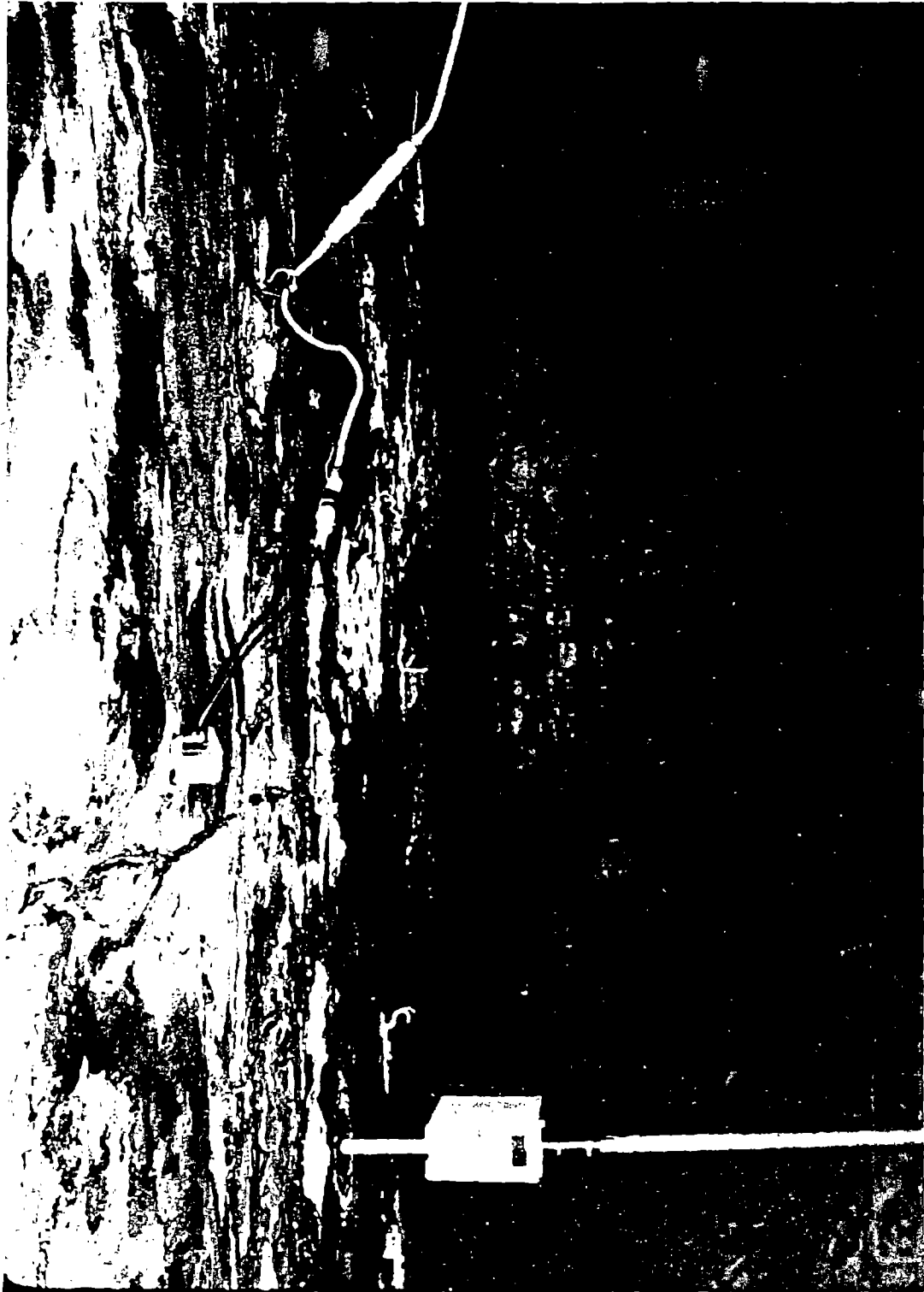


FIGURE 8.—Photograph of underground instrumentation installation. Convergence meter, vibration sensor and paired preamplifier are shown from left to right.



two gain levels. Amplification from -10 to 90 dB in 1 dB increments was available. Record quality was checked in the field by playing the tape back immediately after each blast onto a Honeywell Visacorder galvanometric oscillograph. Final hard copies for analysis were made on a Bureau of Mines fiberoptic device in Denver. An illustration of a fiber-optic record is included on Figure 9.

A time-break contactor was buried with the detonator in a zero-delay shot hole for each blast. This provided a precise start time which was input with a WWVB timing signal onto Channel 14 of the Sangamo Recorder.

To provide a calibration reference, a standard 100 mV rms sine wave was input into each Ithaco amplifier set at 20 db and then onto the corresponding Sangamo channel. Small gain differences in recording and playback were therefore be accounted for during data reduction. The calibration factors derived from these recordings are tabulated in Appendix B, Table B2.

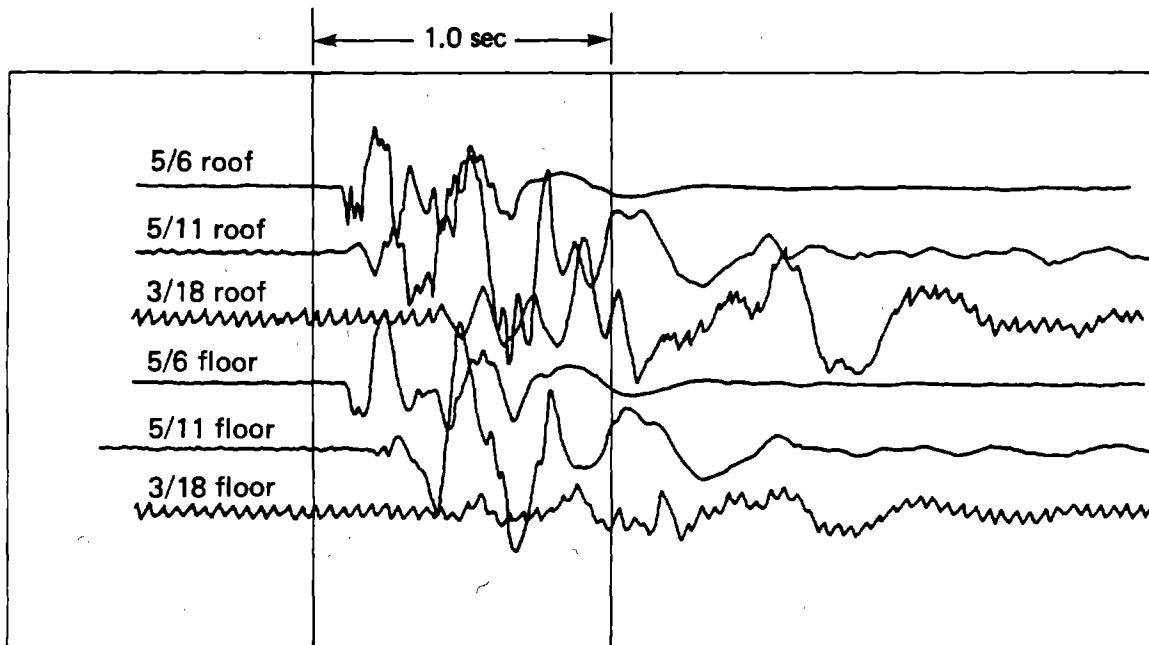
Information on sensor-preamp combinations, record and reproduce channels, gain settings and resulting trace amplitudes for each record is tabulated in Appendix B, Table B3.

### 3.1.2 Recording Vibrations at the Surface

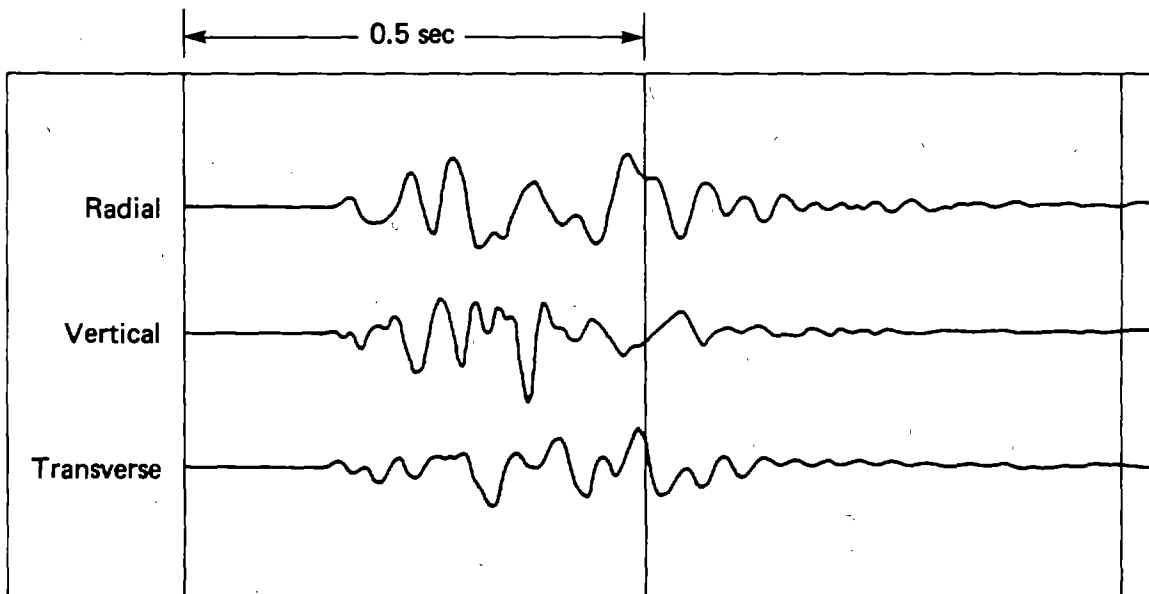
Five surface vibration monitoring stations were established at the sites shown on Figure 7. Stations S1 and S2 were used only for the first two blasts because of interference with mining operations.

Three portable Sprengnether engineering seismographs, model VS-1100, were employed for vibration monitoring at the ground surface. They have a flat response to particle velocities (+3 db) at all gain levels for a frequency range between 2.0 and 200 Hz. The seismographs utilize three orthogonal transducers. Each transducer has a natural frequency of 2 Hz and an inertial mass of 0.5 kilograms. The seismometer cube has a density of 1.6 gm/cc for impedance coupling with average soil.

A four-trace record is produced by the VS-1100 on direct-write linagraph paper. One trace is normally reserved for event marking or air blast monitoring but was unused in this application. The transverse, radial and vertical components of particle velocity were recorded. The seismographs were moved from storage to fixed recording locations where they were set up, and tested before each



Underground sensors - gains vary



Surface location S4 - gain 0.2 in/ips

FIGURE 9.—Tracings of underground and surface vibration records for blast 6.

blast. The radial seismometer was oriented toward the approximate center of the blast. Operation of the instruments was by remote control with the sensitivity preset usually at the least sensitive scale, 0.2 in/in/sec. Peak amplitudes were read from the records following each blast. An example record is shown on Figure 9.

### 3.1.3 Other Vibration Recording

Two other vibration recording systems were used during the monitoring period. A continuously recording seismograph was maintained to measure background vibration levels and to determine the time of occurrence of large rockfalls in the mine should they have occurred. The second system, a downhole array, was implaced only for the final two blasts.

The continuously recording seismograph system consisted of a Sprengnether MEQ-800 drum recorder and a Geospace model HS-10-1 seismometer. The seismometer has a natural frequency of 1 Hz, a flat frequency response above 4 Hz, and is designed to detect distant or low frequency local seismic events.

The sensor was installed near the instrumentation trailer shown in Figure 3. During blast recording, the seismometer was disconnected from the drum recorder to avoid pegging and its output was recorded on a channel of the Sangamo recorder.

The location of the downhole array, is shown on Figure 7. It consisted of two CEC model 4-102-A transducers and a Sprengnether seismograph. The transducers were at depths of 23 and 43 ft. The downhole array was originally intended for study of vibration attenuation versus depth. Only two blasts occurred after implacement of the array, and the gain settings on the recorder were incorrect. The blasting program was abruptly terminated without advance notice, and intended adjustments and further recordings could not be made.

### 3.1.4 Convergence Recording

Continuously recording drum type extensometers, manufactured by Terrametrics, were installed at the three underground mine vibration sensor locations shown on Figure 7. The instruments were mounted on segments of a vertical support leg as shown on Figure 8. The upper portion was anchored in a hole drilled through the

shale at roof level into competent sandstone. The lower portion was attached to the floor in a similar manner. A standard setting provided a twofold gain for the instruments which is reflected on the sample record, Figure 10.

A summary log of these recordings is included in Appendix C.

### 3.2 Documentation

Records were kept of all instrument settings, equipment changes and other items concerned with the recording of vibrations. In addition, information on the location and layout of the blasts and on conditions in the underground mine was gathered and logged. These last two sets of data are discussed below.

#### 3.2.1 Blast Parameters

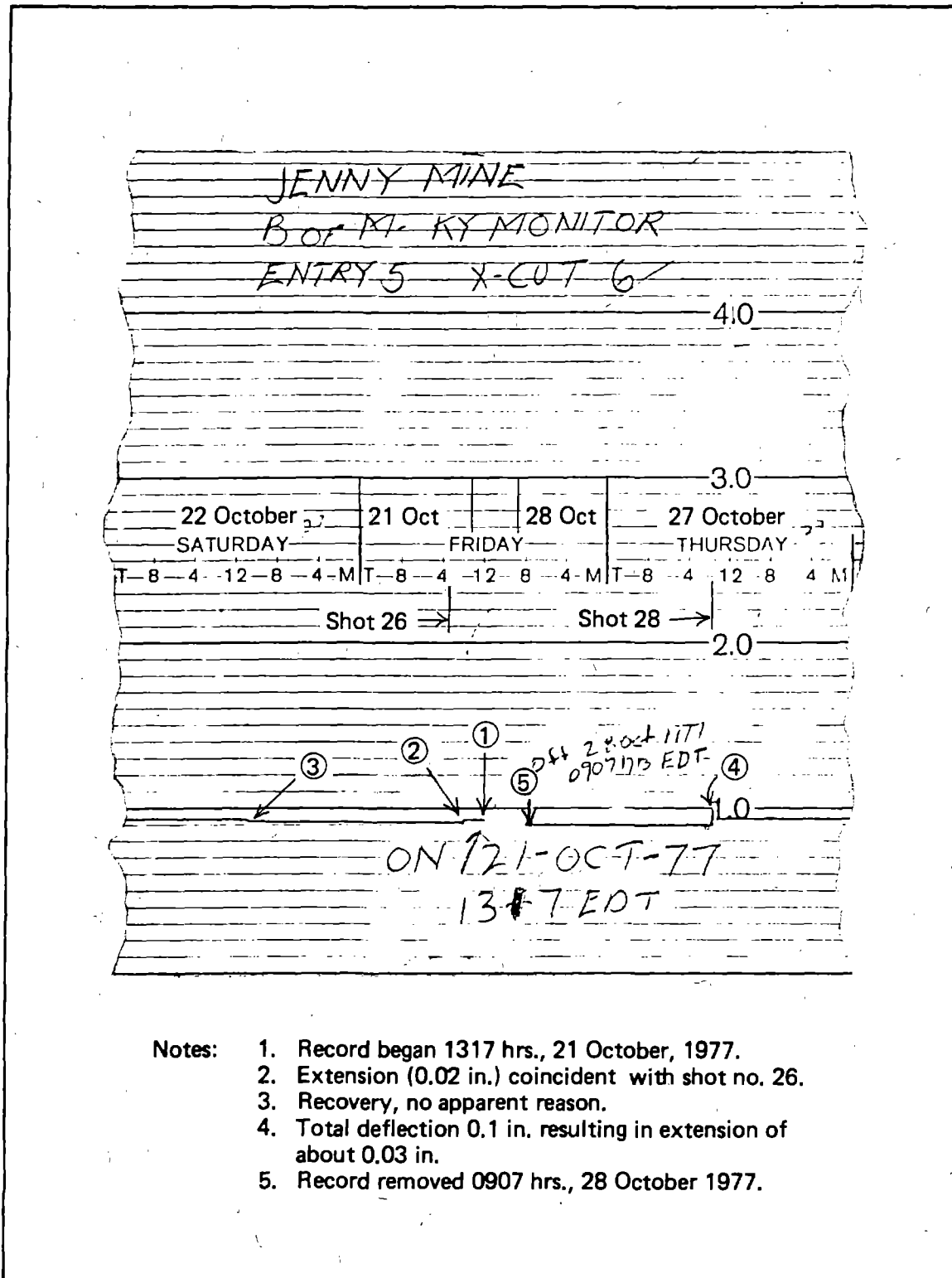
Details of the blasts are presented in Appendix A. Information regarding maximum delay charge weights and distances from vibration sensors are included in the tables in Section 4.1, Data Reduction.

The location and areal extent of each blast was estimated in the field by compass and pace survey and by plotting on a small scale topographic map. This information was refined during later data reduction by reconstructing the blasting sequence from field notes and blast design sketch maps. This procedure also aided in refining elevations estimated in the field. The sketch maps are included in Appendix A.

Particular attention was given in the field to the placement of delays and the number of holes per delay. However, it was not possible to monitor the loading of the holes. The charge weight per hole was based on the blaster's estimate. These figures were combined to provide the maximum charge weights per delay used in the correlations discussed in Section 4.

#### 3.2.2 Mine Inspection

During installation of the underground sensors, the general conditions in the mine were recorded. Periodic inspections were made during the monitoring period. Recent roof falls noted during the inspections or reported by maintenance miners were entered in a daily log.



- Notes:
1. Record began 1317 hrs., 21 October, 1977.
  2. Extension (0.02 in.) coincident with shot no. 26.
  3. Recovery, no apparent reason.
  4. Total deflection 0.1 in. resulting in extension of about 0.03 in.
  5. Record removed 0907 hrs., 28 October 1977.

FIGURE 10.—Portion of convergence meter record with field and editorial annotation.

Near the end of the monitoring period it became apparent that potential damage associated with the levels of vibrations which had been recorded might not be readily apparent. A more rigorous inspection routine was instituted. It consisted of detailed logging of mine entries 3 and 5 on a daily basis and establishment of 23 additional convergence measurement stations.

The convergence stations, located mainly at crosscut intersections in entries 3 and 5, were defined by roof bolts and nails in the floor directly below. Readings using a modified Philadelphia rod were scheduled following each blast. The abrupt termination of the blasting, however, interrupted this program. The limited number of measurements which were obtained are tabulated in Appendix C.

## 4.0 DATA REDUCTION AND STATISTICAL ANALYSIS

### 4.1 Vibration Data Reduction

Peak particle velocities derived from blast vibration recordings described in the previous section are listed on Tables 1 and 2. Charge weight and scaled distance information used in statistical analysis is also included in the tables. This section describes the procedures used for reducing the field records to particle velocities.

#### 4.1.1 Reduction of Underground Data

The peak particle velocities recorded at each of the underground sensors are listed in Table 1. Appendix B contains the necessary data for determining these peak particle velocities from raw field data. Amplitudes measured from the fiber-optic records of the tape-recorded vibration sensor outputs were reduced to peak particle velocity values according to the formula

$$PPV = \frac{A}{S_s \times G_i \times G_r \times C}$$

where PPV = the peak particle velocity in in/sec

A = the maximum zero-to-peak trace amplitude in inches

S<sub>s</sub> = the sensitivity of the sensor-pre-amplifier system in mv/in/sec.

G<sub>i</sub> = the input amplifier-recorder gain.

G<sub>r</sub> = the reproduce system gain.

C = the record-reproduce calibration factor in in/mv.

The sensor-preamp sensitivity was determined by measuring the output of each sensor with a known shunt resistance during shaking at a known level. The sensitivity of the sensors with different preamplifiers was calculated from the different resistances. These sensitivities are tabulated in Table B1, Appendix B.

The calibration factor was determined for each channel by playing a standard calibration signal recorded in the field onto a fiber-optic record at a gain setting of unity. This procedure accounted for the sensitivity of

TABLE 1 - Data for vibrations recorded underground

Shot number	Charge weight <sup>1</sup> lb	Location <sup>2</sup>	Slant distance ft	Scaled distances		Peak particle velocities, ips	
				ft/lb <sup>1/2</sup>	ft/lb <sup>2/3</sup>	Roof	Floor
1...	1,700	( <sup>3</sup> )	—	—	—	—	—
2...	800	5/6	210	7.46	22.7	1.54	—
		5/11	493	17.5	53.2	0.37	—
3...	600	5/6	269	11.0	31.9	0.71	0.49
4...	600	5/6	408	16.7	48.4	0.34	0.24
5...	3,600	5/6	180	3.00	11.7	17.5	2.67
		5/11	416	6.93	27.1	1.12	0.92
6...	1,650	5/6	184	4.54	15.6	9.99	6.20
		5/11	367	9.04	31.1	0.50	0.49
		3/18	947	23.3	80.2	0.14	0.083
7...	12,400	( <sup>3</sup> )	—	—	—	—	—
8...	10,650	( <sup>3</sup> )	—	—	—	—	—
9...	4,600	5/6	216	3.18	13.0	6.26	5.73
		5/11	456	6.74	27.5	0.95	0.78
		3/18	1016	15.0	61.1	0.31	0.42
10..	5,425	5/6	308	4.15	17.5	1.64	1.31
		5/11	457	6.20	26.0	0.83	0.79
		3/18	966	13.1	55.0	0.32	0.33
11..	8,090	5/6	715	7.96	35.7	0.98	0.96
		5/11	912	10.1	45.5	0.56	0.55
		3/18	1408	15.7	70.1	—	0.25
12..	3,095	5/6	589	10.6	40.4	0.72	0.78
		5/11	745	13.4	51.1	0.44	0.57
		3/18	1249	22.5	85.7	—	0.14
13..	2,400	5/6	308	6.29	23.0	1.30	1.10
		5/11	367	7.49	27.4	1.29	1.19
		3/18	859	17.5	64.2	0.34	0.47
14..	2,470	5/6	308	6.21	22.8	2.41	1.98
		5/11	618	12.4	45.8	0.59	0.81
		3/18	1189	23.9	88.0	0.20	0.17
15..	5,250	5/6	375	5.19	21.6	2.40	2.25
		5/11	493	6.82	28.4	1.02	0.92
		3/18	957	13.2	55.1	0.44	0.46
16..	2,600	5/6	493	9.6	35.9	1.60	1.02
		5/11	384	7.54	28.0	2.10	0.93
		3/18	693	13.6	50.4	0.24	0.43
17..	168	5/6	503	38.8	91.1	0.12	0.079
		5/11	657	50.7	119	0.048	0.063
		3/18	1189	91.8	216	—	0.019
18..	3,250	5/6	438	7.69	29.6	1.60	1.31
		5/11	228	4.00	15.4	3.24	1.72
		3/18	674	11.8	45.5	0.47	0.50
19..	5,400	5/6	725	9.87	41.3	0.42	0.35
		5/11	416	5.66	23.7	1.22	0.73
		3/18	572	7.79	32.6	0.62	—
20..	2,445	5/6	266	5.38	19.8	2.88	3.47
		5/11	522	10.6	38.7	0.30	0.26
		3/18	1060	21.5	78.7	0.083	0.10

See footnotes at end of table



TABLE 1 - Data for vibrations recorded  
underground—continued

Shot number	Charge weight <sup>1</sup> lb	Location <sup>2</sup>	Slant distance ft	Scaled distances		Peak particle velocities, ips	
				ft/lb <sup>1/2</sup>	ft/lb <sup>1/3</sup>	Roof	Floor
21..	2,250	5/6	512	10.8	39.1	1.29	0.95
		5/11	292	6.16	22.3	1.51	1.10
		3/18	674	14.2	51.5	1.40	1.22
22..	688	5/6	150	5.7	16.9	2.51	0.93
		5/11	502	19.2	57.0	0.18	0.12
		3/18	1080	41.2	122	—	—
23..	3,000	5/6	1451	26.5	100	0.28	0.16
		5/11	1065	19.4	73.9	0.40	0.38
		3/18	550	10.0	38.2	0.92	0.90
24..	2,200	5/6	684	14.6	52.6	0.62	0.40
		5/11	429	9.16	33.0	0.75	0.60
		3/18	645	13.8	49.6	0.16	0.22
25..	4,600	5/6	1253	18.5	75.3	0.52	0.33
		5/11	868	12.8	52.2	0.71	0.66
		3/18	350	5.16	21.0	2.45	1.76
26..	11,300	5/6	578	5.44	25.8	1.93	1.42
		5/11	316	2.97	14.1	1.87	1.95
		3/18	578	5.44	25.8	1.63	1.21
27A.	6,600	5/6	761	9.37	40.6	1.52	1.27
		5/11	503	6.19	26.8	1.89	1.58
		3/18	475	5.85	25.3	1.64	1.43
27B.	9,000	5/6	1164	12.3	56.0	0.53	0.34
		5/11	751	7.93	36.1	0.74	0.73
		3/18	254	2.68	12.2	3.91	4.47
28..	2,400	5/6	170	3.47	12.7	7.82	4.51
		5/11	455	9.30	34.0	1.33	0.74
		3/18	1011	20.6	75.5	0.22	0.29
29..	276	5/6	283	17.0	44.5	1.44	0.54
		5/11	274	16.5	42.2	0.45	—
		3/18	794	47.8	122	0.061	0.086
30..	801	5/6	390	13.8	42.0	0.86	0.43
		5/11	362	12.8	39.0	0.76	0.36
		3/18	813	28.8	87.6	0.12	0.14

<sup>1</sup> Weight of the largest delay charge.

<sup>2</sup> Locations are designated by entry/crosscut in the underground mine. These are illustrated in Figure 7.

<sup>3</sup> No data recorded.

TABLE 2. - Data for the vibrations recorded  
on the ground surface

Shot number	Charge weight, lb	Location <sup>2</sup>	Slant distance, ft	Scaled distances		Peak particle velocities, ips				
				Ft/lb <sup>1/2</sup>	Ft/lb <sup>1/3</sup>	Vt <sup>3</sup>	Vz <sup>4</sup>	Vr <sup>5</sup>	Vh <sup>6</sup>	Vtot <sup>7</sup>
1...	1,700	( <sup>8</sup> )	--	--	--	--	--	--	--	--
2...	800	S1	230	8.13	24.8	0.60	0.85	1.15	1.30	1.55
		S2	550	19.4	59.2	0.55	0.68	0.70	0.86	0.98
3...	600	S3	351	14.3	41.6	0.35	0.50	0.70	0.78	0.93
		S4	501	20.5	59.5	0.20	0.50	0.30	0.36	0.62
		S5	801	32.7	95.0	0.58	0.36	0.72	0.92	0.99
4...	600	S4	672	27.4	79.7	0.20	0.35	0.22	0.30	0.46
		S5	951	38.8	112	0.21	0.24	0.29	0.36	0.43
5...	3,600	S3	495	8.25	32.3	1.25	1.10	1.70	2.11	2.38
6...	1,650	S3	420	10.3	35.6	1.65	1.10	0.95	1.90	2.01
		S4	540	13.3	45.7	1.45	1.85	1.05	1.79	2.57
7...	12,400	S3	480	4.31	20.7	2.45	1.70	3.40	4.19	4.52
		S4	640	5.75	27.7	1.55	1.95	1.65	2.26	2.99
		S5	930	8.35	40.2	1.15	1.30	1.75	2.09	2.46
8...	10,650	S3	751	7.28	34.1	0.60	1.05	0.75	0.96	1.42
		S4	921	8.93	41.9	1.30	1.00	1.35	1.87	2.12
9...	4,600	( <sup>8</sup> )	--	--	--	--	--	--	--	--
10...	5,425	S3	290	3.94	16.5	1.15	2.35	3.70	3.88	4.53
		S4	450	6.12	25.6	1.95	1.45	2.30	3.02	3.35
11...	8,090	S3	1100	12.2	54.8	1.05	1.00	1.50	1.83	2.09
12...	3,095	( <sup>8</sup> )	--	--	--	--	--	--	--	--
13...	2,400	S3	380	7.76	28.4	1.15	2.00	2.95	3.17	3.74
14...	2,470	S3	670	13.5	49.6	2.60	2.25	1.85	3.19	3.90
15...	5,250	S3	220	3.04	12.7	2.05	4.60	4.20	4.67	6.56
		S4	400	5.53	23.0	2.20	2.00	2.00	2.97	3.58
16...	2,600	S3	400	7.85	29.1	1.15	1.45	1.15	1.62	2.17
		S4	570	11.2	41.5	0.55	0.85	0.85	1.01	1.32
17...	168	S3	950	73.3	172	0.15	0.05	0.10	0.18	0.19
		S4	1030	79.5	186	0.10	0.05	0.15	0.18	0.19
		S5	1330	103	241	0.08	0.05	0.08	0.12	0.13
18...	3,250	S3	580	10.2	39.2	1.70	3.05	4.00	4.34	5.31
19...	5,400	S4	831	11.3	47.3	0.40	0.60	0.40	0.57	0.82
20...	2,445	( <sup>8</sup> )	--	--	--	--	--	--	--	--
21...	2,250	S3	550	11.6	42.0	0.55	0.85	1.85	1.93	2.11
		S4	730	15.4	55.7	0.35	0.85	0.65	0.74	1.13
22...	688	S3	450	17.2	51.0	1.15	0.95	0.50	1.25	1.57
		S4	540	20.6	61.2	1.00	1.00	0.45	1.10	1.48
23...	3,000	S3	1700	31.0	118	0.50	0.35	0.95	0.99	1.05
		S4	1870	34.1	130	0.55	0.25	0.15	0.57	0.62
		S5	2130	38.9	147	0.61	0.29	0.32	0.69	0.75
24...	2,200	S3	580	12.4	44.6	0.25	0.45	0.75	0.79	0.91
		S4	750	16.0	57.7	0.15	0.55	0.45	0.47	0.73
		S5	1000	21.3	76.9	0.45	0.35	0.60	0.75	0.83
25...	4,600	S3	1520	22.4	91.3	0.50	0.45	0.50	0.71	0.84
		S4	1690	24.9	101	0.25	0.45	0.35	0.43	0.62
		S5	1960	28.9	118	0.52	0.39	0.55	0.76	0.85
26...	11,300	( <sup>8</sup> )	--	--	--	--	--	--	--	--

See footnotes at end of table.

TABLE 2. - Data for the vibrations recorded on the ground surface--continued

Shot number	Charge weight, lb	Location <sup>2</sup>	Slant distance, ft	Scaled distances		Peak particle velocities, ips				
				ft/lb <sup>1/2</sup>	f/lb <sup>1/3</sup>	Vt <sup>3</sup>	Vz <sup>4</sup>	Vr <sup>5</sup>	Vh <sup>6</sup>	Vtot <sup>7</sup>
27A.	6,600	S3	750	9.23	40.0	1.35	2.00	3.00	3.29	3.85
		S4	930	11.5	49.6	0.45	1.70	1.10	1.19	2.07
27B.	9,000	S3	1380	14.5	66.3	0.70	0.50	0.70	.99	1.11
		S4	1550	16.3	74.5	0.30	0.45	0.25	0.9	0.60
28..	2,400	S3	400	8.16	29.9	1.25	1.85	1.70	2.11	2.81
		S4	500	10.2	37.3	1.50	0.85	1.15	1.89	2.05
		S5	800	16.3	59.8	0.35	0.40	0.54	0.64	0.77
29..	276	S3	480	28.9	73.7	1.85	1.15	1.80	2.58	2.83
		S4	630	37.9	96.8	0.65	0.50	0.85	1.07	1.18
30..	801	S3	380	13.4	40.9	0.80	1.05	1.10	1.36	1.71
		S4	550	19.4	59.2	0.30	0.30	0.35	0.46	0.55

<sup>1</sup>Weight of largest delay charge.

<sup>2</sup>Locations shown on Figure 7.

<sup>3</sup>Transversely oriented sensor.

<sup>4</sup>Vertically oriented sensor.

<sup>5</sup>Radially oriented sensor.

<sup>6</sup>Vector sum of peak horizontal values.

<sup>7</sup>Vector sum of peak values of all three axes.

<sup>8</sup>No recording.

the fiber-optic unit and also allowed for any small differences between preamplifiers or tape recorder channels. Calibration factors for each channel are listed in Table B2, Appendix B.

The gains included in the formula were logged from instrument settings during recording and playback. Gain settings, sensor-preamp combinations and zero-peak record amplitudes are included on Table B-3 in Appendix B.

#### 4.1.2 Reduction of Surface Data

The Sprengnether seismographs used to measure surface vibrations were factory calibrated. The manufacturer's specifications indicate the peak-to-zero calibration pulse amplitudes are within  $\pm 5\%$ . A calibration pulse is automatically recorded with each set of vibration data to insure that the instrument remains within tolerances.

Reduction of the field records consists of measuring the maximum amplitude of each vibration trace and dividing by the selected sensitivity, usually 0.2 in/sec. Peak particle velocities for each of the three orthogonal directions; radial, vertical, and transverse, are shown in Table 2. Vector sums of the peak horizontal values ( $V_t + V_r$ ) and of the peak values for all three directions ( $V_t + V_z + V_r$ ) have been calculated. The measured surface vibrations result from the additive effects of several different types of waves; compressional, shear, and surface waves. These waves do not travel at the same velocity and the maximum amplitudes recorded in the three orthogonal directions do not occur simultaneously. Therefore, the calculated vector sums may not represent instantaneous values of particle velocity. The vector sum values, however, are commonly used in field applications to represent a conservative upper bound on particle velocity. They are presented here to facilitate comparison of data from the Jenny mine study with previously reported data.

### 4.2 Selection of Appropriate Scaling Factors

#### 4.2.1 Background

It has become generally accepted in the literature that the relationship between vibration levels, distance and charge weight follows the form of the equation:

$$V = K (D/W^\alpha)^\beta$$

where V = the peak particle velocity, in/sec.

D = the distance from the source, ft.

W = the weight of the explosive charge, lbs.

$\alpha$  = the scaling exponent on W.

K = the intercept of the regression line at  $D/W = 1$

$\beta$  = the slope of the regression line.

This equation plots as a straight line on a logarithmic graph and provides a convenient method of estimating vibration levels from distance and charge weight parameters once the values of  $\alpha$ , K and B have been determined.

Once the value of  $\alpha$  has been selected, the values K and  $\beta$  applicable to a particular site are calculated by simple least squares regression of V versus  $D/W^\alpha$ . In previous studies, simple fractions such as 1/2 or 1/3 have been found to be suitable values for the scaling exponent. However, it has not been established in the literature which value is more appropriate for the specific geometry of the Jenny mine study.

Nicholls (12) noted that for the case of quarry blasting and vibration measurements made at the ground surface, square root scaling provided the best grouping of the data. Other authors have suggested different scaling factors for similar conditions. Ambraseys and Hendron (1) preferred cube root scaling. Langfors and Kihlstrom (6) recommended scaling to the 2/3 power. Oriard (19) used cube root scaling for blast waves in water, and sometimes for seismic body waves in rock, but recommended square root scaling for surface ground motion.

Numerous authors have selected either cube root or square root scaling to best group the data in particular situations. Nicholls (11) found that cube root scaling best grouped the data from blasts in an underground evaporite

mine for vibration measurements made on the mine roof. The curve he developed allowed prediction of vibration levels from a nuclear blast at a distance of 8.6 miles. On the other hand, Olson (14), found that square root scaling was more appropriate for similar measurements in an underground copper mine in sedimentary rocks. In another study, Olson (16), sought to apply square root scaling developed for quarry blasting to vibrations measured in one opening of a large underground complex in granite, from blasting in other openings. He reported that cube root scaling was more appropriate.

Snodgrass and Siskind (22) compared the results of mine roof vibrations from underground blasting at four sites and found that while cube root scaling provided the best grouping in some cases, only small errors resulted in the use of square root scaling instead.

#### 4.2.2 Direct Statistical Analysis

The available background literatures does not provide a definite value of the scaling factor for use in the analysis of underground vibrations originating from surface blasting. Therefore, multiple least squares linear regression analysis was used to directly investigate the relationships between charge weight, distance and peak particle velocity for the various sets of data collected at the Jenny mine. The method used was developed for implementation on a computer by Daniel and Wood (4).

The propagation equation defined in Section 4.2.1 is of the form

$$V = K (D/W^\alpha)^\beta$$

This equation may be expressed as

$$\ln V = a + b \cdot \ln D + c \cdot \ln W$$

$$Z = a + bx + cy, \text{ where}$$

$$a = \ln K \quad z = \ln V$$

$$b = \beta$$

$$c = -\alpha \cdot \beta$$

This is the linear equation used for the multiple regression analysis.  $K$  is the intercept of the regression line,  $\beta$  the slope, and  $\alpha$  the scaling exponent.

Table 3 gives the results of multiple regression analysis for the various data sets. It is apparent that the scaling exponents for all of the surface data fall close to  $1/2$  which is consistent with findings of previous studies. The underground roof data, do not appear to follow the same scaling. The value of  $\alpha$  for the roof data is close to  $1/3$  while the value of  $\alpha$  for the floor data, is close to  $1/2$ .

#### 4.2.3 Range of Regression Coefficients

The results of the multiple regression calculations were used to perform a non-linear regression analysis (Daniel & Wood(4)) on selected sets of data to determine the range of the coefficients  $K$ ,  $\alpha$  and  $\beta$ , at the 95% confidence level. The data set which includes the maximum peak particle velocity recorded on any of the three components at the surface was chosen to represent all of the surface data. As shown on Table 3, this "maximum" set has a relatively high correlation coefficient. Furthermore, the maximum value in any direction is commonly used for controlling vibrations at surface structures and takes into account the possibility of misalignment of the sensor and significant elevation changes between the blast and the sensor.

Limits of the coefficients at the 95% confidence level are shown in Table 4. The standard error of the estimate for each of the three resulting equations is also given on the table for comparison with the same values included on Table 3. These values show that the standard error results of the multiple linear and non-linear calculations were the same.

The range of  $\alpha$  for the three sets is of particular interest. As shown in Table 4, the 95% confidence limits on  $\alpha$  for the roof data includes  $1/3$  but does not include  $1/2$ . For the floor data, the limits include  $1/2$  but not  $1/3$ . For the surface maximum data, the limits are relatively wide, due to the scatter of the data, and include both  $1/3$  and  $1/2$ .

From a strictly statistical viewpoint, therefore, for the data collected at the Jenny mine, it would be appropriate to scale the roof data by the cube root of the

TABLE 3 - Multiple linear regression results

Data Set	Direct coefficients			Derived Values		SE <sup>6</sup>	C.C. <sup>7</sup>
	lnK <sup>1</sup>	-αβ <sup>2</sup>	β <sup>3</sup>	K <sup>4</sup>	α <sup>5</sup>		
<u>Underground</u>							
Roof	5.683	.665	-1.79	294	.37	.490	.819
Floor	3.438	.705	-1.51	31.1	.46	.428	.853
<u>Surface</u>							
Radial	3.484	.486	-1.14	32.6	.42	.531	.690
Vertical	3.273	.547	-1.19	26.4	.48	.467	.772
Transverse	1.872	.403	-.83	6.5	.49	.616	.499
Horiz. Sum	3.466	.448	-.99	32.0	.45	.516	.654
Total Sum	4.015	4.75	-1.05	55.4	.45	.464	.723
Maximum <sup>8</sup>	3.096	4.68	-1.03	22.1	.46	.468	.713

<sup>1</sup> Intercept at  $-\alpha\beta = \beta = 0$

<sup>2</sup> Regression coefficient for charge weight (W)

<sup>3</sup> Regression coefficient for distance (D) which is equivalent to the slope of the trend line for exponential form of the equation

<sup>4</sup> Intercept at  $D/W^\alpha = 1$

<sup>5</sup> Scaling exponent on W for the exponential form of the equation

<sup>6</sup> Standard error of the estimate for the equation (residual root mean square)

<sup>7</sup> Multiple correlation coefficient ( $r^2$ )

<sup>8</sup> The set of data which includes for peak particle velocity, the highest value of the three components measured for each site monitored for each shot.



TABLE 4 - Limits of regression coefficients at the 95% confidence level calculated by non-linear regression

Data Set	$K^1$		$\alpha^2$		$\beta^3$		SE <sup>4</sup>
	lower	upper	lower	upper	lower	upper	
<u>Underground</u>							
Roof	64.7	1466	.29	.44	-2.20	-1.57	.494
Floor	8.33	134	.38	.55	-1.71	-1.33	.431
<u>Surface</u>							
Maximum of 3 components	4.00	121	.31	.60	-1.27	-0.78	.468

<sup>1</sup>Intercept at  $D/W^2 = 1$

<sup>2</sup>Scaling exponent on W

<sup>3</sup>Slope of the regression line

<sup>4</sup>Standard error of the estimate for the non-linear equation

maximum delay charge weight and the floor data by the square root. At the 95% confidence level, either scaling factor for the surface data would be satisfactory. However, since the calculated value of  $\alpha$  is closer to 1/2, statistical errors resulting from the use of square root scaling would be less than from cube root scaling.

It should be noted that the statistical analysis was performed on a relatively small amount of data gathered under less than ideal test conditions. The results, therefore, could change considerably if more data points were to become available. One anomaly in particular is apparent from the non-linear regression on the surface maximum value data set. From recording many thousands of data points, Oriard (20) has noted that the slope,  $\beta$ , of the regression line for surface data plotted against square root scaled distance for a particular site is generally close to -1.6. As shown on Table 4, the 95% confidence limits for the present surface data do not include that number. This apparent anomaly is discussed further in Section 5.3.

#### 4.3 Conventional Presentation of the Data

A trend line was calculated for each data set by simple linear least squares regression using both square root and cube root scaled distance. These analyses were done to provide an additional check on the relative effect of the scaling factor for each data set and to provide a basis for comparison with other data scaled by either of these factors. The results of these analyses are shown on Table 5.

In the simple linear regression analysis the standard propagation equation

$$V = K (D/W^\alpha)^\beta \quad \text{is written in the form}$$

$$y = a + bx \quad \text{where}$$

y = the logarithm of the peak particle velocity

a = the intercept of y at x = 0

b = the slope of the regression line on a linear graph

x = the logarithm of the scaled distance  $D/W^\alpha$

TABLE 5 - Simple linear regression results

Data Set	Versus $D/W^{1/2}$				Versus $D/W^{1/3}$			
	K <sup>1</sup>	β <sup>2</sup>	S.E. <sup>3</sup>	C.C. <sup>4</sup>	K <sup>1</sup>	β <sup>2</sup>	S.E. <sup>3</sup>	C.C. <sup>4</sup>
<u>Underground</u>								
Roof	30.1	-1.58	.520	.793	592	-1.84	.491	.816
Floor	18.7	-1.47	.427	.852	255	-1.66	.461	.828
<u>Surface</u>								
Radial	13.5	-1.04	.531	.684	112	-1.24	.537	.676
Vertical	15.4	-1.14	.465	.770	146	-1.34	.487	.747
Transverse	5.85	-0.82	.610	.499	28.3	-0.95	.624	.476
Horiz. Sum	19.0	-0.94	.512	.652	122	-1.11	.524	.636
Total Sum	32.8	-0.99	.461	.721	235	-1.17	.477	.702
Maximum	13.6	-0.98	.465	.711	93.7	-1.15	.481	.691

<sup>1</sup> Intercept at  $D/W^0 = 1$

<sup>2</sup> Slope of regression line

<sup>3</sup> Standard error of the estimate for the equation (residual roof mean square)

<sup>4</sup> Correlation coefficient ( $r^2$ )

A comparison of correlation coefficients in Table 5 produces the same conclusions as derived earlier in selecting the best scaling factors. A value  $1/3$  for  $\alpha$  better groups the data from the underground roof and  $1/2$  appears best for underground floor and the surface data.

A further comparison of correlation coefficients is shown in Table 6 which summarizes the results of all of the statistical analyses. It is apparent that a considerable reduction in scatter is obtained by using either the square root or cube root of the charge weight for scaling rather than simply plotting peak particle velocity versus distance from the blast. However, the differences among the results of using either of the scaling factors or that determined directly from the data by multiple regression are relatively small.

The peak particle velocity data recorded at the Jenny mine are presented graphically on Figures 11, 12, and 13 as functions of the conventional scaled distance which best groups the particular data set. From a statistical standpoint, the regression lines shown on the graphs would therefore be appropriate for estimating vibration levels at the various monitoring stations for additional blasting at the surface at the Jenny mine site.

It is apparent from the graphs that the least scatter was encountered from measurements on the mine roof. The 95% confidence limits, which define the range of expected future data points, are considerably narrower than for the floor or surface data.

The maximum peak particle velocity of the three components measured at the surface was chosen to represent the surface data on Figure 13. The component which recorded the highest value for each station and shot are shown by different symbols. Of the 53 data points, 31 are represented by peak values on the radial component, 14 on the vertical, and 8 on the transverse component.

Table 6 - Comparison of correlation coefficients with respect to scaling factors

Data Set	Correlation coefficients ( $r^2$ )				$\alpha^1$
	V vs D	V vs $D/W^{1/2}$	V vs $D/W^{1/3}$	V vs $D/W^\alpha$	
<u>Underground</u>					
Roof	.508	.793	.816	.819	.37
Floor	.465	.852	.828	.853	.46
<u>Surface</u>					
Radial	.322	.684	.676	.690	.42
Vertical	.268	.770	.747	.772	.48
Transverse	.195	.499	.476	.499	.49
Horiz. Sum	.286	.652	.636	.654	.45
Total Sum	.314	.721	.702	.723	.45
Maximum	.208	.711	.691	.713	.46

<sup>1</sup>Scaling exponent resulting from multiple linear regression analysis

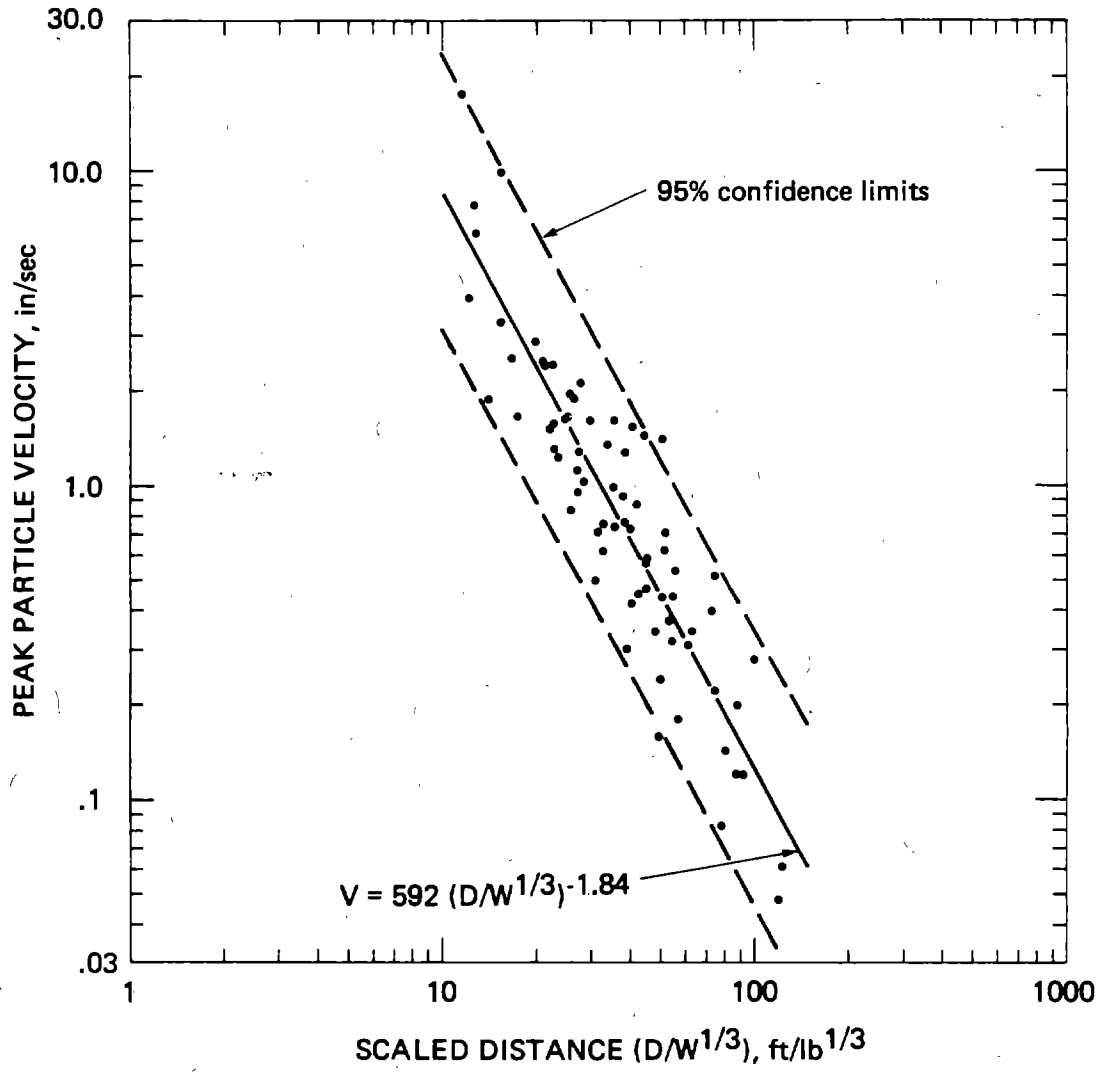


FIGURE 11.—Underground roof peak particle velocity versus cube root scaled distance.

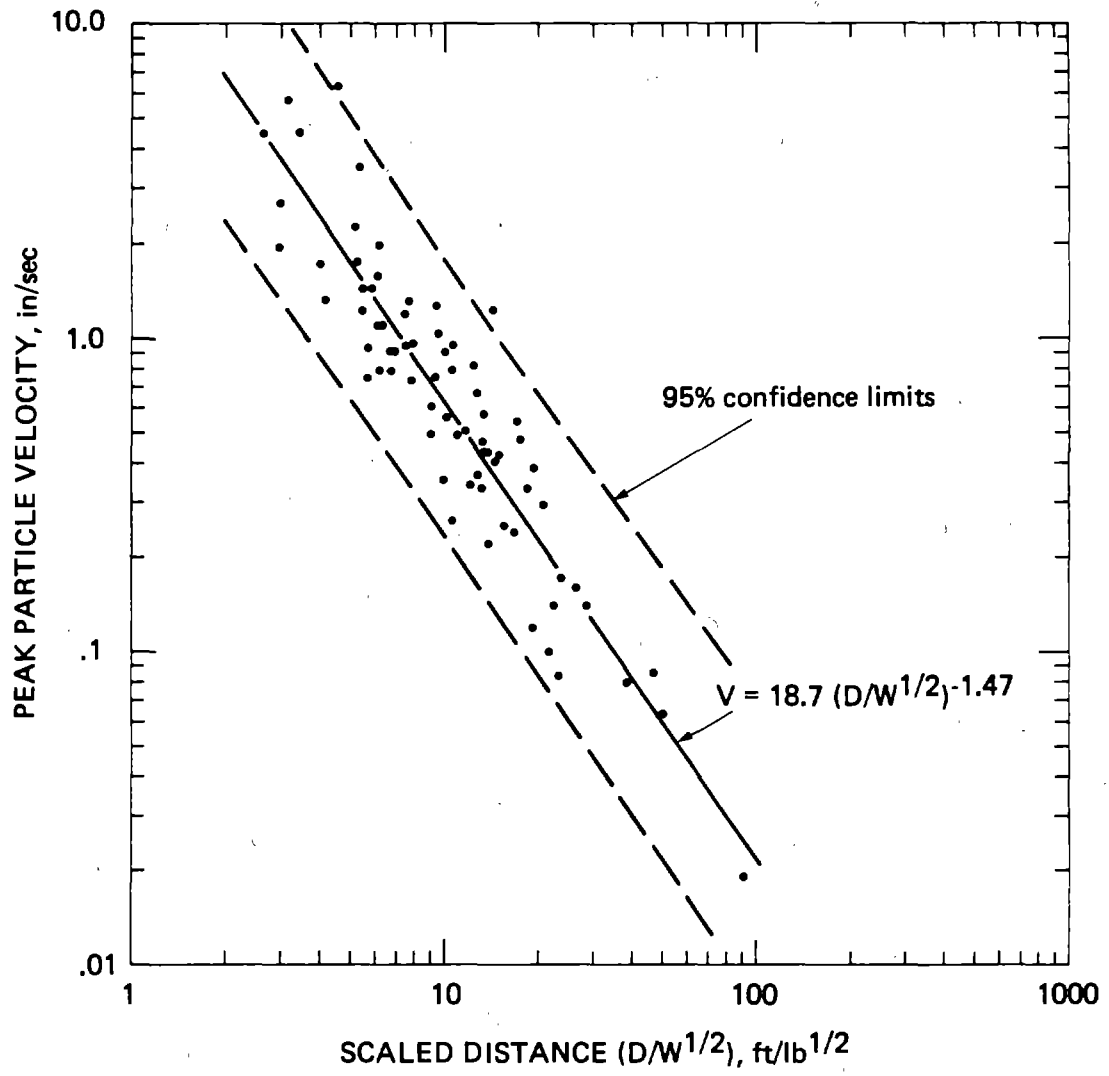


FIGURE 12.—Underground floor peak particle velocity versus square root scaled distance.

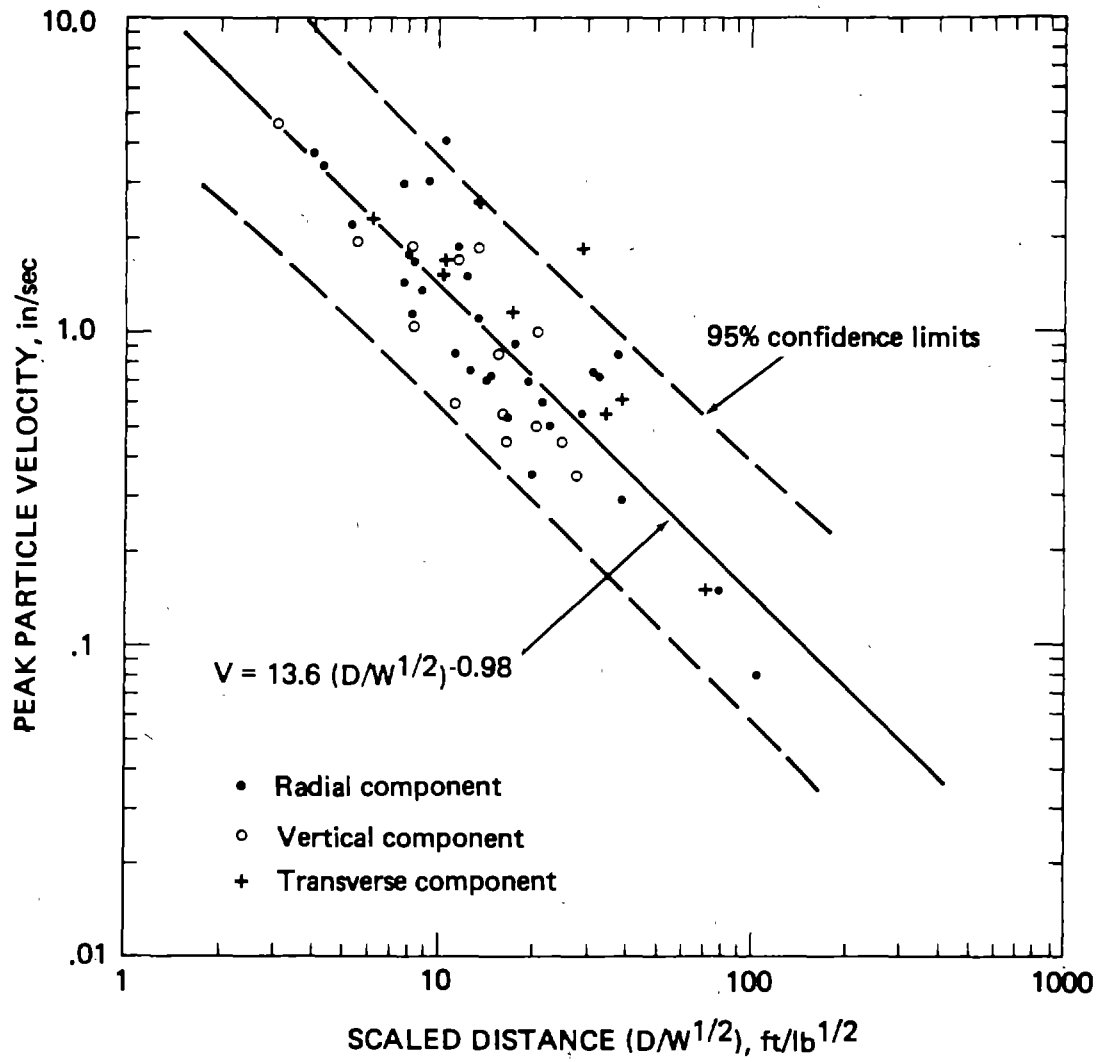


FIGURE 13.—Maximum peak particle velocity of the three components measured at the surface versus square root scaled distance.



## 5.0 DISCUSSION OF VIBRATION ANALYSIS

### 5.1 Propagation Equation for Underground Roof Vibrations

The results of the statistical analysis of underground roof data provide a clear picture of the relationships among particle velocity, distance, and maximum delay charge weight at the Jenny mine site. Scaling by the cube root of the charge weight produces a relatively well grouped data set with relatively narrow 95% confidence limits over the range of data recorded.

Studies of underground vibrations from surface blasts have been made by investigators from the University of Missouri at Rolla (25) but the data had not been published at the time this report was prepared. No data sets for similar blast-recorder geometry were found in the literature. Therefore, it is not possible to compare the Jenny mine data to other data sets collected under identical conditions. However, the present data may be compared with sets of data from underground production blasts recorded underground as presented in four separate Bureau of Mines reports reviewed by Snodgrass and Siskind (22). The regression line from the Jenny mine roof data falls slightly above those derived from the four underground blasting sites. The slopes of all five trend lines are similar. The Jenny mine data shows somewhat less scatter than for the underground blasting sites.

One site in particular appears to have some geometric similarity to the Jenny Mine site. Olson (16) reported the results of blasting in one chamber and recording in an adjacent chamber during development of the underground NORAD complex in Colorado. While the NORAD blasting was in granite, the site was similar to the present site in that solid rock separated the blasts from the monitoring points.

Olson's data are plotted on Figure 14 with the data points and 95% confidence limits from the present roof recordings. The blasts at the NORAD site were considerably smaller and closer to the monitoring points than in the present case and resulted in somewhat larger scaled distances. Olson also found that scaling by the cube root of the charge weight produced the best grouping of the data.

### 5.2 Relationship Between Floor and Roof Vibrations

In future work, especially under production conditions, it would be easier to measure underground vibration levels at the floor of the mine than having to attach

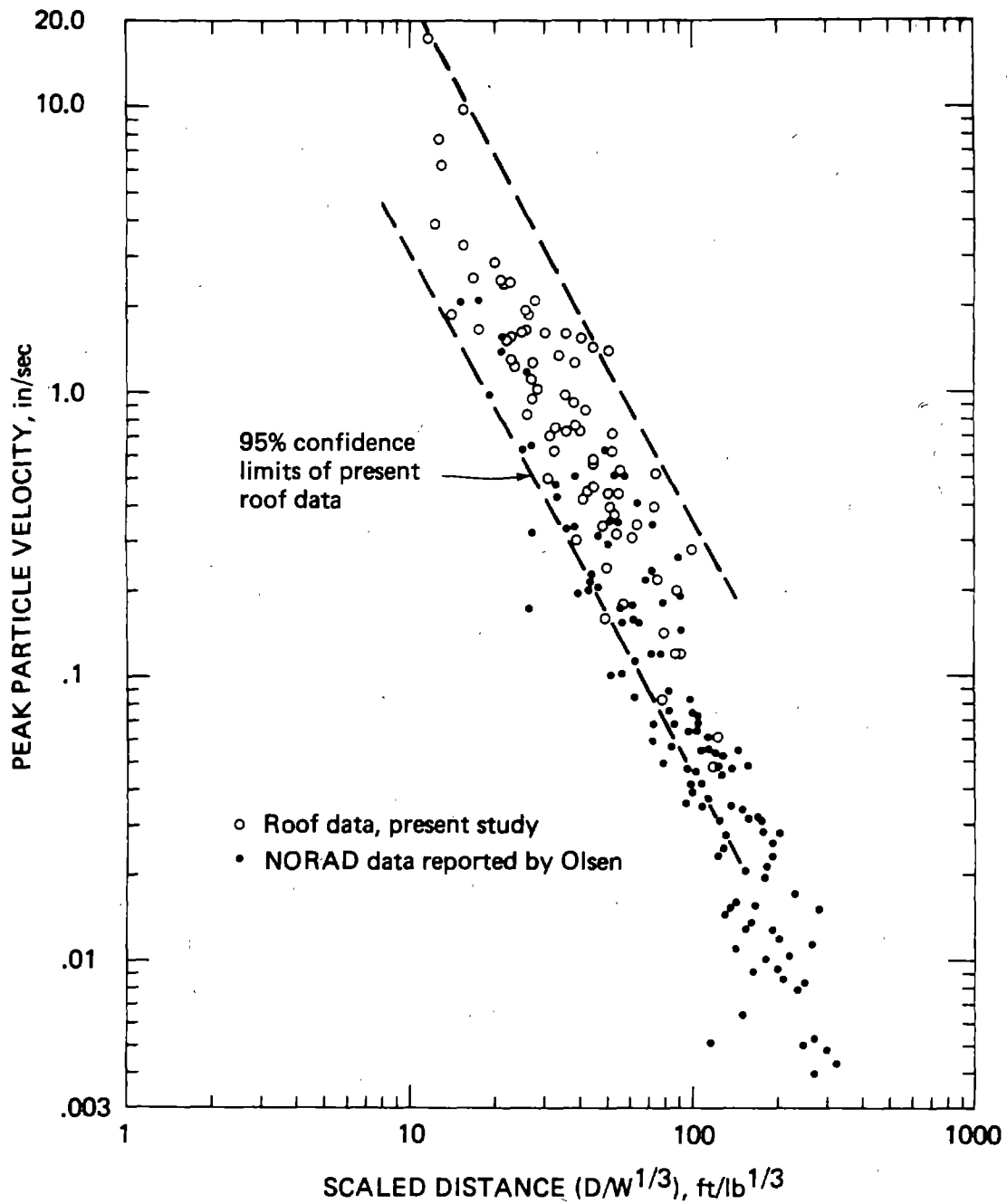


FIGURE 14.—Comparison of vibration data from the Jenny mine roof with that collected by Olsen from production blasting monitored in an adjacent underground opening. Both plotted versus cube root scaled distance.

sensors to the roof. At the Jenny mine, measurements were made at both the floor and roof to investigate possible differences.

Data from both sets are plotted together as functions of square root scaled distance on Figure 15. The 95% confidence limits overlap almost entirely within the range of the data indicating that the two sets are not statistically dissimilar. A careful examination of the figure shows that the floor data groups somewhat below the roof data. A comparison of the peak particle velocity values for each monitoring point and blast on Table 1 shows that considerable differences exist. The floor velocity exceeded the roof velocity in approximately 20% of the measurements. No discernable pattern was found to explain these occurrences and the present data base appears to be insufficient to explain the observed relationship. Further analysis and additional studies as recommended in Section 8.0 may be helpful in understanding the complex relationship between roof and floor particle velocities in an underground opening.

The regression lines derived from the two data sets tend to diverge at higher peak particle velocity values. Thus, at the Jenny mine site, a prediction curve developed from vibration recordings on the mine floor would not yield conservative results. This is shown on Figure 16 which is a plot of expected particle velocities for the roof and floor given the distance and charge weight. Additional data and study are required to develop a numerical relationship between roof and floor velocities in an underground opening.

### 5.3 Relationship Between Surface and Roof Vibrations

Roof and surface data are plotted together on Figure 17 as functions of square root scaled distance. Also shown on the figure are relations developed by Oriard (18) and Nicholls (12) from large numbers of surface vibration recordings from surface blasting.

The Oriard (18) curves define a band of typical vibration data observed on over a hundred projects. They were originally developed from surface blasts in volcanic rocks but have been found to be applicable in a wide range of conditions (Oriard, 20).

Nicholls (12) compiled data from several years of quarry blast monitoring and found that no peak particle velocity values measured fell above the line shown on Figure 18. Nicholls' data falls within the limits defined by Oriard.

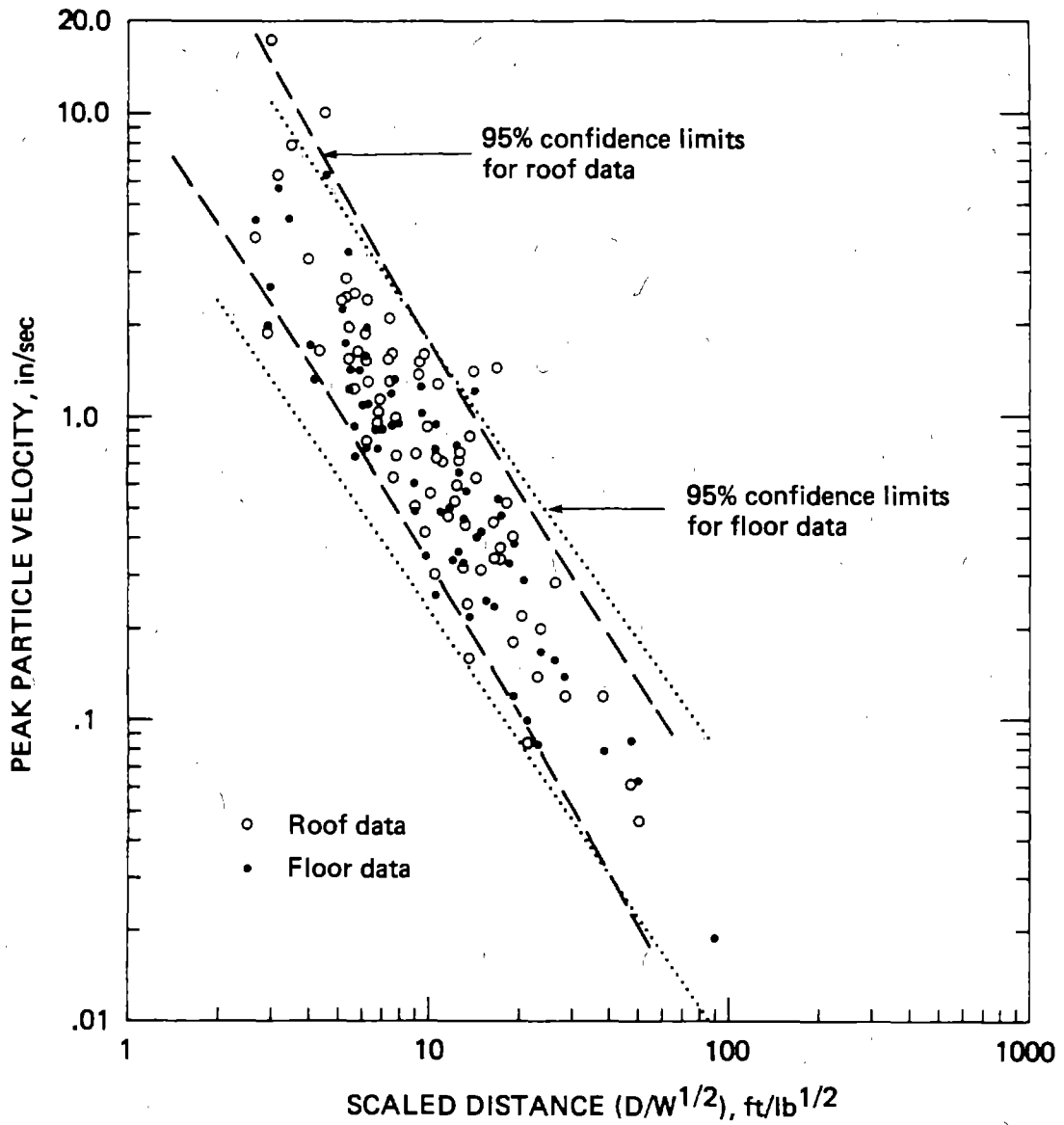


FIGURE 15.—Data and 95% confidence limits for roof and floor vibration measurements plotted versus square root scaled distance.

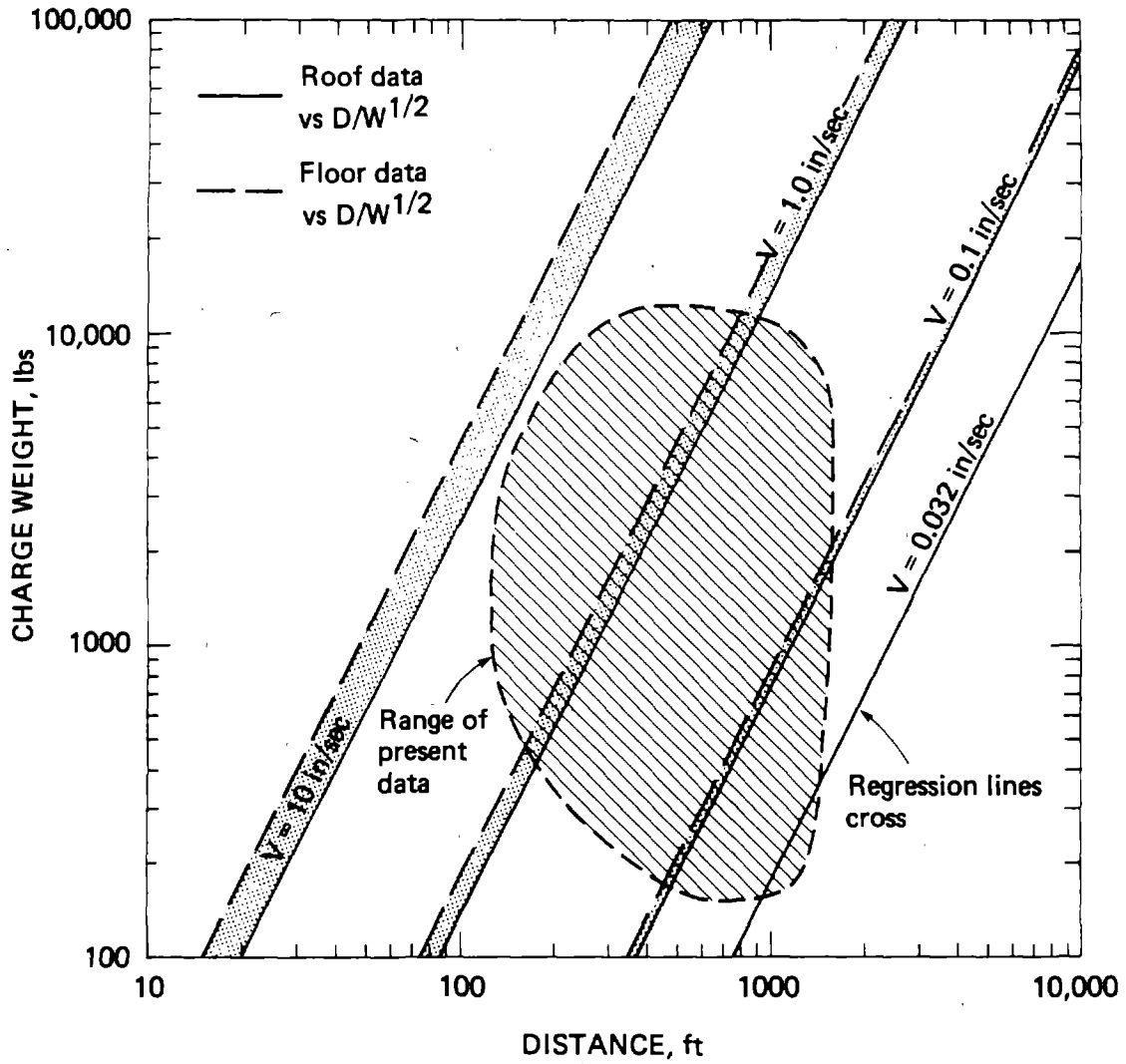


FIGURE 16.—Distance versus charge weight relationships for peak particle velocity values predicted by regression lines derived from roof and floor data versus square root scaled distance.

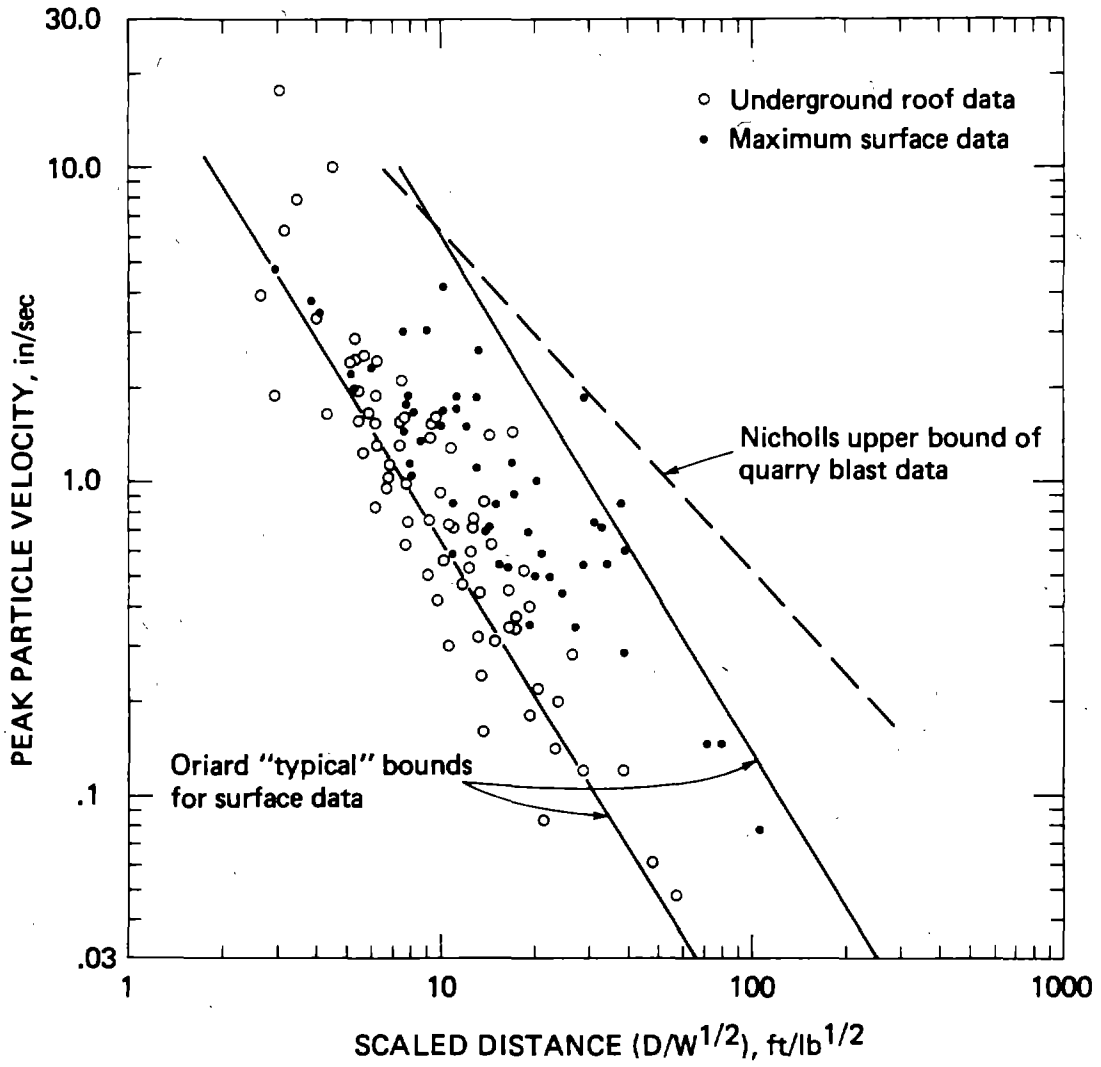


FIGURE 17.—Roof and surface velocities versus square root scaled distance showing relationships to compilations of previous workers.

The present surface data falls very well within the typical limits established by Oriard. Also, none of the data exceeds the limits observed by Nicholls. It appears, therefore, that the surface data gathered at the Jenny mine is not significantly different than that recorded from many other projects.

Figure 17 shows that Oriard's upper bound for surface data also appears to be a limiting value for roof data. This relationship may be unique for the Jenny mine site but if it could be shown to hold for other sites as well, it may lead to a simple, conservative method of predicting mine roof vibrations.

For the Jenny mine data, however, predictions of particle velocities in the underground mine based on the trend line from surface recordings appear to be less conservative at higher velocity values where damage might be expected. Figure 18 is a graph of charge weight and distance relations, for selected velocity values, based on trend lines for both the roof and surface data. This is similar to Figure 16 for the roof and floor data. Figure 18 shows that the conservatism of predictions based on surface data at low velocity values decreases as particle velocities increase.

As previously mentioned, the slope of the regression line derived from the Jenny mine surface data is flatter than that predicted by Oriard (-1 vs -1.6). If, however, the surface data had produced a steeper regression line the conservatism of predictions based on the surface data would extend to higher velocity values. Based on Oriard's studies (18), a regression line slope of -1.6 might be expected from a large number of samples over a large scaled distance range. However, there is no physical basis for this value. The observed particle velocities represent the vector sum of motions from several wave types (compressional, shear, surface) and are further complicated by reflected and refracted arrivals resulting from local geologic conditions and the mine structure. Blasting patterns and possible mine resonance may also influence the observed motions. Figures 17 and 18 show that the Jenny mine surface data occurs within a relatively narrow range of scaled distances. It would be desirable to extend this range to determine the effect on the slope of the regression line.

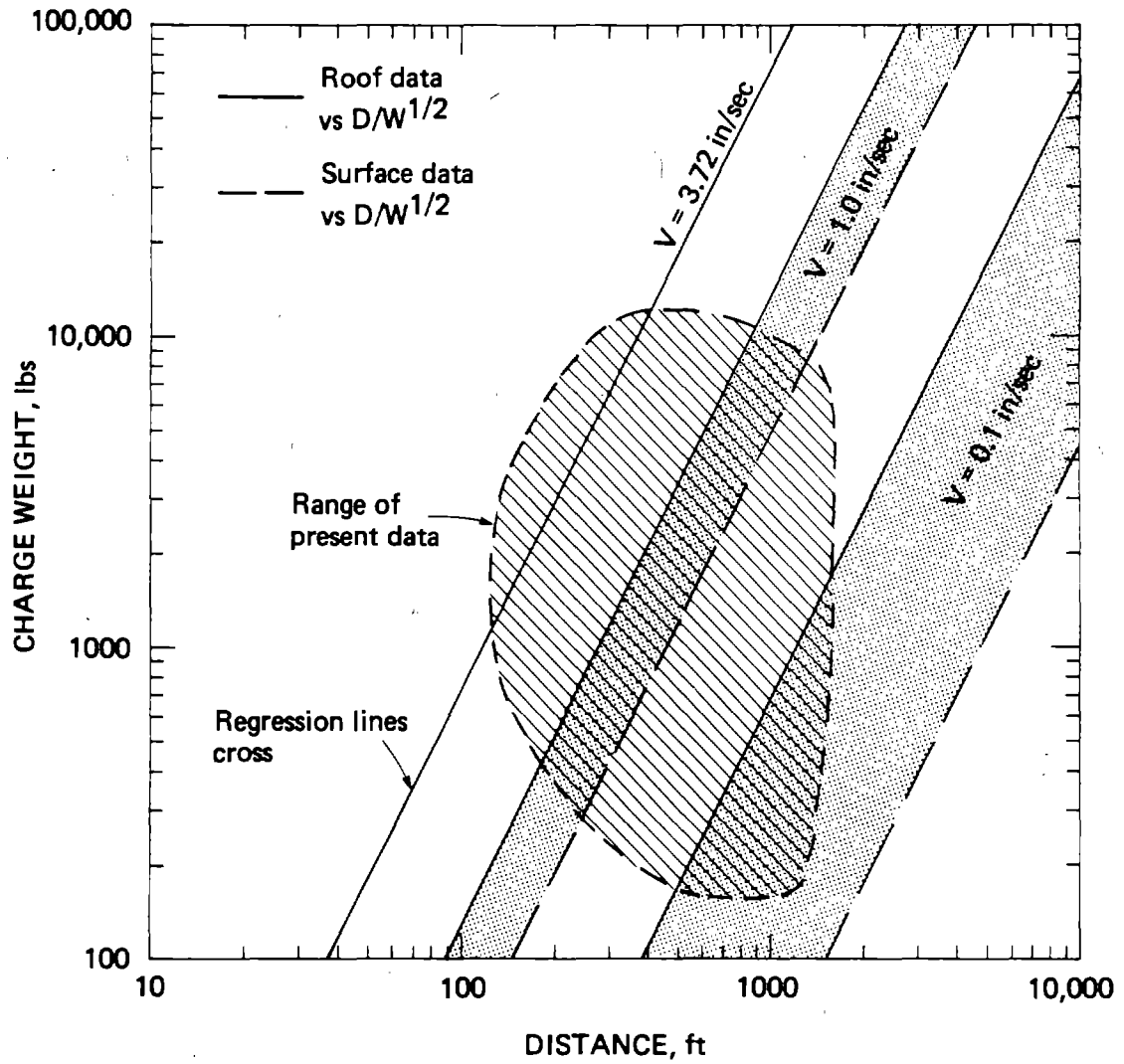


FIGURE 18.—Distance versus charge weight relationships for peak particle velocity values predicted by regression lines derived from roof and surface data versus square root scaled distance.



## 6.0 INDICATIONS OF PHYSICAL CHANGES IN THE UNDERGROUND MINE

Formal procedures for monitoring physical changes in the Jenny mine are discussed in Section 3.0. These observations included extensometer recordings at vibration sensor locations, convergence measurements elsewhere in the mine, background vibration recording, visual inspections, and observations of the roof strata with a borescope. In addition, miners and other persons associated with the mine were interviewed for information or opinions as to the frequency of roof failures before and during the surface blasting. No evidence of damage which could be directly attributed to blasting was found from any of these studies. These subjects are discussed in the following paragraphs. Reports of major damage from other investigations are summarized in Section 6.5

### 6.1 Roof Falls

It was the opinion of those familiar with the mine that loose rock which fell from the mine roof during the monitoring period would have fallen regardless of the blasting. Evidence of several past large roof failures, some almost filling the opening, were observed in the mine. No failures of that magnitude were observed during the blasting.

Efforts to quantify roof fall frequency and magnitude were intensified during the final stages of the project. Rigorous logging of entries 3 and 5, as described in Section 3.2.2, however, proved inconclusive due to unexpected termination of the blasting.

Few references are made in the literature to vibration levels associated with roof failures. Langefors and Kihstrom (10) cite approximately 12 in/sec as being associated with the "fall of stones in galleries and tunnels" but offer no additional details.

One substantial case history is presently available. Blasting above an underground crushing chamber at Dwarshak Dam in Idaho was described by Faris (7) and expanded upon by Oriard (20) who acted as consultant to the project. The project involved approximately 6 years of blasting in granite above the underground chamber, gradually approaching it until only a 30 ft shell remained over the chamber. When particle velocities reached 5 in/sec, 1 or 2 loose stones fell from an unsupported, unreinforced section of access tunnel. That was the only known rockfall during the 6 years

with particle velocities reaching about 10 in/sec. The chamber arch was bolted. The arch rose about 5/8 in. relative to the floor as a result of elastic rebound from excavation of the mountain above the chamber.

## 6.2 Convergence Measurements

Convergence measurements have been effective in monitoring roof and pillar failures in previous studies (23, 24). At the Jenny mine, two methods of measuring convergence were used. These were 1) installation of continuously recording drum extensometers at vibration sensor locations, and 2) physical measurements at fixed stations in other areas.

The drum recorders provided little information for this particular project. Two of the recorders (at locations 5/11 and 3/18) showed no deflections. The third recorder operated for about 70% of the monitoring period and showed several deflections of from .01 to .03 in. Most of these changes indicated divergence of the roof from the floor rather than convergence. The cumulative total for the meter was a divergence of less than 0.1 in. A graphic log of these records is included in Appendix C.

Convergence measurements made at 23 other points in the mine were also not conclusive. The measurements were made with a modified Philadelphia surveyor's rod between fixed points on the floor and roof at each station. During the eight days prior to the termination of blasting, readings at most stations registered positive or negative changes of 0.001 to 0.002 ft. Apparent cumulative changes over that period ranged from zero to a maximum convergence of 0.002 ft. A log of these readings is also included in Appendix C.

## 6.3 Borescope Suvey

After the termination of blasting, holes were drilled 10 ft into the roof at entry/crosscut locations 5/11, 5/14, and 3/18 for inspection of the strata with a borescope. In each of these holes, the strata was found to be intact with only minor partings at bedding surfaces. Nothing which could be considered a crack or bed separation was noted. It would have been preferable to have drilled the holes prior to blasting to determine as precisely as possible the condition of the strata at the beginning of the program as well as the end.

#### 6.4 Background Vibration Recording

The seismograph used to monitor background vibrations during the project recorded a large number of events. Some of the events were attributed to blasting in nearby mines and traffic noise at the site. If rockfalls or seismic events in or near the mine occurred they could not be distinguished on the seismic record. Since only one seismometer was used, the location of the events could not be determined.

One of the prime purposes of the seismograph was to determine the time of occurrence of any large roof failures which might have happened during the project. The idea was to investigate the time relationship between blasting and such a failure. However, no large failure occurred during the monitoring period.

#### 6.5 Likelihood of Major Damage

Several modes of damage in mines and tunnels due to blast vibrations and other phenomena have been noted in literature. The following paragraphs discuss these modes and their likelihood of occurrence under conditions at the test site or in similar circumstances.

The following may be considered types of major damage which result from blasting. These are not mutually exclusive categories but are presented as such for ease of discussion.

- . Crushing
- . Fracturing of confined rock
- . Fracturing at free surfaces
- . Failure due to addition of dynamic stresses to existing static stresses

The first three modes are discussed together because they can be considered to occur in originally intact rock affected predominantly by stresses of the blast. Addition of dynamic stresses is discussed in Section 6.5.2.

### 6.3.1 Crushing, Confined Fracturing and Free Surface Fracturing

Crushing and fracturing in confined rock and fracturing at free surfaces have been studied by several authors and the mechanisms for these modes of damage are fairly well understood.

Crushing and fracturing occur in zones near an explosion where stresses from the shock wave and expanding gases far exceed the shear strength of the rock. Oriard (19) listed 5 mechanisms for failure. These included (1) tensile parallel slabbing at a free surface, (2) conical failure under quasi-static compressive loading, (3) radial cracking under the action of tangential stresses, (4) peripheral cracking at the discontinuous shock front, and (5) mass shifting due to the venting of the explosive gases.

The confined fracturing zone is roughly equivalent to the transition zone between propagation of energy by shock and propagation as elastic waves. In this zone, compressive forces are greater than the strength of the rock, especially along existing planes of weakness. Beyond these zones, true elastic propagation is approximated with no damage occurring in confined rock. At a free surface, however, a compressional pulse is reflected as a tensional pulse which constructively interferes with the oncoming portion of the incident wave. The summed tensile stress may exceed the strength of the rock and produce spalling.

The extent of these zones has been examined in relation to tunnel damage which might result from nuclear blasts (3, 8). Experiments have ranged from model tests in a weak grout with 2 lbs of explosives to field tests using from 750 lbs of chemical explosives to the nuclear equivalent of 5.1 kilotons. Field tests were made in several rock types including sandstone, granite, basalt and tuff. The results of these tests are relatively consistent even though there were large scale differences in the experiments.

The following formula has been used by Clark (3) and other investigators to estimate the radii of the zones of damage:

$$R_i = K_i W^{1/3} \quad \text{where:}$$

$$R_i = \text{radius of zone of damage}$$

W = yield of explosive source expressed as pounds of chemical exposure

$K_i$  = an empirically determined constant which is a function of rock type and other variables

Average values of  $K_i$  have been reported by Hendron and others (8).  $K_i$  is expressed in  $\text{ft}/\text{lb}^{1/3}$ .

ZONE (i)	GRANITE	SANDSTONE
Zone of Crushing	1.3	1.3
Zone of Compressive Failure	2.5	3.3
Zone of Spalling	4.4	5.1

The results of other experiments are comparable to the tunnel closure tests. Olson and others (17) found large drops in sonic pulse velocities, indicating rock fabric damage, within scaled distances of 0.9 to 1.7  $\text{ft}/\text{lb}^{1/3}$  from small charges in granite. Obert and Duval (13) found severe cracking of metamorphic rock at a scaled distance of 1.3  $\text{ft}/\text{lb}^{1/3}$ . D'Andrea (5) used 3.1  $\text{ft}/\text{lb}^{1/3}$  to correlate the results of crushed zone measurements for small charges in laboratory studies in granite.

In the tunnel closure studies, charges were concentrated and assumed to be spherical. This is different than the design of blasts in the present case where charges were dispersed both in time and space. For comparison, however, the effects predicted for an instantaneous concentrated charge might be considered as an upper bound as to what might have occurred at the Jenny mine. Assuming a 12,000 lb charge, the largest delay charge in the Jenny mine blast program, and K values derived from sandstones the following damage radii would be calculated:

- . Zone of crushing 30 ft
- . Zone of compressive failure 75 ft
- . Zone of spalling 117 ft.

These distances are less than the minimum distances at Jenny mine and the modes of failure would not be expected to have occurred during this blasting program.

#### 6.5.2 Addition of Dynamic Stresses

The design of an underground mine is generally based on a consideration of static loads many times greater than any expected dynamic stresses. However, if conditions are such that static stresses are near the strength of supporting rock, added dynamic stresses from blast vibrations could cause failure.

Tincelin and Sinou (24) monitored deterioration of mine roofs near production blasts. They observed that strains larger than those which could be attributed to increasing static stresses occurred as blast vibrations passed gage locations. They compared total strains with those in openings driven by continuous mining methods and found the values associated with blasting to be significantly larger. They were able to correlate damage induced by blasting with peak partical velocity and duration of shaking.

Isaacson (9) reported failures in mine openings due to rock bursts initiated on planes of weakness away from the openings were caused by the addition of dynamic stresses from vibrations to existing high static stresses. Campbell and Dodd (2) used added dynamic stresses from predicted possible earthquake shaking in design consideration for an underground power plant.

Although techniques have been developed for estimating both static and dynamic stresses there is not sufficient information about the conditions at Jenny mine to make an accurate estimate of these stresses during the blasting program. The previous work described above indicates that dynamic stresses may be a critical consideration in estimating potential damage from blasting near underground openings.

## 7.0 SUMMARY: OBSERVATIONS AND CONCLUSIONS

The major observations and conclusions which can be inferred from the Jenny mine study are summarized below:

- . Surface and underground vibration levels observed at Jenny mine can be related to blast distance and charge weight using previously developed propagation formulas.
- . A significant reduction in data scatter is obtained by scaling rather than simply plotting velocity versus distance. However, only minor differences in parameters result from the use of square root scaling, cube root scaling or scaling by the fractional root determined directly from the data by multiple regression analysis.
- . Peak particle velocities measured at the mine roof are best grouped by using cube root scaling. Velocities measured on the mine floor and at the ground surface are best grouped by square root scaling. The reason for the difference in scaling factors is not defined by these observations.
- . The results of analysis of the data measured at the mine roof are similar to those of previous studies where vibrations from underground blasts were measured on the roof of the underground mine or tunnel. Particular similarity was noted with a case where vibrations were monitored in an underground opening separate from the opening where blasting took place.
- . Vibration levels measured on the mine floor were generally lower than those measured at the roof.
- . The slope of the regression line derived from surface data versus square root scaled distance is flatter than expected from previous studies. This may be a result of the widely spread blast patterns used at the site. However, the data lie within the bounds, based on a slope of  $-1.6$ , developed by Oriard (18) from numerous previous projects.

- . Roof vibration levels are consistently less than those measured at the surface at equal scaled distances. Although the regression line from the roof data crosses the regression line of the present surface data, it closely parallels the value of -1.6 developed from previous surface vibration studies.
- . Based on Jenny mine data alone, predictions of roof vibration levels from measurements on the mine floor would be slightly low at low particle velocity values and would become even less conservative at higher levels. Predictions of roof vibration levels from surface measurements would be conservative at low levels but less conservative at higher levels.

Only limited conclusions can be drawn regarding the relationship between damage and vibration levels as there were no observed underground failures attributable to the surface blasting. However, it is significant that no apparent damage occurred even at the peak measured particle velocity of 17.5 in/sec.. The following points can be related to the levels of blast induced vibrations recorded.

- . Neither the frequency nor magnitude of roof falls noticeably increased during the project.
- . No significant convergence of the roof to the floor was noted.
- . Borescope observation showed roof strata at the three points investigated to be intact after the blasting.

Analysis of the results of the Jenny mine project has indicated several areas in which improvements could be made in the investigative approach. Recommendations are made in Section 8.0 for improving the amount and quality of data obtained in future studies.



## 8.0 RECOMMENDATIONS

The relationships developed from the Jenny mine observations represent a significant first step in defining the impact of surface blasting over underground workings. However, these relationships are presently not sufficiently well defined to use in general production situations without a high degree of conservatism. Furthermore, it is not presently clear what vibration levels might be associated with undesirable physical effects in the underground mine on a long-term basis.

Our recommendations are directed toward procedures to obtain data supplemental to that presented in this report. These recommendations fall into two categories: additional tests at the Jenny mine and monitoring blasts over underground openings at other sites.

### 8.1 Additional Tests at Jenny Mine

In order to better understand the results of the Jenny mine monitoring program, tests should be performed to provide additional definition of site conditions and the behavior of elastic waves in the local strata. These tests would also be useful for comparing the Jenny mine site data with other sites where additional data might be gathered or where application of the relationships developed in this report might be contemplated. Also, it would be desirable to conduct tests to relate observable damage to vibration and strain levels.

Procedures to better define the Jenny mine site would require material property tests of the rock. We recommend one or more core borings at the site from which a complete log of the strata could be made. This log would include a petrographic description and information on discontinuities such as joints and bed separations. Downhole photographs would be useful to investigate discontinuities. Field tests could be conducted to study anisotropy and seismic velocities. Laboratory tests of compressive, tensile and shear strength, and of density of representative strata could be performed on core samples.

Although it would not be feasible to continue blasting on a large scale above the mine, there would be a feasibility of conducting definitive research at carefully chosen locations within the mine. Several locations could be chosen to represent different conditions of

stability. These locations could be selected in areas where a roof failure would not be disastrous. These roof sections could then be subjected to vibrations while the rock was carefully monitored to observe its behavior.

One suggested approach would be to detonate a series of blasts a short distance above the monitored roof sections. These could be small blasts, at a short distance, and would necessarily be very limited in number. However, this limitation would be offset by the detailed study of the rock that could be made before, during and after the blasting. Because of the limited number of blasts that would be possible, it would be desirable to increase the charges rapidly until immediate damage occurred.

A different approach could be made to the question of the long-term effects of low-level vibrations. In this instance, a mechanical vibrator could be installed a short distance above a roof section of interest. The vibrator could be operated electrically and allowed to run continuously or intermittently, at the option of the observers. The method of installing the vibrator would depend on its physical size and location. It could be brought in through a small raise and adit, or lowered into a large-diameter hole from above.

Although additional case histories of open-pit mining above underground openings are desirable, there are certain advantages to the small-scale research efforts that could be conducted at the Jenny mine. This research could be conducted without the time pressures that would be present if the researchers were merely monitoring actual mining operations at some other location. At the Jenny mine, there would be ample opportunity to make as elaborate and detailed a study as would suit the purposes of the research, and there would not appear to be any time limits to hinder the work.

Additional information may be obtained from the existing vibration records from the Jenny mine. The records contain complete wave traces. They can be digitized and a computer could be used to analyze the observed frequencies. The frequency content of the incident shock wave and the subsequent response of the rock may be important parameters in assessing potential damage.

## 8.2 Tests at Additional Sites

Monitoring blasts from surface operations over underground mines at other sites is essential to developing general guidelines. At these sites, the procedures for defining site properties discussed in the previous section should be implemented. Core holes used for logging and testing could also be used for installation of downhole vibration sensors to obtain free field vibration data during the blasting.

If sufficient lead time or records are available, it would be desirable to conduct a pre-blast study or review of the rock behavior in the mine in order to evaluate the influence of seasonal changes. A cursory investigation would be of relatively little value, and available man-power should be concentrated to obtain a detailed survey of a limited zone.

An evaluation of long-term effects should include monitoring of acoustic emission in and around the mine. A sufficiently large array of sensors should be used to determine the location of the microseisms. Monitoring should begin far enough in advance of blasting to provide adequate base level data.

In the event that lead time was insufficient to provide a base for evaluating any changes in rock behavior at low levels of vibration, the next best information would be a correlation of increasing levels of vibration with effects that could be observed immediately. This would require some control over blasting operations so that charge sizes could be increased to the point of producing immediate effects. In order to detect the first signs of loosening or deterioration of roof and/or pillar rock, instrumentation and tests in addition to the convergence monitors and borescope observations used at the Jenny mine would be useful. Multiple point borehole extensometers would better define the mode of a failure. Repeated sonic velocity tests could detect cracking and deterioration before it became visible. If convergence meters are used, steps should be taken to insure their proper function. Borescope observations should be made before and periodically during the blasting period.

Documentation of operations should be more complete than at the Jenny mine. The location, layout and loading of blasts should be a primary concern in additional studies. This would include the use of surveying equipment to determine locations and careful observations of explosives loading. Accurate determination of charge weight is essential.

As in the present study, we recommend that vibrations at the ground surface and on the mine floor be measured as well as on the roof. Hopefully, this will lead to a simplified method of evaluating roof vibrations in general operations. Also, surface measurements provide a means of comparing data with the large available surface vibration data base.

Strain as well as particle velocity should be measured underground. Where displacement or frequency values would be expected to exceed the measuring capabilities of presently available velocity gauges, accelerometers should be used, and data derived therefrom converted to velocity values.

### 8.3 Development of a Model

It would be desirable to begin as soon as possible to develop a model for damage produced by blasting over an underground mine. Data from the present study and information from the literature could be used as a starting point. The model could then be altered as additional data became available until such time as researchers were satisfied that it indeed reflected actual physical conditions.

At that point, the model could be made available for general use by the industry and its consultants, much as the model developed by Nicholls (12) is used where potential damage to surface structures from surface blasting is a concern.

## References

1. Ambraseys, N.R., and A.J. Hendron Jr. Dynamic Behavior of Rock Masses. Rock Mechanics in Engineering Practice, Ed. by K.G. Stagg and O.C. Zienkiewicz, John Wiley & Sons, New York, 1968, pp. 203-236.
2. Campbell, R.B., and J.S. Dodd. Estimated Rock Stresses at Morrow Point Underground Power Plant from Earthquakes and Underground Nuclear Blasts. Proceedings of the Ninth Symposium on Rock Mechanics. Society of Mining Engineers of the American Institute of Mining, Metallurgical and Petroleum Engineers, Port City Press, Baltimore, Md., 1968, pp. 84-114.
3. Clark, G.B. Some Basic Principles of Scaling Explosion Produced Damage to Deep Unlined Openings in Rock. U.S. Army Engineers Waterways Experiment Station, Vicksburg, Mississippi, Technical Report 1-695, 1965, 42 pp.
4. Daniel, C., and F.S. Wood. Fitting Equations to Data. Wiley-Interscience, New York, 1971, 342 pp.
5. D'Andrea, D.V., R.L. Fischer, and A.D. Hendrickson. Crater Scaling in Granite for Small Charges. BuMines RI 7409, 1970, 28 pp.
6. Devine, J.F., R.H. Beck, A.V.C. Meyer, and W.I. Duvall. Effect of Charge Weight on Vibration Levels From Quarry Blasting. BuMines RI 6774, 1966, 37 pp.
7. Faris, C.O. Dworshak Dam Underground Crushing Chamber. Symposium on Underground Rock Chambers. American Society of Civil Engineers, N.Y., 1971, pp. 159, 160.
8. Hendron, A.J., Jr., G.B. Clark, and J.N. Strange. Damage to Model Tunnels Resulting from an Explosively Produced Impulse. U.S. Army Engineer Waterways Station, CE, Vicksburg, Mississippi, Research report 1-6, 1965, 33 pp.

9. Isaacson, E.Q. Stress Waves Resulting from Rock Failure. Fourth Symposium on Rock Mechanics. Bulletin of the Mineral Industries Experiment Station, Pennsylvania State University (University Park), 1961, pp. 153-161.
10. Langefors, U., and B. Kihlstrom. The Modern Technique of Rock Blasting. Almquist & Wiksell, Stockholm, 1963.
11. Nicholls, H.R. Case Study of Validity of Scaling Laws for Explosion-Generated Motion. BuMines RI 6472, 1964, 14 pp.
12. Nicholls, H.R., C.F. Johnson, and W.I. Duvall. Blasting Vibrations and Their Effects on Structures. BuMines Bull. 656, 1971, 105 pp.
13. Obert, L., and W.I. Duvall. Generation and Propagation of Strain Waves in Rock - Part I. BuMines RI 4683, 1950, 19 pp.
14. Olson, J.J., R.A. Dick, J.L. Condon, A.D. Hendrickson, and D.E. Fogelson. Mine Roof Vibrations from Underground Blasts. BuMines RI 7330, 1970, 55 pp.
15. Olson, J.J., R.A. Dick, D.E. Fogelson, and L.R. Fletcher. Mine Roof Vibrations from Production Blasts, Shullsburg Mine, Shullsburg, Wis. BuMines RI 7462, 1970, 35 pp.
16. Olson, J.J., D.E. Fogelson, R.A. Dick, A.D. Hendrickson. Ground Vibrations from Tunnel Blasting in Granite. BuMines RI 7653, 1972, 25 pp.
17. Olson, J.J., R.J. Willard, D.E. Fogelson, and K.E. Hjelmstad. Rock Damage from Small Charge Blasting in Granite. BuMines RI 7751, 1973, 44 pp.
18. Oriard, L.L. Blasting Operations in the Urban Environment. Bulletin of the Association of Engineering Geologists, vol. IX, no. 1, 1972, pp. 27-46.

19. Oriard, L.L. Blasting Effects and Their Control in Open Pit Mining. Geotechnical Practice for Stability in Open Pit Mining. Proceedings of the Second International Conference on Stability in Open Pit Mining, Vancouver, B.C., Nov., 1971, Soc. Min. Eng. of AIME, New York, 1972.
20. Oriard, L.L. Personal Communications on file at Woodward-Clyde Consultants, P.O. Box 1149, Orange, CA., 92668.
21. Siskind, D.E. Mine Roof Vibrations from Underground Blasts, Pilot Knob, MO. BuMines RI 7764, 1973.
22. Snodgrass, J.J., and D.E. Siskind. Bureau of Mines Research on Vibrations from Underground Blasting. Proceedings of the 1974 Rapid Excavation and Tunneling Conference, Soc. Min. Eng. of AIME, New York, 1974, pp. 1561-1577.
23. Statehan, R.M. Field Studies on an Unsupported Roof. BuMines RI 7886, 1974, 18 pp.
24. Tincelin, E., and P. Sinou. Control of Weak Roof Strata in the Iron Ore Mines of Lorraine. Internat. J. Rock Mech. and Min. Sci., v. 1, no. 1, 1964, pp. 341-383.
25. University of Missouri. Establishment of Criteria for the Proximity of Surface Blasting Operations and Underground Coal Mines. BuMines Contract No. H0242015, 1974, report pending.

APPENDIX A  
Blast Documentation

Basic information about the surface blast program during the vibration monitoring period is presented in this Appendix. Table A1 is a summary of blast data. Layouts for each shot are shown on Figures A1 through A12. An explanation of the symbols used in the drawings is included on Figure A1.

Blast operations were conducted by the Rebel Mining Company from 13 September 1977 to 4 November 1977. Blast holes were drilled with 6 in augers to depths of 10 to 40 ft in the irregular terrain. Prilled ammonium nitrate and fuel oil was the principal blasting agent. Primers were 1 in. 60% dynamite sticks initiated by primacord. Holes were generally spaced on 10 to 12 ft centers but the spacing varied considerably for some shots.

Shots 11, 12, 13, 17, 20, 22, 28, 29 and 30 were relatively small, shallow blasts in the shale binder between the two coal seams. The remainder of the blasts were located in the overburden above the upper coal seam.

The spacing and location of the shot holes were estimated by compass and pace survey. Charge sizes were estimated by the blaster based on the number of boxes of prills used in each hole.



TABLE A1. - Blast data summary

Blast number	Date	Time (est)	Total charge		Number of delays	Maximum delay	
			No. holes	Weight, lb		No. holes	Weight, lb
1...	9-13-77	1300	55	5,500	5	17	1,700
2...	9-15-77	1227	42	4,200	5	8	800
3...	9-17-77	1137	47	4,700	8	6	600
4...	9-17-77	1452	52	5,200	9	6	600
5...	9-20-77	1450	51	6,450	2	18	3,600
6...	9-23-77	1403	62	9,300	5	11	1,650
7...	9-26-77	1505	62	12,400	0	62	12,400
8...	9-28-77	1455	129	19,350	3	71	10,650
9...	10-01-77	1256	71	11,900	5	23	4,600
10...	10-03-77	1340	94	18,800	5	27	5,400
11...	10-03-77	1807	311	8,086	0	311	8,086
12...	10-04-77	1130	119	2,975	0	119	2,975
13...	10-05-77	1646	68	8,800	5	17	2,400
14...	10-06-77	1149	180	4,680	1	95	2,470
15...	10-07-77	1513	148	51,400	13	15	5,250
16...	10-11-77	1450	176	35,200	19	13	2,600
17...	10-12-77	1710	259	2,072	14	21	168
18...	10-13-77	1516	67	18,500	6	13	3,250
19...	10-14-77	1630	45	9,900	1	27	5,400
20...	10-15-77	1618	343	8,918	3	94	2,445
21...	10-17-77	1544	106	14,660	9	15	2,250
22...	10-18-77	1330	187	2,992	4	43	688
23...	10-18-77	1643	60	6,000	1	30	3,000
24...	10-19-77	1530	67	6,700	4	22	2,200
25...	10-20-77	1507	184	18,659	8	46	4,600
26...	10-21-77	1510	169	16,900	3	113	11,300
27A.	10-25-77	1543	143	14,443	3	66	6,600
27B.	10-25-77	1544	90	9,000	0	90	9,000
28...	10-27-77	1501	203	3,248	2	150	2,400
29...	11-02-77	1505	418	1,254	5	92	276
30...	11-04-77	1801	644	5,796	9	89	801

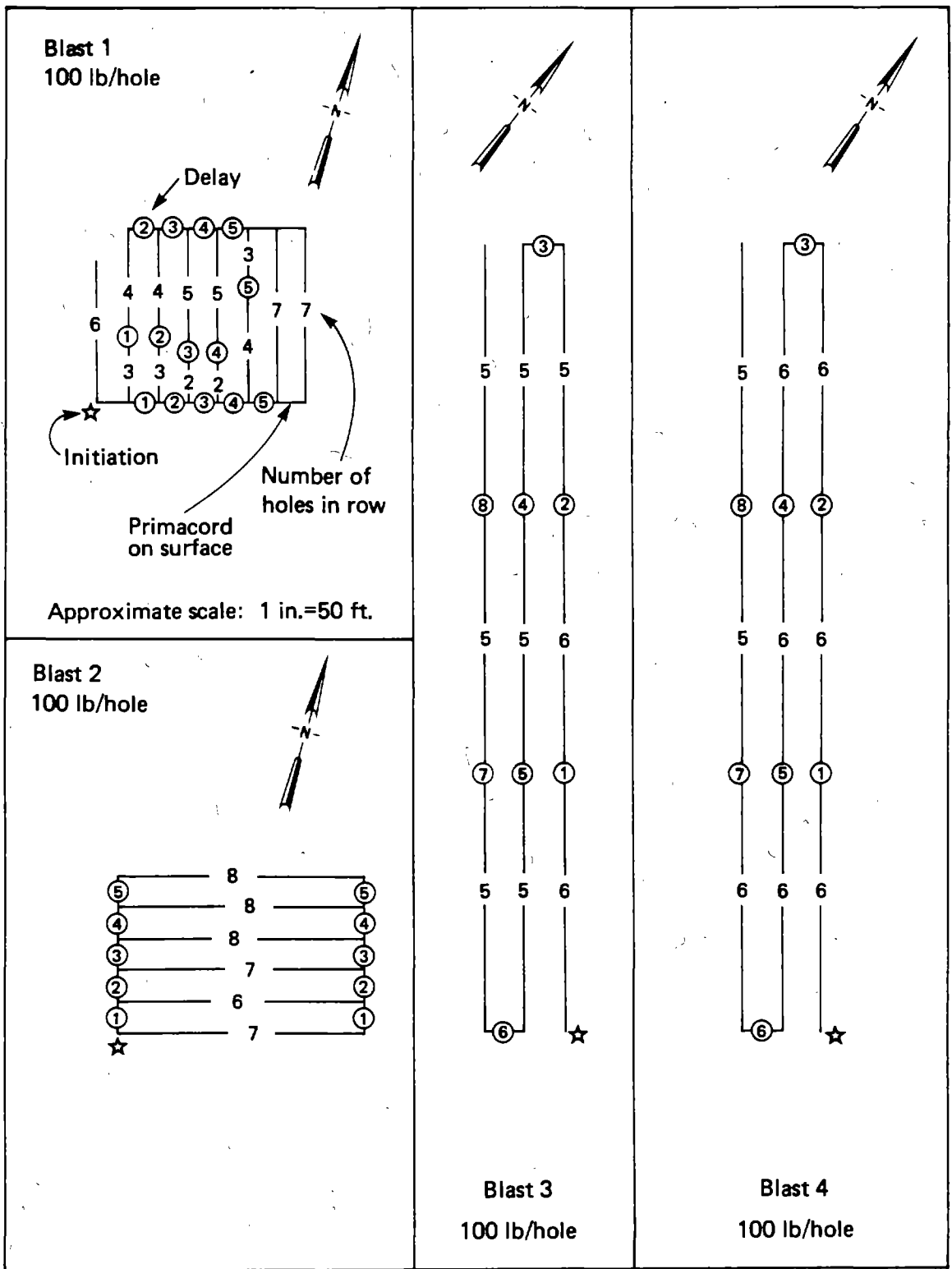


FIGURE A-1.— Layout of blasts 1, 2, 3, and 4.

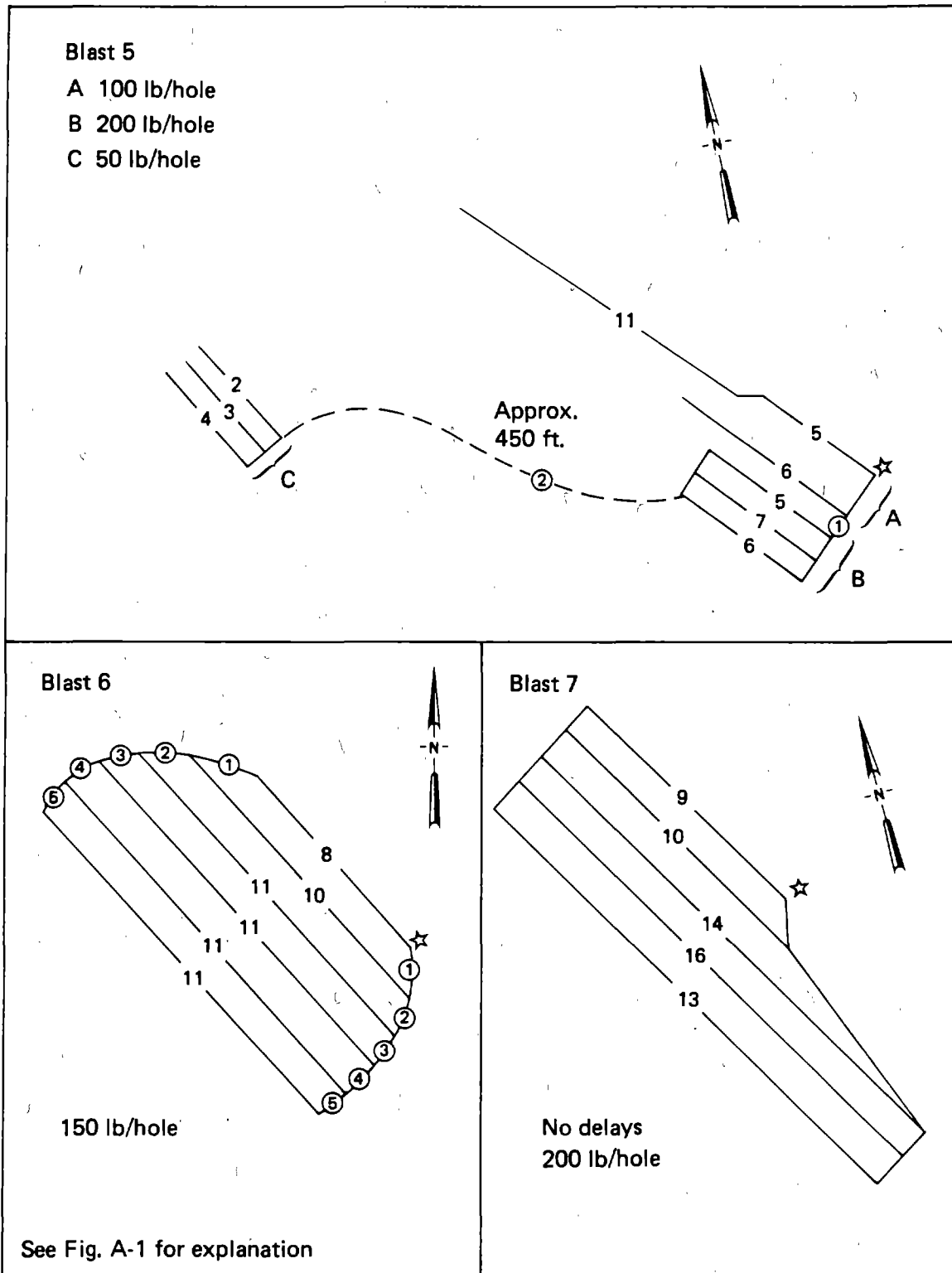


FIGURE A-2.—Layout of blasts 5, 6, and 7.

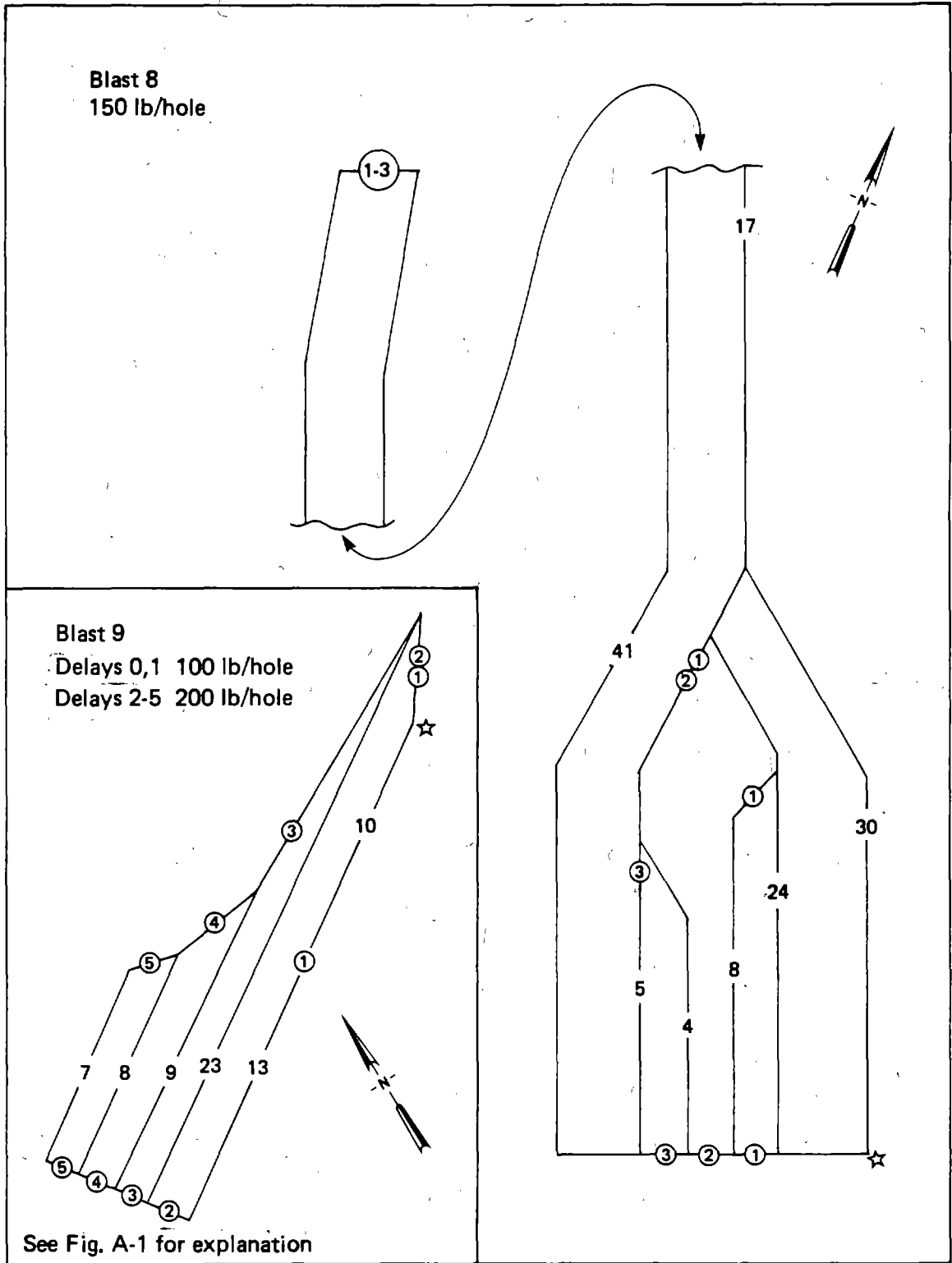


FIGURE A-3.—Layout of blasts 8 and 9.

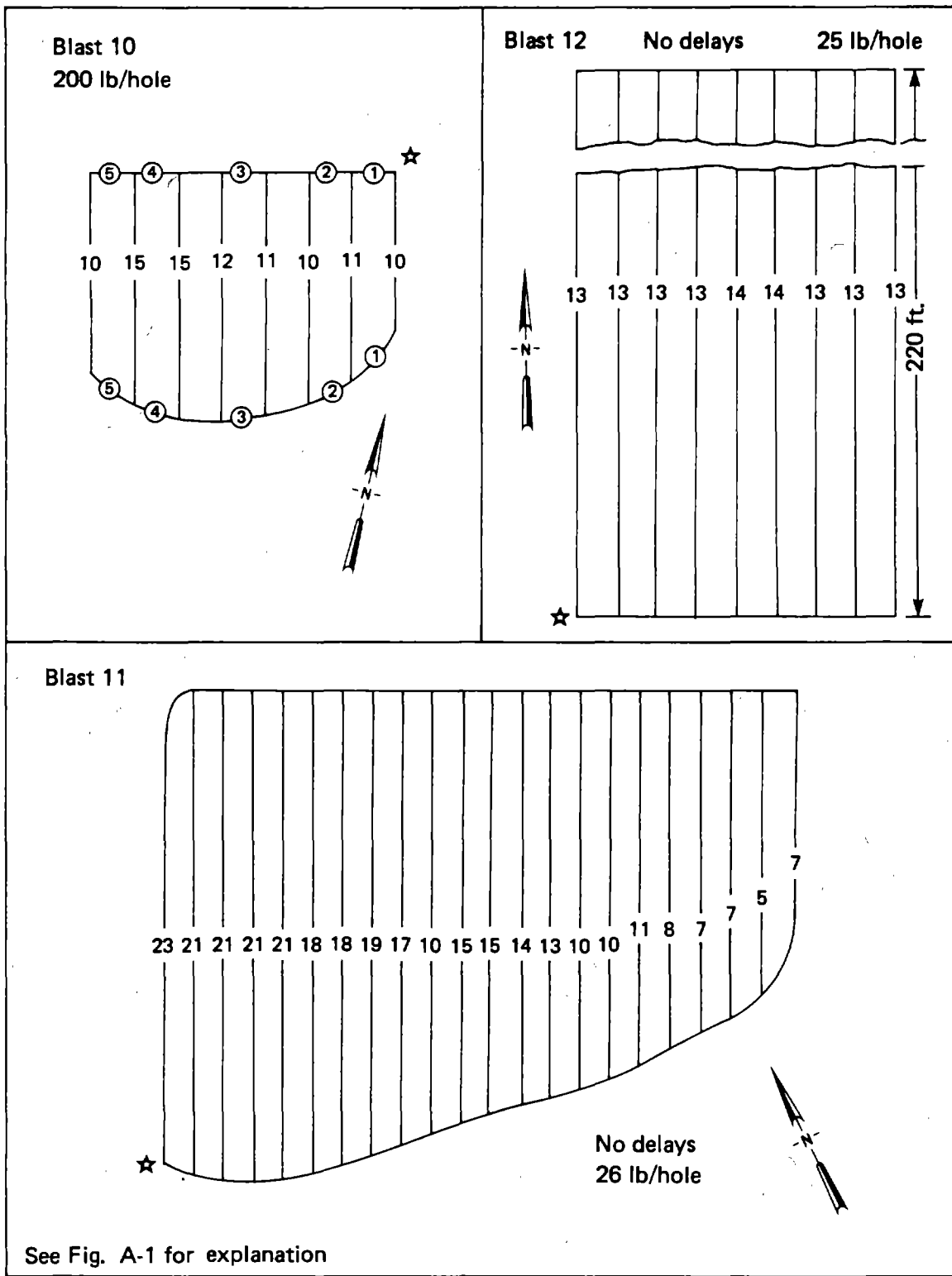


FIGURE A-4.— Layout of blasts 10, 11, and 12.

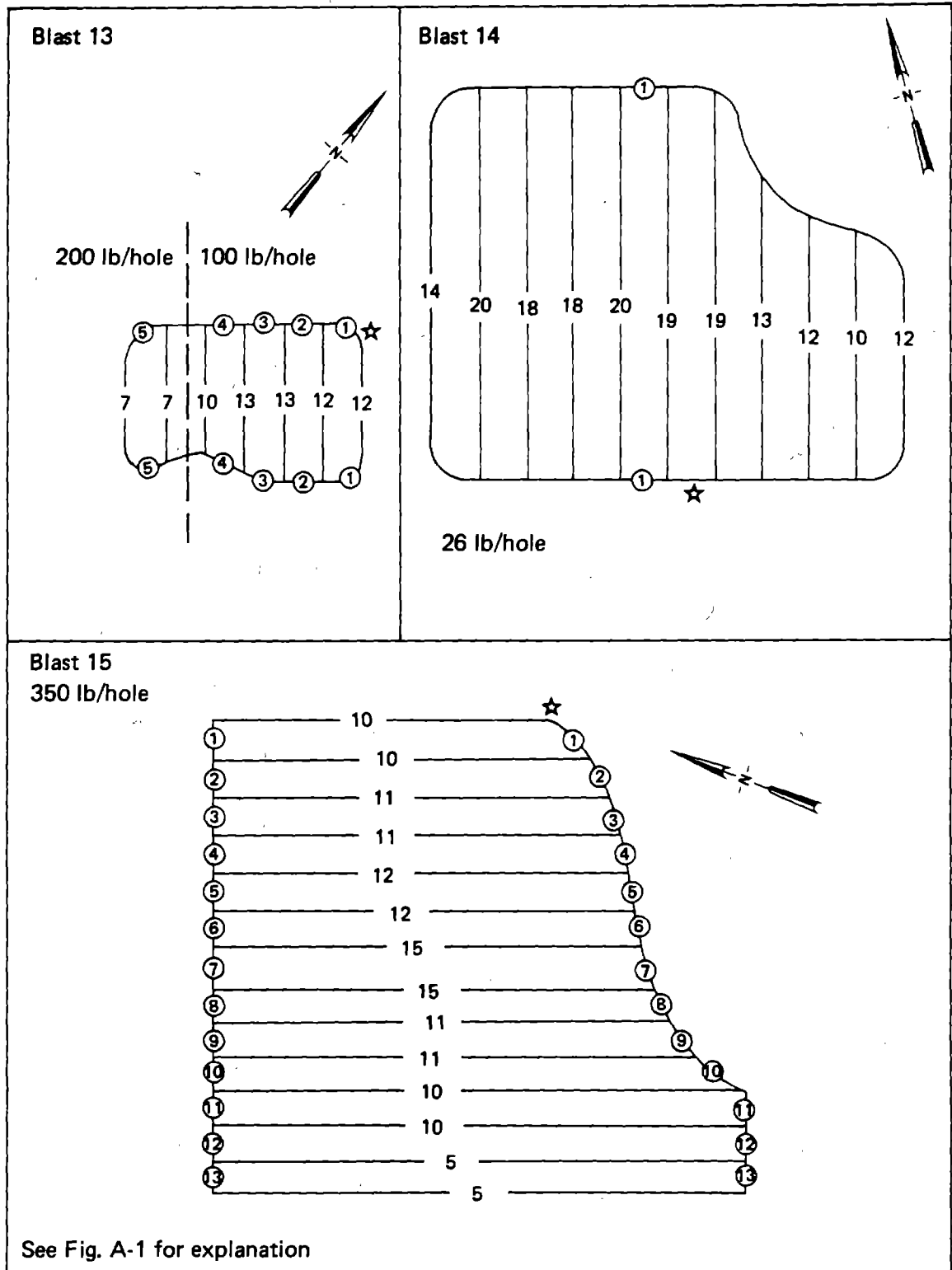


FIGURE A-5.— Layout of blasts 13, 14, and 15.

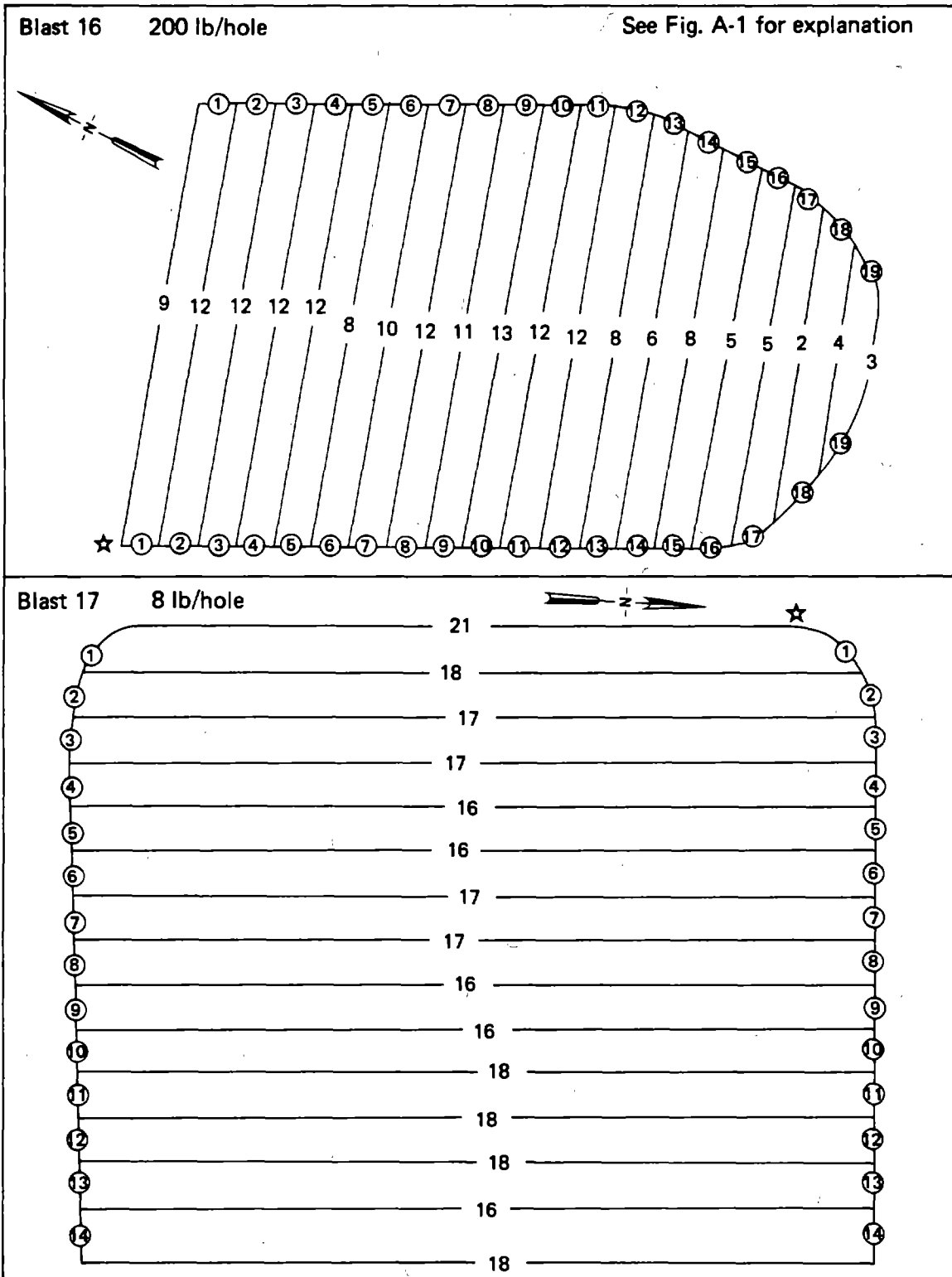


FIGURE A-6.—Layout of blasts 16 and 17.

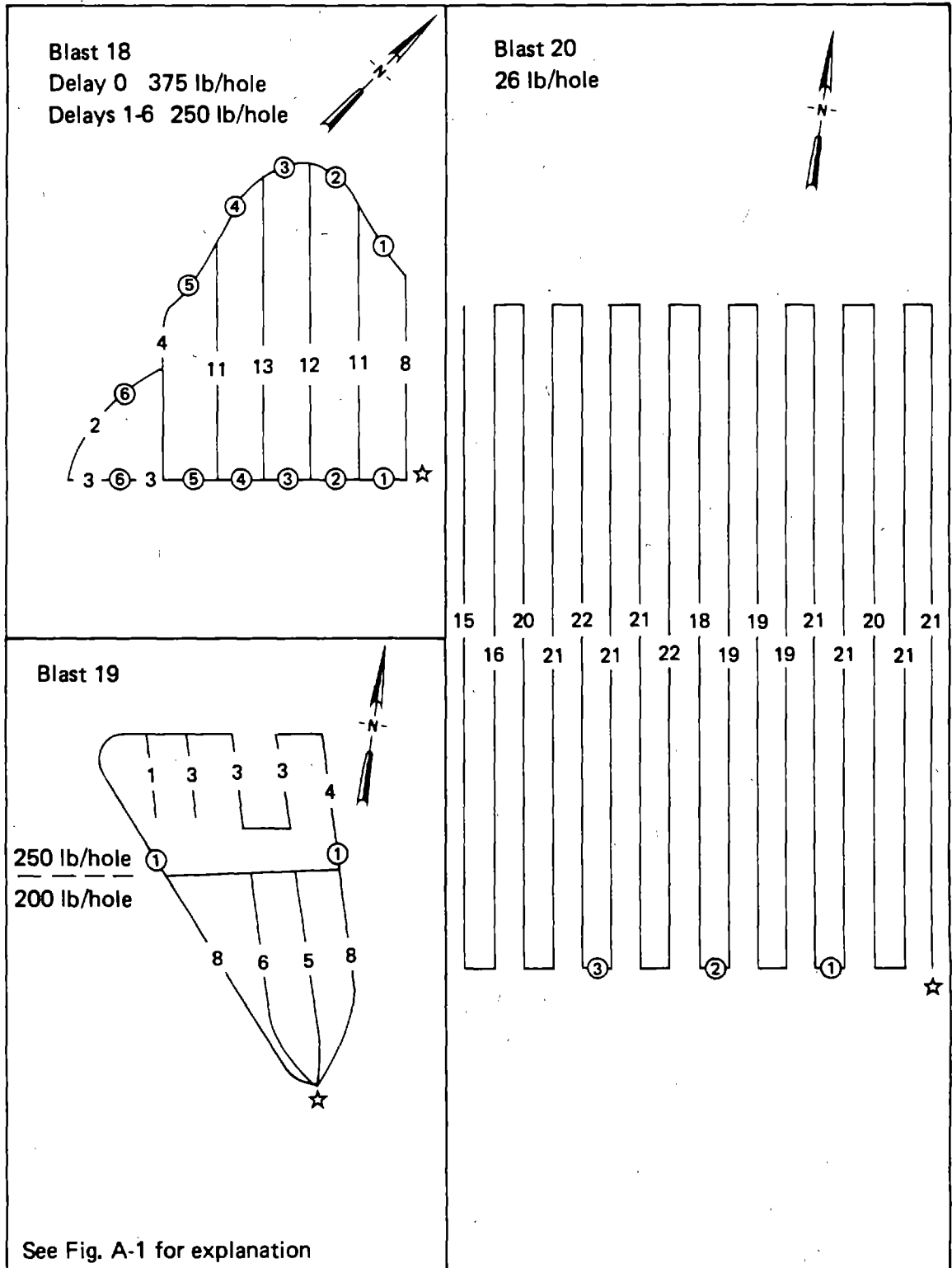


FIGURE A-7.—Layout of blasts 18, 19, and 20.



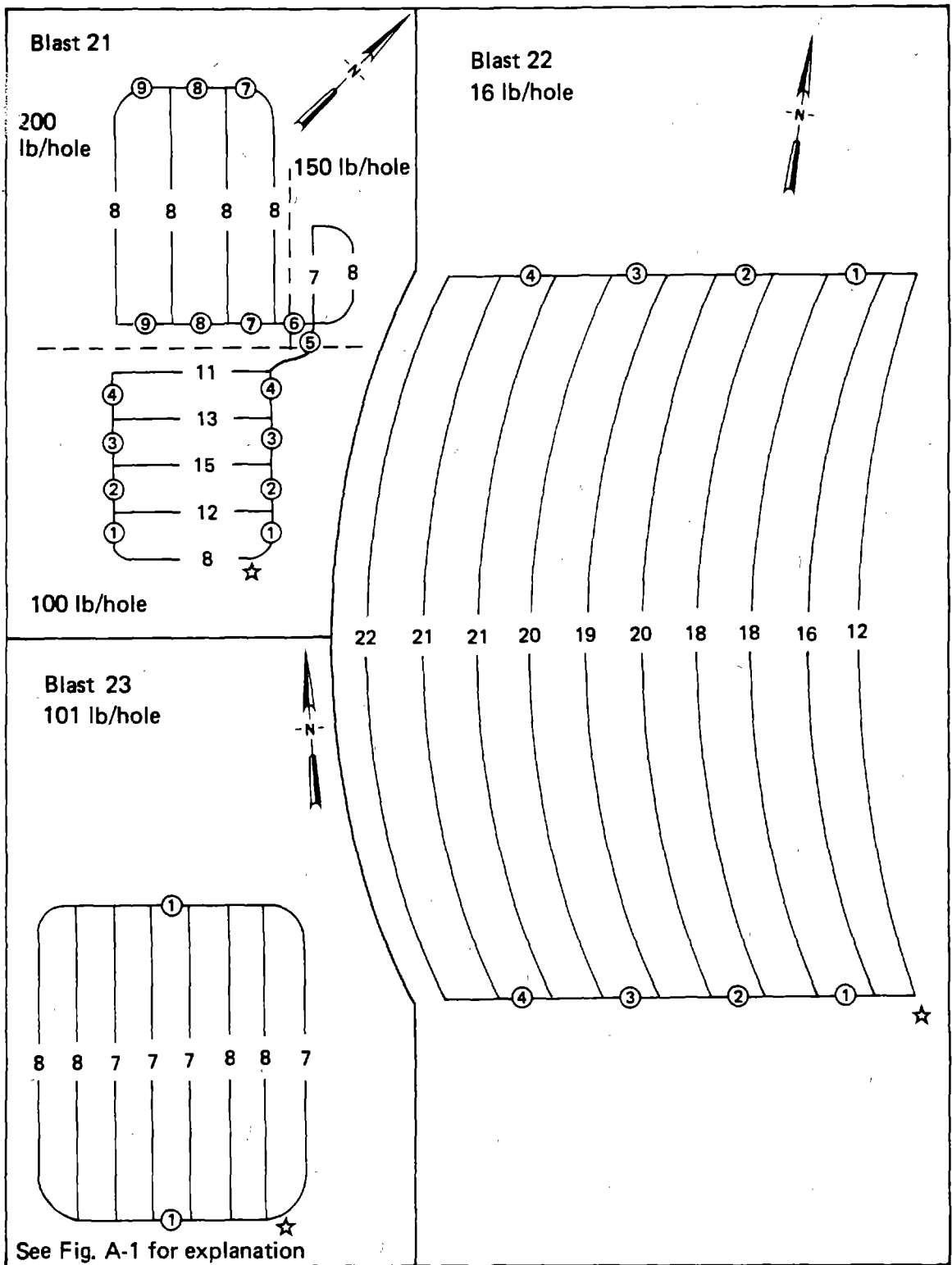


FIGURE A-8.—Layout of blasts 21, 22, and 23.

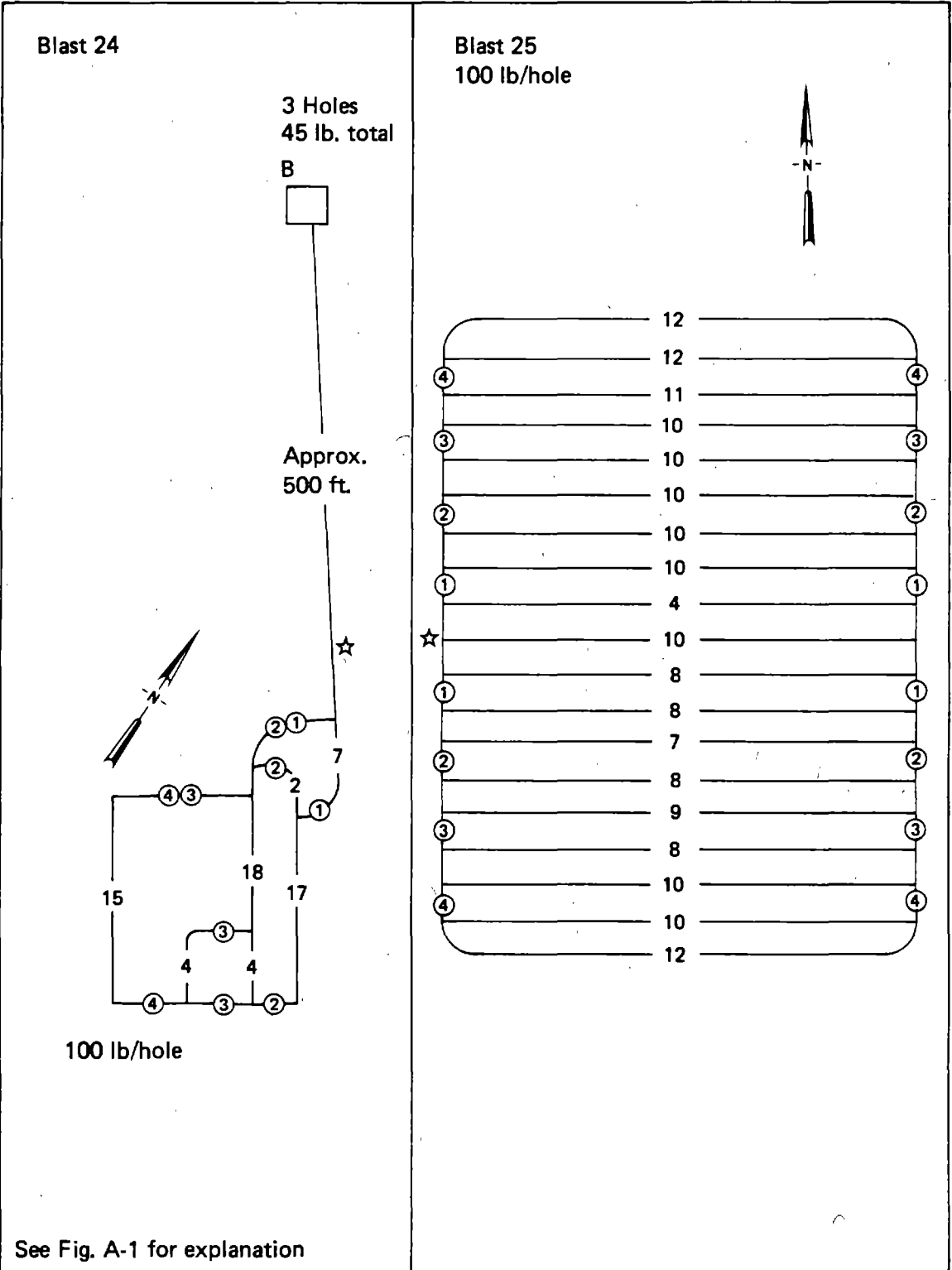


FIGURE A-9.— Layout of blasts 24 and 25.

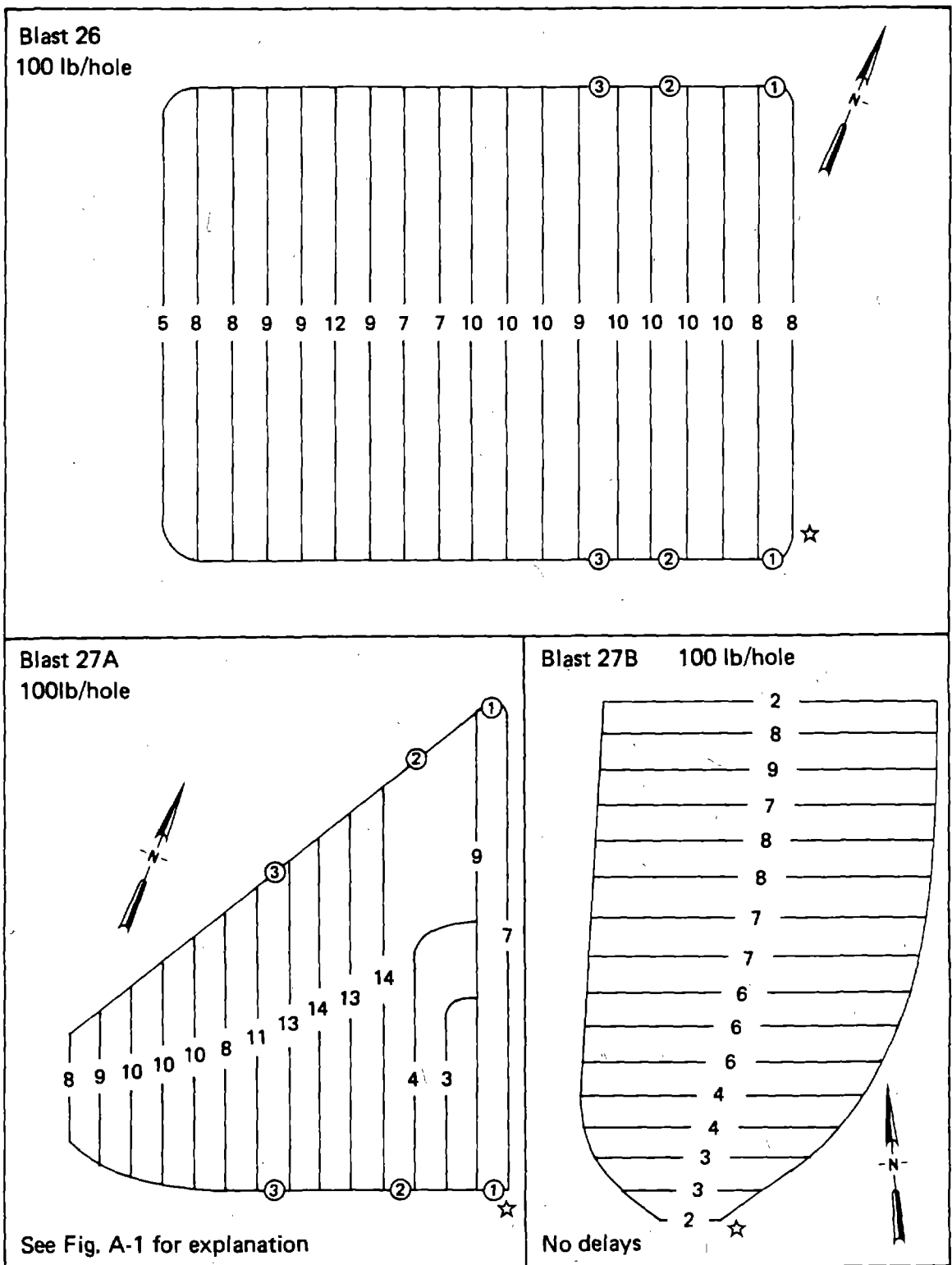


FIGURE A-10.—Layout of blasts 26, 27A, and 27B.

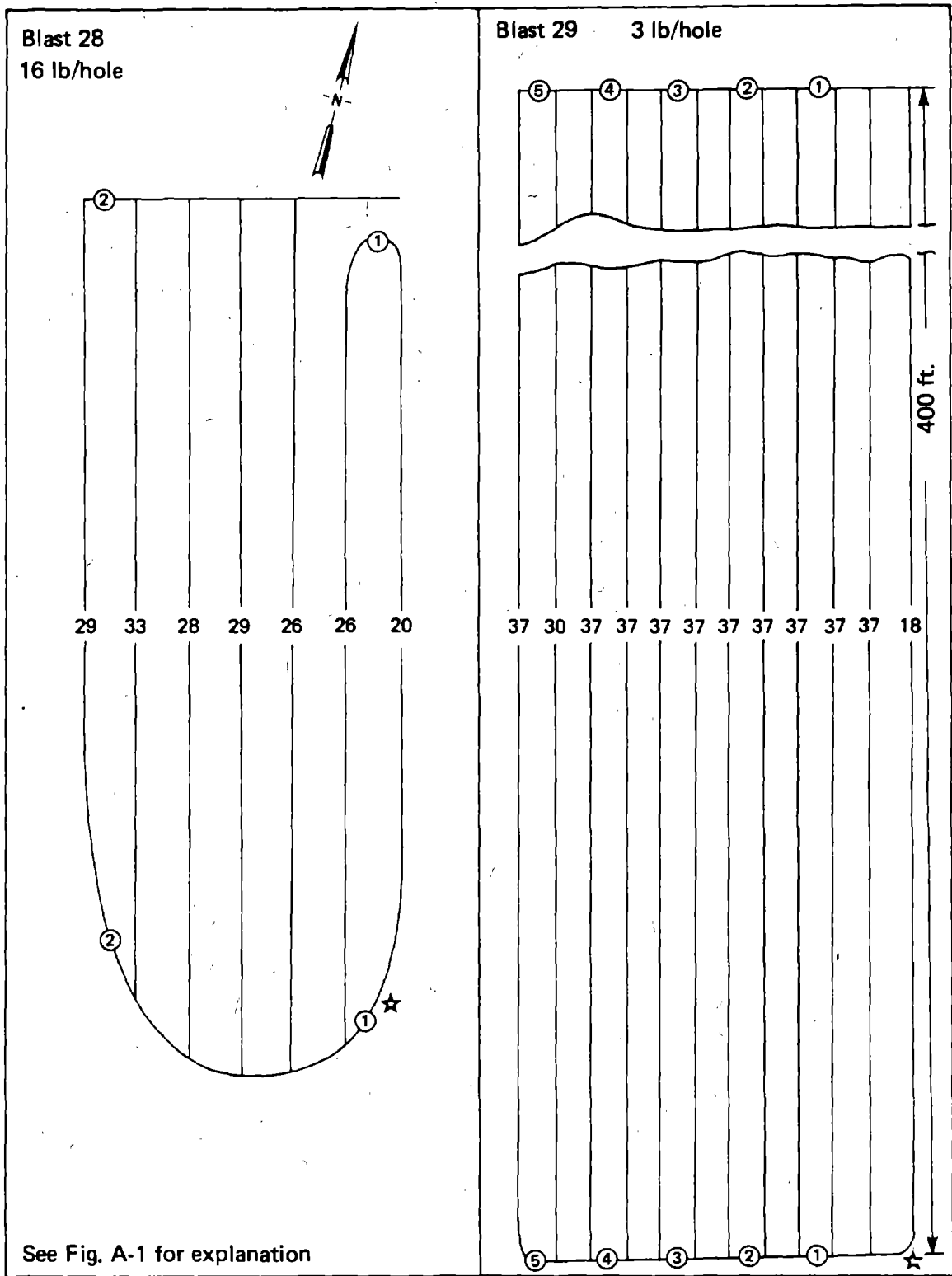


FIGURE A-11.—Layout of blasts 28 and 29.

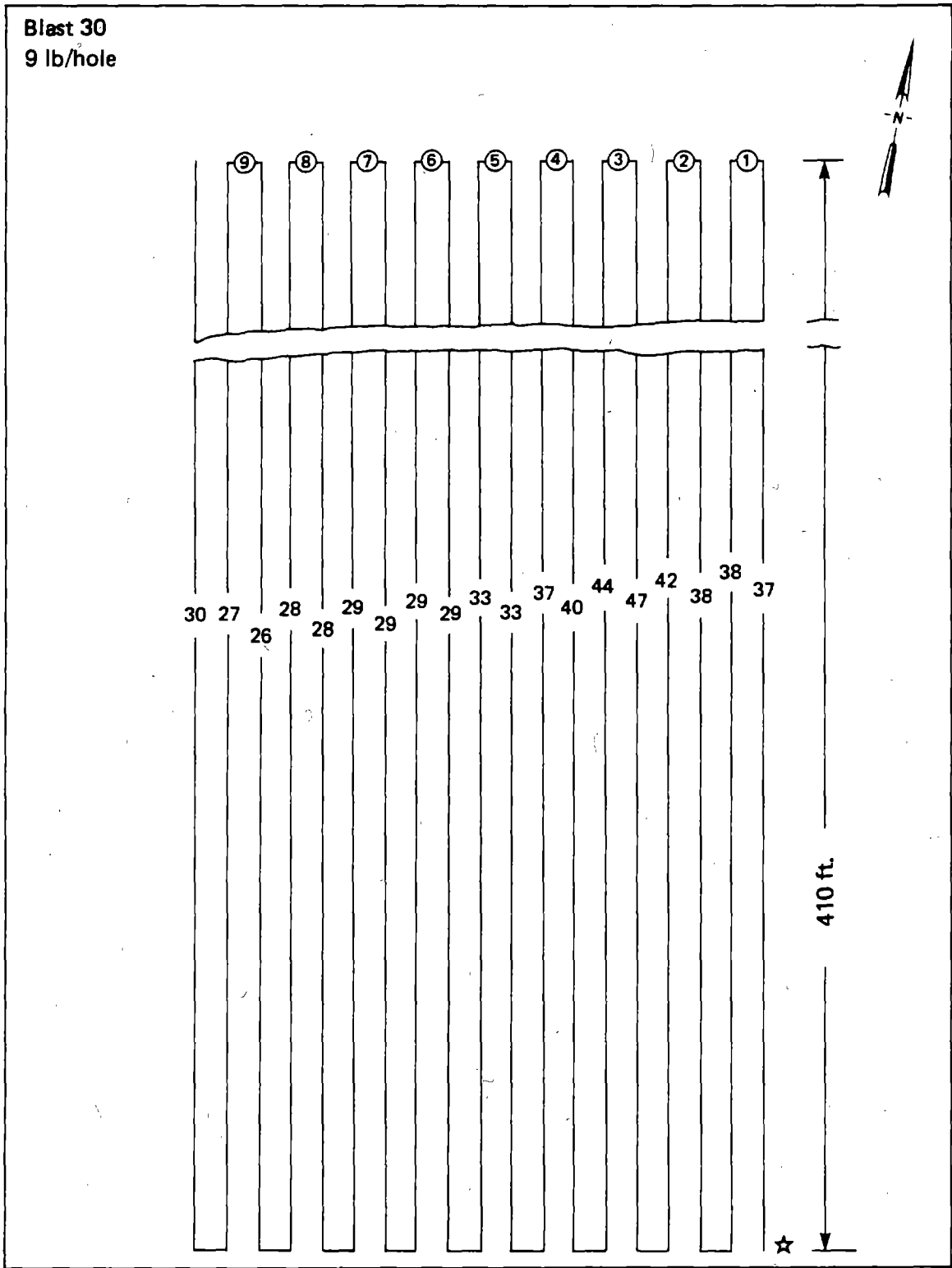


FIGURE A-12.—Layout of blast 30.

APPENDIX B  
Underground Vibration Recording Data

The three tables in this Appendix provide the information necessary for reduction of the recorded underground vibration data. The reduction procedures are discussed in Section 4.1 of the report. Table B1 lists the sensitivity of each sensor-preamplifier combination used. Table B2 lists the calibration factor for each channel of the record-reproduce system. Table B3 lists sensors and preamps used for each blast, gain settings, recorder channels, and amplitudes of the resulting records.

TABLE B1 - Sensitivity of underground sensors

Location <sup>1</sup>	Period	Sensor	Coil resistance, ohms	Measured sensitivity, <sup>2</sup> mV/in/sec	Preamp <sup>3</sup>	Shunt resistance, <sup>4</sup> ohms	Installed sensitivity, mV/in/sec
5/6 R	13Sep	12029	638	18.45	9	151.5	17.15
	-29 Sep						
	30Sep	2144	638	18.34	( <sup>5</sup> )	( <sup>5</sup> )	17.04
5/6 F	27Oct	( <sup>5</sup> )	( <sup>5</sup> )	( <sup>5</sup> )	1	152.2	17.10
	-12Nov						
	17Sep	12022	637	18.33	4	152.4	17.12
5/11 R	-12Nov	12026	642	18.48	8	152.4	17.25
	15Sep						
5/11 F	23Sep	12024	637	18.47	13	162.2	18.13
	-29Sep						
	30Sep	12033	632	18.62	( <sup>5</sup> )	( <sup>5</sup> )	18.28
	-11Oct	( <sup>5</sup> )	( <sup>5</sup> )	( <sup>5</sup> )	12	150.7	17.23
3/18 R	3Nov	( <sup>5</sup> )	( <sup>5</sup> )	( <sup>5</sup> )	14	166.0	18.62
	-12Nov						
	23Sep	2187	694	17.09	14	166.0	17.09
3/18 F	-4Oct	( <sup>5</sup> )	( <sup>5</sup> )	( <sup>5</sup> )	3	149.9	15.72
	5Oct						
3/18 F	23Sep	2186	641	18.33	5	169.6	18.64
	-29Sep						
	30Sep	13697	670	17.44	( <sup>5</sup> )	( <sup>5</sup> )	17.74

<sup>1</sup> Locations referenced by entry/crosscut; R refers to roof sensors, F refers to floor sensors.

<sup>2</sup> Measured at 100 Hz; particle velocity 1.0 in/sec peak; shunt resistance 166.0 ohms.

<sup>3</sup> Designation of impedance matching preamplifier installed with sensor and which contained the shunt resistance.

<sup>4</sup> Measured at DC; variation at 1000 Hz was  $-0.5 \times 10^{-4}$

<sup>5</sup> Not changed.

TABLE B2 - Record-reproduce system calibration factor

Recorder channel	Reproduce amplitude, <sup>1</sup> inches peak to peak				Calibration factor, <sup>2</sup> in/mV
	End of tape 1	Start of tape 2	End of tape 2	Average	
1	2.40	2.41	2.41	2.41	0.000852
2	2.41	2.44	2.45	2.43	0.000859
3	2.39	2.40	2.40	2.40	0.000849
4	2.30	2.32	2.33	2.32	0.000820
5	2.29	2.33	2.31	2.31	0.000816
6	2.31	2.39	2.36	2.35	0.000831
7	2.21	2.28	2.28	2.26	0.000799
8	2.34	2.38	2.38	2.37	0.000838
9	2.31	2.32	2.31	2.31	0.000816
10	2.29	2.31	2.31	2.30	0.000813
11	2.29	2.32	2.32	2.31	0.000816
12	2.30	2.38	2.37	2.35	0.000831
13	2.34	2.40	2.39	2.38	0.000842

<sup>1</sup>100 mVrms input at 1 kHz with 20db (10x) amplification; effective input to recorder 2828 mV peak to peak.

<sup>2</sup>Factor determined by dividing average reproduce amplitude by 2828 mV.



TABLE B3 - Underground recording information

Blast No.	Sensor	Amplifier-recorder <sup>1</sup>		Reproduce		Zero-peak amplitude of trace, in.	
		Preamp	channel	gain, db	channel		gain, X
Sensor location: entry 5, crosscut 6, roof (5/6 R)							
1	( <sup>3</sup> )	—	—	—	—	—	
2	12029	9	5	30	5	2	1.36
3			3	40	3	1	1.03
4			3	40	3	5	2.49
5			1	20	1	0.2	.51
6				20		0.5	.73
7				—		—	( <sup>2</sup> )
8				—		—	( <sup>2</sup> )
9	2144			20		2	1.83
10			8	30		2	1.49
11				22		5	.89
12				22		5	.65
13				30		2	1.18
14				32		1	1.38
15				20		2	.69
16				25		2	.82
17				36		5	.54
18				25		2	.82
19				33		5	1.34
20			1	22		2	1.06
21			8	30		2	1.17
22				30		1	1.14
23				45		2	1.41
24				32		2	.71
25				32		2	.60
26			1	30		1	.89
27A			8	36		1	1.38
27B				36		2	.97
28		1		18		1	.89
29				28		2	1.04
30				28		2	.62
Sensor location: entry 5, crosscut 6, floor (5/6 F)							
1	( <sup>3</sup> )	—	—	—	—	—	—
2	( <sup>3</sup> )	—	—	—	—	—	—
3	12022	4	6	40	6	2	1.40
4			6	40	6	5	1.74
5			4	20	4	2	.75
6				20		1	.87
7				—		—	( <sup>2</sup> )
8				—		—	( <sup>2</sup> )
9				20		2	1.61
10			11	30		2	1.16
11				22		5	.84
12				22		5	.69
13				30		2	.97
14				30		2	1.75
15				20		2	.63
16				25		5	1.27

See footnotes at end of table

TABLE B3 - Underground recording information - continued

Blast No.	Sensor	Preamp	Amplifier-recorder <sup>1</sup> channel	gain, db	Reproduce channel	gain, X	Zero-peak amplitude of trace, in.
Sensor location: entry 5, crosscut 6, floor (5/6 F) continued							
17	12022	4	11	36	4	5	.35
18				25		2	.65
19				33		5	1.09
20				22		2	1.22
21				31		2	.94
22				30		2	.82
23				45		2	.80
24				32		2	.45
25				32		5	.91
26				38		1	1.58
27A				36		2	2.24
27B				36		5	1.51
28				18		2	1.00
29				28		5	.94
30				28		5	.75
Sensor location: entry 5, crosscut 11, roof (5/11 R)							
1	( <sup>3</sup> )	—	—	—	—	—	—
2	12026	8	6	30	6	5	.84
3				—		—	( <sup>2</sup> )
4				—		—	( <sup>2</sup> )
5			9	40	2	1	1.57
6				40		2	1.42
7				—		—	( <sup>2</sup> )
8				—		—	( <sup>2</sup> )
9				32		2	1.07
10				30		2	.74
11				28		5	.99
12				28		5	.77
13				30		2	1.15
14				32		2	.66
15				20		5	.72
16				33		1	1.32
17				38		5	.27
18				33		0.5	1.02
19				33		1	.77
20				32		5	.85
21				30		2	1.34
22				34		5	.62
23				40		2	1.13
24				32		2	.85
25				32		2	.80
26				28		1	.66
27A				28		1	.67
27B				28		5	1.31
28				35		1	1.05
29				38		2	1.00
30				28		2	.54

See footnotes at end of table

TABLE B3 - Underground recording information - continued

Blast No.	Sensor	Preamp	Amplifier-recorder channel gain, db	Reproduce channel gain, X	Zero-peak amplitude of trace, in.
Sensor location: entry 5, crosscut 11, floor (5/11 F)					
1	( <sup>3</sup> )	--	--	--	--
2	( <sup>3</sup> )	--	--	--	--
3	( <sup>3</sup> )	--	--	--	--
4	( <sup>3</sup> )	--	--	--	--
5	12024	13	5	20	5
6			12	40	2
7					( <sup>2</sup> )
8					( <sup>2</sup> )
9	12033			32	2
10				30	2
11				28	5
12				28	5
13				30	2
14				30	5
15				20	5
16				33	1
17		12		38	5
18				33	1
19				33	2
20				30	5
21				31	2
22				35	5
23				40	2
24				32	2
25				32	2
26				28	2
27A				28	2
27B				28	5
28				35	2
29				--	( <sup>2</sup> )
30		14		28	5
Sensor location: entry 3, crosscut 18, roof (3/18 R)					
1	( <sup>3</sup> )	--	--	--	--
2	( <sup>3</sup> )	--	--	--	--
3	( <sup>3</sup> )	--	--	--	--
4	( <sup>3</sup> )	--	--	--	--
5	( <sup>3</sup> )	--	--	--	--
6	2187	14	10	40	3
7					( <sup>2</sup> )
8					( <sup>2</sup> )
9				32	5
10				30	1
11			3	22	2
12			3	32	1
13		3	10	30	2
14				32	5
15				20	5

See footnotes at end of table

TABLE B3 - Underground recording information - continued

Blast No.	Sensor	Preamp	Amplifier-recorder <sup>1</sup> channel	gain, db	Reproduce channel	gain, X	Zero-peak amplitude of trace, in.
Sensor location: entry 3, crosscut 18, roof (3/18 R) continued							
16	2187	3	3	39	3	2	58
17			10	45		2	( <sup>4</sup> )
18				45		2	2.12
19				45		2	2.83
20				35		5	.30
21				37		2	2.54
22				40		2	( <sup>4</sup> )
23				25		2	.42
24				36		2	.26
25				28		2	1.57
26				38		1	1.65
27A				35		1	1.18
27B			3	18		2	.83
28			10	46		2	1.13
29				46		5	.78
30				42		5	.93
Sensor location: entry 3, crosscut 18, floor (3/18 F)							
1-5	( <sup>3</sup> )	—	—	—	—	—	—
6	2186	5	13	40	6	2	.26
7				—		—	( <sup>2</sup> )
8				—		—	( <sup>2</sup> )
9	31697			32		5	1.26
10				30		2	.31
11				38		2	.60
12				38		5	.82
13				30		5	1.11
14				30		5	.40
15				20		5	.34
16			6	50		1	2.00
17			13	45		2	.10
18			13	45		2	2.68
19			6	39		0.2	( <sup>4</sup> )
20			3	32		5	.30
21				37		2	2.54
22				40		2	( <sup>4</sup> )
23				25		2	.48
24				36		2	.42
25				28		2	1.32
26				38		1	1.44
27A				35		1	1.20
27B			6	14		2	.66
28			13	46		2	1.73
29				46		5	1.28
30				42		2	.51

Footnotes:

<sup>1</sup> Gain in db must be converted for use with formula given in Section 4.1.

<sup>2</sup>Not recorded; <sup>3</sup>Not installed; <sup>4</sup>Poor record

APPENDIX C  
Convergence Measurements

Convergence measurements were made to observe any changes in the roof-floor distance which may have resulted from the blasting or overburden removal. Two methods of measurement were used. The results of these measurements are presented in this Appendix

A modified Philadelphia rod was used to make direct measurements at 23 locations. These measurements were made during the period 2 Nov.- 9 Nov. 77. Readings are listed in Table C1.

Drum recording extensometers were placed at the three underground sensor locations. Although designed to be continuously recording, the records are intermittent due to instrumentation problems. Figures C1, C2, and C3 shows the deflections recorded by the meters.

TABLE C1 - Convergence measurements made with modified Philadelphia surveyors rod

Station	2 Nov 77	3 Nov 77	4 Nov 77	7 Nov 77	8 Nov 77	9 Nov 77	Overall Change
<b>Entry 3</b>							
Crosscut 5	5.447	5.447	5.448	5.447	5.447	5.446	-0.001
Do. 6	5.086	5.086	5.085	5.085	5.085	5.085	-0.001
Do. 7	5.215	5.215	5.215	5.214	5.213	5.213	-0.002
Do. 8	5.693	5.693	5.693	5.693	5.693	5.693	0
Do. 9	5.865	5.864	5.864	5.864	5.865	5.865	0
Between 9 and 10	5.854	5.854	5.853	5.852	5.853	5.852	-0.002
Crosscut 10	5.686	5.685	5.685	5.685	5.685	5.685	-0.001
Between 10 and 11	5.819	5.819	5.818	5.818	5.818	5.817	-0.002
Crosscut 11	5.922	5.921	5.921	5.921	5.921	5.921	-0.001
Between 11 and 12	5.234	5.234	5.234	5.234	5.234	5.234	0
Crosscut 12	4.975	4.975	4.974	4.975	4.973	4.974	-0.001
Between 12 and 13	5.092	5.091	5.091	5.091	5.091	5.090	-0.002
Crosscut 13	5.122	5.122	5.121	5.122	5.121	5.122	0
Do. 14	5.214	5.213	5.213	5.212	5.212	5.212	-0.002
Do. 15	4.817	4.817	4.817	4.817	4.817	4.817	0
Do. 16	4.564	4.564	4.563	4.564	4.563	4.563	-0.001
Do. 17	4.653	4.653	4.653	4.653	4.654	4.652	-0.001
<b>Entry 5</b>							
Crosscut 5	-	5.504	5.505	5.505	5.504	5.504	0
Do. 7	-	5.667	5.667	5.666	5.666	5.666	-0.001
Do. 8	-	5.029	5.207	5.028	5.027	5.028	-0.001
Do. 9	-	5.853	5.853	5.852	5.853	5.852	-0.001
Do. 10	-	4.805	4.805	4.805	4.805	4.805	0
Between 11 and 12	-	5.143	5.144	5.143	5.143	5.143	0
Time of measurements	0857 to 0946hrs	0947 to 1142hrs	1105 to 1225hrs	0858 to 1028hrs	1053 to 1151hrs	1001 to 1048 hrs	

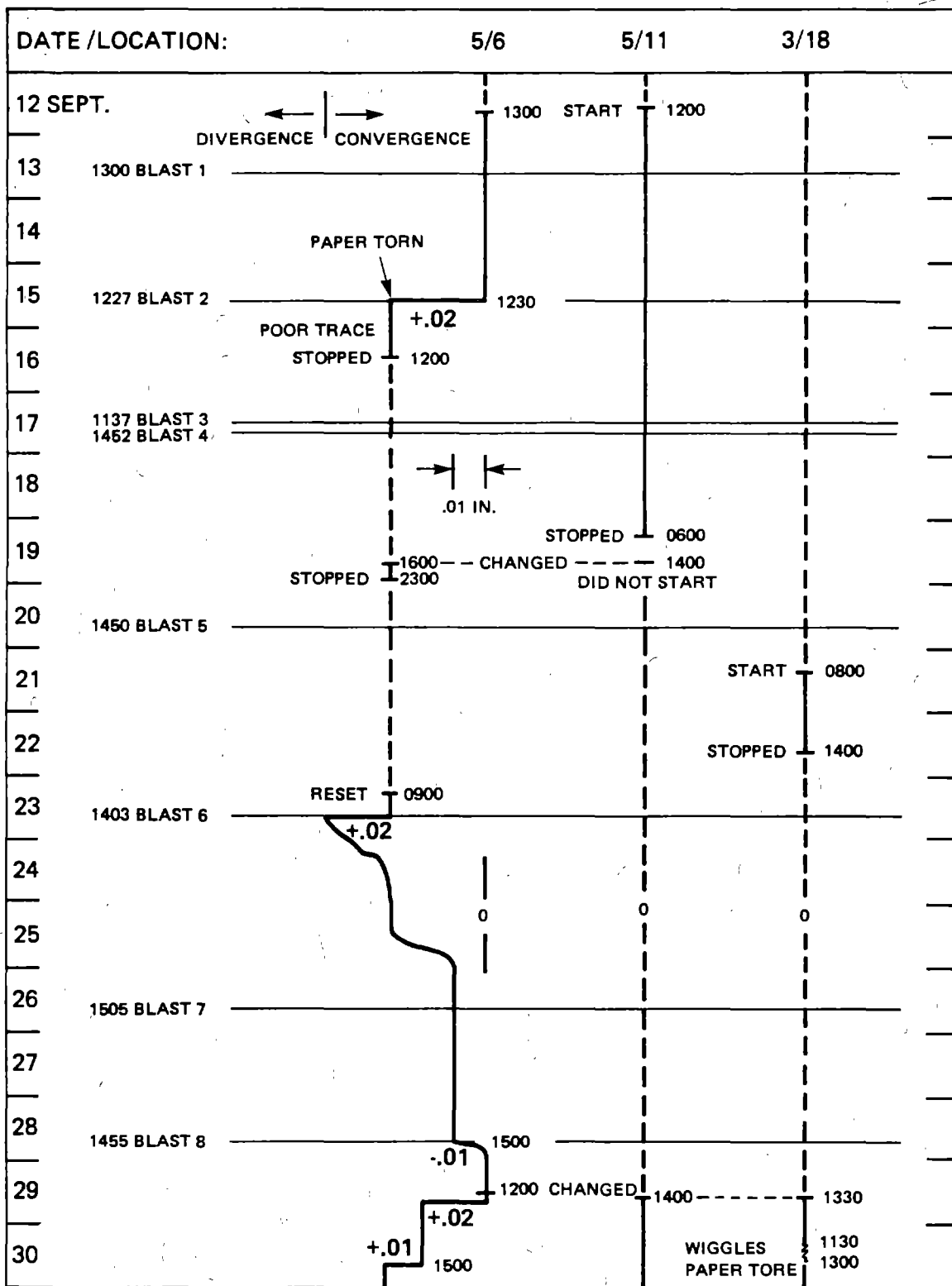


FIGURE C-1.—Convergence meter deflections, 12 to 30 September, 1977.

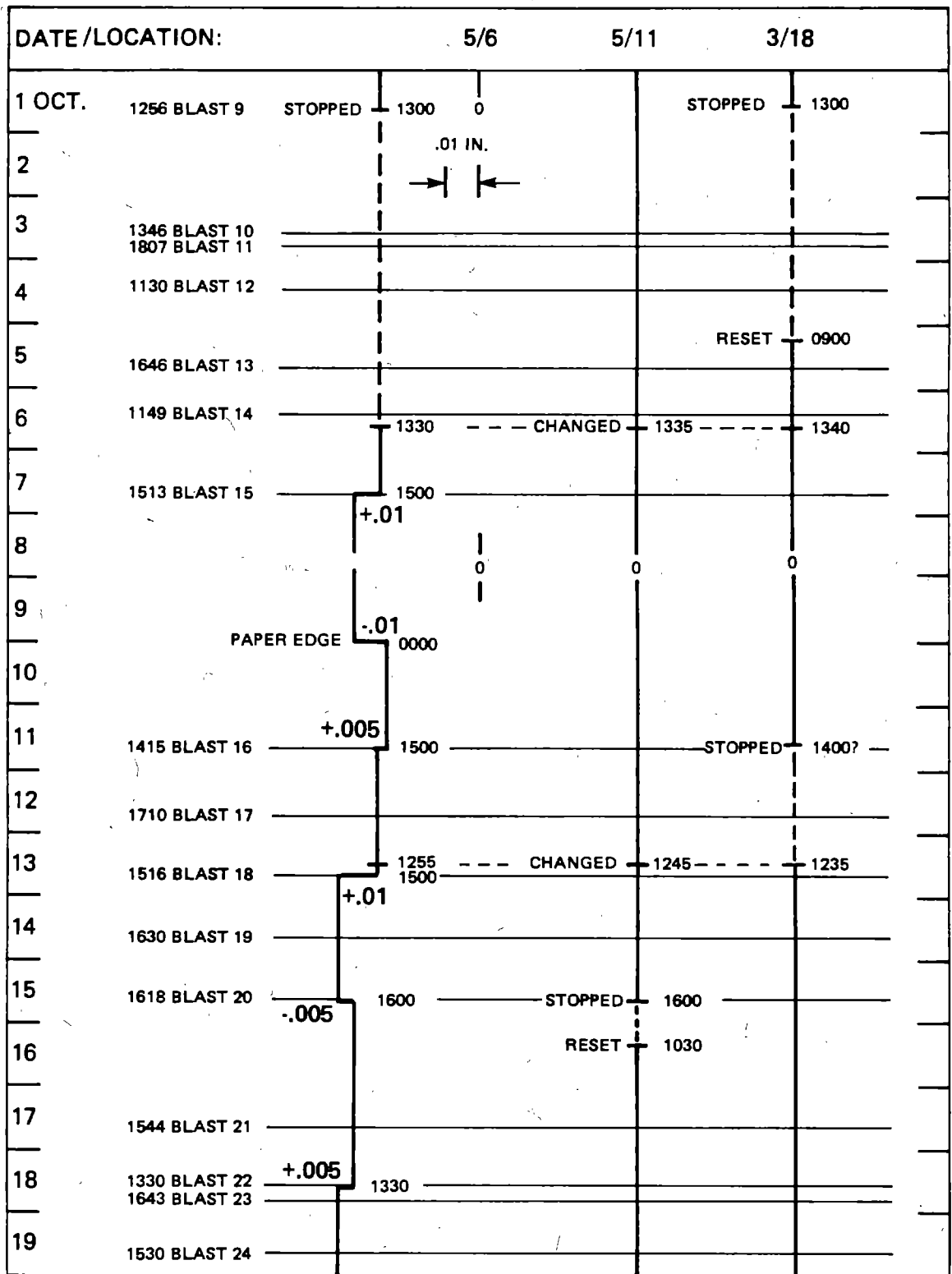


FIGURE C-2.—Convergence meter deflections, 1 to 19 October, 1977.



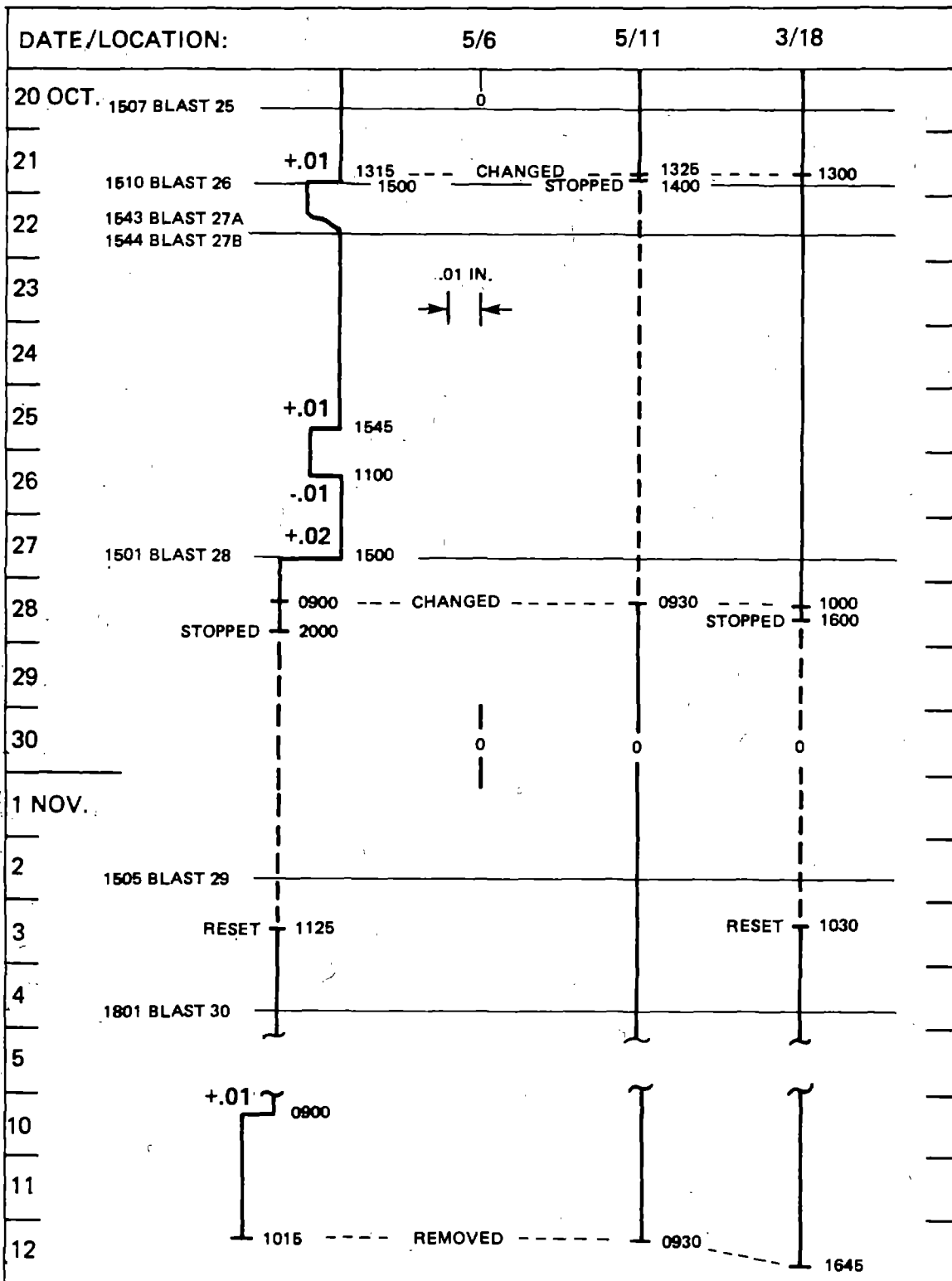


FIGURE C-3.—Convergence meter deflections, 20 October to 12 November, 1977.